Fakultät für Ingenieurwissenschaften, Informatik und Psychologie

Institut für Psychologie und Pädagogik

Abteilung Klinische & Biologische Psychologie

Leiterin: Prof. Iris-Tatjana Kolassa

Diagnosis and prognosis of disorders of consciousness:

Classification and prognostication of clinical outcome of patients after traumatic and non-traumatic brain injuries

Dissertation zur Erlangung des Doktorgrades Dr. rer. nat.

der Fakultät für Ingenieurswissenschaften, Informatik und Psychologie

der Universität Ulm

vorgelegt von

Barbara Zeller

Geb. in Bonn

Neu-Ulm

2018

Amtierender Dekan: Prof. Dr.-Ing. Maurits Ortmanns

Gutachter/in: 1. Prof. Dr. Iris-Tatjana Kolassa

2. Prof. Dr. Andreas Bender

3. Prof. Dr. Cornelia Herbert

Tag der Promotion: 16. Januar 2019

Danksagung aus Gründen des Datenschutzes entfernt.

Table of content

Abstract

The improved medical care for craniocerebral injuries caused by traumatic or non-traumatic events leads to a constantly increasing number of patients who remain in a changed state of consciousness after intensive medical treatment. Usually the first stage is the *Unresponsive Wakefulness Syndrome* (UWS), which may change into a *Minimally Conscious State* (MCS) from which patients may eventually regain full consciousness. Especially for UWS patients the early detection of first signs of consciousness could support the creation of individual treatment plans. However, in addition to the classification of disorders of consciousness, the prediction of the clinical course is also an important point in the daily lives of practitioners and, above all, the relatives of patients.

The thesis deals with the question of how reliably different electroencephalographic (EEG) parameters can determine consciousness in these patients and whether a regaining of consciousness in these patients can be predicted by EEG markers identified in ERP and resting-state EEG data. To this end, it was examined how reliable event-related potentials (ERP) can be measured in patients with impaired consciousness (Study 1, Schorr et al., 2014) and whether UWS patients can be distinguished from MCS patients on the basis of these measurements. Patients were tested with an oddball paradigm several times on the same day and on different days. In the next step, connectivity, more precisely, coherence, i.e., the synchronous activation of different brain areas, was examined in UWS and MCS patients. On the one hand, with regard to the differentiation between these two states of consciousness and on the other hand with regard to the significance of coherence patterns for the course of the disease. EEG data from 73 patients was evaluated (coherence within parietal and frontal brain areas and coherence between frontal and parietal lobe) and patients were reassessed after one year to determine the current state of consciousness (Study 2, Schorr et al., 2016).

The aim of the last study was to compare the usefulness of different EEG parameters, to distinguish between non-reactive and minimally conscious patients and to predict an improvement in the state of consciousness. For this purpose, already established methods (such as coherence, power analysis, entropy, microstates and complex network analyses) were compared together on a single data set for the first time and an attempt was made to determine whether an automated prediction is possible (Study 3, Stefan et al., 2018).

In summary, it was demonstrated that a) the occurrence of ERPs is subject to strong fluctuations and this is reflected in a low retest reliability; a lack of ERP could be quickly interpreted as a lack of awareness, which could be prevented by repeated measurements at short time intervals; it was also demonstrated that b) coherence, power analysis, entropy, microstates and complex network analyses all predict the recovery of consciousness in UWS patients, and that c) an automated classification scheme can be used to predict recovery from UWS. The results suggest that the above measurements might be useful as biomarkers in predicting a positive course of unconsciousness disorders. This work lays the foundation for further research to apply the methods described on an individual basis in the future.

Zusammenfassung

Die verbesserte medizinische Versorgung bei Schädel-Hirnverletzungen durch traumatische oder nicht-traumatische Ereignisse führt zu einer stetig ansteigenden Zahl von Patienten, die nach intensiv-medizinischer Behandlung in einem veränderten Bewusstseinszustand verbleiben. Meist ist die erste Stufe das *Syndrom Reaktionsloser Wachheit* (engl.: Unresponsive Wakefulness Syndrome, UWS), das dann eventuell in einen Zustand des *minimalen Bewusstseins* (engl.: Minimally Conscious State, MCS) übergeht, woraus Patienten dann unter Umständen wieder zu vollem Bewusstsein erwachen. Gerade bei UWS-Patienten könnte die Früherkennung erster Anzeichen von Bewusstsein die Erstellung von individuellen Behandlungsplänen unterstützen. Neben der Klassifizierung der Bewusstseinsstörung ist aber auch die Vorhersage des klinischen Verlaufs ein wichtiger Punkt im Alltag von Behandlern und vor allem auch den Angehörigen der Patienten.

Diese Dissertation beschäftigt sich mit der Frage, wie zuverlässig verschiedene elektroenzephalographische (EEG) Parameter Bewusstsein bei diesen Patienten feststellen können und damit, ob ein Wiedererlangen des Bewusstseins bei diesen Patienten mit Hilfe von EEG Markern vorhergesagt werden kann. Dazu wurde überprüft, wie reliabel ereignis-korrelierte Potentiale (engl.: event-related potentials, ERP) bei bewusstseinsgestörten Patienten gemessen werden können (Studie 1, Schorr et al., 2014) und ob anhand dieser Messungen UWS-Patienten von MCS-Patienten unterschieden werden können. Die Patienten wurden mehrmals täglich sowie an verschiedenen Tagen mit einem Oddball-Paradigma getestet. Im nächsten Schritt wurde die Konnektivität, genauer gesagt, Kohärenz, also die synchrone Aktivierung verschiedener Gehirnareale, bei UWS- und MCS-Patienten untersucht. Zum einen im Hinblick auf eine

Abgrenzung dieser beiden Bewusstseinszustände und zum anderen im Hinblick auf die Aussagekraft von Kohärenzmustern für den Krankheitsverlauf. Es wurden EEG-Daten von 73 Patienten ausgewertet (Kohärenz innerhalb parietaler und frontaler Hirnareale, sowie Kohärenz zwischen Frontal- und Parietallappen) und die Patienten wurden nach einem Jahr noch einmal besucht, um den aktuellen Bewusstseinszustand zu erheben (Studie 2, Schorr et al., 2016). Das Ziel der letzten Studie war ein Vergleich der Nützlichkeit verschiedener EEG-Parameter, um reaktionslose von minimalbewussten Patienten zu unterscheiden und eine Verbesserung des Bewusstseinszustandes im klinischen Verlauf vorherzusagen. Hierzu wurden bereits etablierte Methoden (wie Kohärenz, Poweranalyse, Entropie, Microstates und Komplexe Netzwerkanalysen) erstmals zusammen an einem einzigen Datensatz verglichen und darüber hinaus wurde versucht zu ermitteln, ob eine automatisierte Vorhersage eines positiven klinischen Verlaufs möglich ist (Studie 3, Stefan et al., 2018).

Zusammengefasst konnte gezeigt werden, dass a) ein Auftreten von ERPs starken Fluktuationen unterliegt und sich dies in einer niedrigen Retest-Reliabilität widerspiegelt; Das Fehlen eines ERPs könnte vorschnell als ein Fehlen von Bewusstsein gedeutet werden, was durch wiederholte ERP-Messungen in kurzen Zeitabständen verhindert werden könnte; ebenso konnte gezeigt werden, dass b) Kohärenz, Poweranalyse, Entropie, Microstates und Komplexe Netzwerkanalysen getrennt voneinander bei UWS-Patienten die Wiedererlangung von Bewusstsein vorhersagen und dass c) ein automatisiertes Klassifikationsschema zur Vorhersage genutzt werden kann. Die Ergebnisse sprechen dafür, dass die oben genannten Messungen EEG-Marker erfassen können, die einen positiven Verlauf bei Bewusstseinsstörungen vorhersagen können. Die vorliegende Arbeit legt einen Grundstein für weitere Forschung mit dem Ziel, zukünftig die beschriebenen Methoden auch auf individueller Basis anwenden zu können.

Abbreviations

ApEn Approximate entropy

CRS-R Coma Recovery Scale - Revised

DOC Disorders of consciousness

DRS Disability Rating Scale

EEG Electroencephalography

ERP Event-related potential

fMRT Functional magnetic resonance imaging

GCS Glasgow Coma Scale

Hz Hertz

KRS Koma-Remissions-Skala

LIS Locked-In-Syndrome

MCS Minimally conscious state

(FDG-) PET Fluordesoxyglucose positron emission tomography

REM sleep Rapid eye movement sleep

ROI Regions of interest

SBH Subarachnoid hemorrhage

SFFS Sequential floating forward selection

TE Symbolic transfer entropy

UWS Unresponsive wakefulness syndrome

wSMI Weighted symbolic mutual information

Part I Synopsis

1 Introduction

1.1 Theoretical background

Consciousness comprises multiple dimensions (Zeman, 2008): The *qualitative* aspect of consciousness is described as awareness (Guldenmund, Stender, Heine, & Laureys, 2012), which focuses on content. A person is aware of their surroundings and their own self. Awareness can, for example, be compromised in patients with schizophrenia, who experience hallucinations (Poeck & Hacke, 2001). The *quantitative* aspect is described as wakefulness or arousal (Faymonville et al., 2004) and instead focuses on a patient's ability to react to external stimuli or initiate contact with their environment. This ability is to different degrees compromised in patients with disorder of consciousness (DOC).

1.2 Spectrum of quantitative disorders of consciousness (DOC)

1.2.1 Coma

Coma is the most severe manifestation of a DOC. The main causes are lesions to the brainstem or thalamus as well as bi-hemispheric cortical damages (Giacino & Kalmar, 1997; Jennett, 2002). Patients no longer show any signs of arousal or awareness (Lücking & Wallesch, 1992) and do not react to any external stimuli or show signs of spontaneous directed behaviour. Their sleep-wake cycle is disrupted, as is shown by EEG measurements, and they are not able to breathe independently (Jennett, 2002; Plum & Posner, 1982). When patients recover from coma, they usually drift into a state of unresponsive wakefulness first.

1.2.2 Unresponsive wakefulness syndrome

The term "Unresponsive wakefulness syndrome" (UWS) was first introduced by Laureys et al. (2010). Until then, the condition was known as *(persistent) vegetative state*, *appallic syndrome* or *coma vigile* (Laureys et al., 2010). UWS describes more accurately the state in which patients do not show reproducible behaviour or any response to environmental stimuli. Furthermore, it is characterized by intermittent wakefulness and preserved sleep-wake cycles, as well as preserved brainstem and autonomic nervous system function. UWS can be caused by traumatic and non-traumatic brain injuries (Oder & Wurzer, 2011), and it can be permanent.

1.2.3 Minimally conscious state

Patients in a minimally conscious state (MCS) are able to follow commands, fixate on objects with their eyes and may show visual pursuit (Guldenmund et al., 2012; PVS TM-STFo, 1994a b). But clinicians should be aware that these signs may be inconsistent. Since DOC present themselves as a spectrum, abilities can vary widely, e.g. depending on the time of day at the point of testing, and between different patients. Some patients may even show the ability to respond to simple yes/no questions with behavioural reactions (Giacino et al., 2002). In an attempt to even further differentiate within the MCS spectrum, Bruno et al. (2011) defined the categories of MCS+ and MCS- patients. The former follow commands, show basic verbalization or non-functional communication. MCS- patients show visual pursuit, can localize adverse stimuli or react contingently to emotional stimuli (Perrin, Castro, Tillmann, & Luauté, 2015)

1.2.4 Locked in syndrome – not a DOC

Patients in a locked-in state have preserved cerebral function and are fully awake and aware (Laureys, Perrin, & Brédart, 2007; Plum & Posner 1966), but lost any muscle control (although they sometimes preserve some control over eye muscles). The state is usually the result of

brainstem hemorrhage or infarction resulting in damages to cortico-spinal and cortico-bulbar pathways (Laureys et al., 2005).

1.3 Prevalence

Van Erp et al. (2014) systematically reviewed 1032 papers. Based on the reviewed studies they assumed the prevalence of UWS to vary between 0.2 and 6.1 patients per 100 000. They pointed out that the quality of the studies differed widely, especially regarding inclusion criteria and diagnosis verification which led to a poor reliability of prevalence figures. For MCS, Giacino et al. (2002) estimated a prevalence of 48-96 patients per million. Even though diagnostic methods improved over the last decades, around 40% of patients are still thought to be misdiagnosed (Andrews, Murphy, Maunday, & Littlewood, 1996, Schnakers et al., 2006), and the rate per million patients is also thought to be too high (Wade, 2018). In his review, Wade (2018) stated that this rate is misinterpreted. Underlying physical causes, such as brainstem or thalamic damage, which are suggested to be the main causes of DOC, and also pharmacological treatment which could cause unresponsiveness, may not have been evaluated thoroughly. This in turn could have led to a classification error, which could be avoided by taking both neurological evidence and behavioural assessment into account. This discussion proves that it is difficult to determine the exact prevalence of UWS and MCS in the general population (Zeman, 1997).

2 Diagnostic methods of disorders of consciousness

2.1 Clinical methods

The *Glasgow Coma Scale* (GCS, Teasdale & Jennett, 1974) is usually used to assess the state of consciousness during the first diagnostic exam in a patient (Lesko et al., 2013; Teasdale & Jennett, 1974). It comprises three subscales: motor response, verbal functions and eye opening. It is a fast and simple method to assess level of consciousness. However, it has been shown that the interrater reliability is poor (32% of conformity between raters on the complete scores; only 55% to 74% on the sub scales; (Gill, Reiley, & Green, 2004)), and also Reith, Van den Brande, Synnot, Gruen and Maas (2016) found varying reliability depending on the quality of the scale's administration. Additionally, its validity can be compromised where patients have impairments to motor or verbal behaviour and the scale lacks sensitivity when it comes to differentiating between levels, both within and between UWS and MCS.

A second, widely-used, coma scale is the German *Coma Remission Scale* (Koma-Remissions-Skala [KRS]; Voss, 1993). It comprises six sub-scales: arousal, motor response, reaction to acoustic stimuli, reaction to visual stimuli, and verbal function. Like the GCS, the KRS recognises only rough categories of patient reactions, and cannot assess subtle changes in the patient's behaviour; it is therefore difficult to measure small changes in the patient's state of consciousness (Stepan, Haidinger, & Binder, 2004a).

The *Coma Recovery Scale* was first developed in 1991 (Giacino, Kezmarsky, DeLuca, & Cicerone, 1991) to assess the ability of patients to respond to stimuli. It not only assesses the state of arousal of the patient, but also measures behaviour on a total of six sub-scales: arousal, auditory function, visual function, motor function, oromotor and verbal function, and communicative skills. The

categories of each sub-scale are ordered hierarchically, starting with reflexive behaviour and ending with willful conscious behaviour. There is a specific standardized protocol, which has to be followed during the assessment, leading to a satisfying inter-rater-reliability (O'Dell et al., 1996). The validity was assessed alongside the GCS and the Disability Rating Scale (DRS, Rappaport, Hall, Hopkins, Belleza, & Cope, 1982). The DRS predicts the outcome after traumatic brain injury (TBI) and assesses cognitive abilities as well as a patient's dependency on external help. It is not able to differentiate between different levels of DOC.

Based on clinical experience with the CRS, Giacino, Reiley, & Green (2004) revised the scale, which resulted in the *Coma Recovery Scale-revised* (CRS-R) (Giacino et al., 2004). Single items were replaced or added to render the scale more sensitive; however the overall structure of the scale remained the same. Additionally, greater detail was added to the descriptions in the administration protocol of the CRS-R in order to increase standardization. Giacino et al. (2004) showed that the CRS-R has a good test-retest-reliability of $\kappa = .23$ to $\kappa = 1.00$ and an interrater reliability of $\kappa = .58$ to $\kappa = .88$. Compared to the GCS and KRS, the CRS-R is more sensitive in the differential diagnostics of different levels of consciousness and can also show the recovery of neuro-behavioural functions.

The CRS-R is widely accepted as the highest standard in the clinical diagnosis of DOC (Giacino et al., 2004; Schnakers et al., 2006; Schnakers, Giacino, & Laureys, 2010). Yet, misdiagnosis due to physical impairments in the patients still remains a major problem (Andrews et al., 1996; Guldenmund et al., 2012). In order to circumvent these limitations, imaging and electrophysiological methods have been used increasingly in recent years to add to the methodological tool set (Bender, Jox, Grill, Straube, & Lulé, 2015; Bekinschtein, Manes, Villareal, Owen, & Della-Maggiore, 2011; Fischer, Morlet, & Giard, 2010; Vanhaudenhuyse et al., 2010).

2.2 Functional magnetic resonance imaging (fMRI) & Fluordesoxyglucose positron emission tomography (FDG-PET)

It is important to explore the applicability of imaging techniques such as FDG-PET, fMRI and EEG, as an addition to the everyday clinical routine as tools for the classification of the level of consciousness. It has been shown that active tasks are, however, sometimes insensitive to preserved consciousness (Monti et al., 2010; Stender et al., 2014), which has led to the exploration of resting-state markers of consciousness. FDG-PET and fMRI studies yielded promising results: glucose metabolism in DOC patients is altered in comparison to healthy controls (DeVolder et al., 1990; Tommasino, Grana, Lucignani, Torri, & Fazio, 1995), and can moreover differentiate between UWS and MCS patients with high sensitivity and specificity (Stender et al., 2015). Furthermore, resting-state fMRI analyses yielded markers distinguishing DOC patients from healthy controls, with a focus on functional connectivity in different neural networks, such as the default mode network (Demertzi et al., 2014; Vanhaudenhuyse et al., 2010). Later studies found differences between UWS and MCS patients (Demertzi et al., 2015; Wu et al., 2015). A recent study by Golkowski and colleagues (2017) using simultaneous EEG-PET-fMRI, demonstrated that absolute occipital glucose metabolism was the best predictor for differentiating between UWS and MCS, with higher metabolism in MCS patient compared to UWS patients. Similar findings were reported by Chennu and colleagues (2017), who found that connectivity hubs in EEG data correlate with metabolism measured with PET.

The prognostic value of fMRI assessments has also been demonstrated in a variety of studies: For example, Silva et al., (2015) reported that unresponsive patients who improved after brain injury showed significant differences in the connectivity between their medial prefrontal cortex and posterior cingulate cortex compared to those patients who did not recover consciousness. When

patients were presented with their own names as stimuli, the activation in the auditory cortex successfully predicted the outcome of UWS patients (Wang et al., 2015). FDG-PET has proved useful for clinical prognosis as well: In a large cohort study, Stender et al. (2014) were able to show that FDG-PET correctly predicted long-term outcome in 74% of their patients using FDG-PET.

2.3 Electroencephalography (EEG) in DOC patients

In a meta-analysis, Bender et al. (2015) showed that quantitative EEG has a high sensitivity and specificity for detecting minimal consciousness, directly followed by functional magnetic resonance imaging (fMRI), and event-related potentials (ERP). Quantitative EEG describes the automated analysis of EEG characteristics such as frequency, amplitude, and synchrony between signals. ERP analysis explores the brain's reaction to single events reflected in the EEG data. ERPs can differentiate between states of consciousness (Donchin, Karis, Bashore, Coles, & Gratton, 1986; Risetti et al., 2013), they can be used to communicate with patients via brain computer interfaces and detect the ability to follow commands in otherwise behaviourally unresponsive patients (Lulé et al., 2013). They may also predict the recovery of patients with DOC (Cavinato et al., 2011; Fischer et al., 2006; Fischer Morlet, & Giard, 2000; Kotchoubey, 2005). Auditory oddball paradigms are frequently used in DOC research: a patient is presented with tones (targets and distractors) or other acoustic stimuli (e.g., the patient's own name among other names) and is instructed to either listen passively or to actively count the target stimuli (Fischer et al., 2010; Cavinato et al., 2010; Schnakers et al., 2008). The P300, which is the ERP component elicited by the oddball task, varies depending on the patient's state of awareness but also depending on the frequency of the target stimulus among the distractors (Pritchard, 1987; Johnson, 1986). A passive paradigm can already give information on the brain's ability to process basic external stimuli. Comparing active vs. passive conditions can yield additional information on the patient's

attentiveness, which would be represented by a higher P300 in the active condition (Schnakers et al., 2008), and may be a marker for the level of consciousness.

As DOC patients may be visually or acoustically impaired, the analysis of resting-state data bypasses these limitations. Power spectrum analysis, connectivity, and specifically entropy have previously yielded promising results in the differentiation between MCS and UWS and even in predicting the outcome of UWS patients (Manganotti et al., 2013; Jordan et al., 2013; Grosseries et al., 2011; Sara et al., 2011; Sitt et al., 2014; Golkowksi et al., 2017). Entropy describes the complexity of a signal. In EEG, entropy reflects the content of the processed information; the stronger the stimulation, the higher the information content in the EEG signal and, therefore, the higher the entropy. For example, entropy is lower during sedation (Jordan et al., 2013), and increased during stimulus processing (Thomeer et al., 1994) in comparison to a resting-state. Sara and colleagues found that patients with relatively low approximate entropy (ApEn) either remained in an unresponsive state, whereas patients with higher ApEn regained consciousness or made a full recovery (Sara & Pistoia, 2010; Sara et al., 2011).

Brain connectivity can be assessed with different analysis techniques. Coherence, weighted symbolic mutual information (wSMI) and symbolic transfer entropy (TE) represent three frequently used analysis techniques. Coherence describes the level of synchrony between two EEG signals collected at different locations on the scalp (Cavinato et al., 2015; Pereda, Quiroga, & Bhattacharya, 2005). Damages to subcortical structures, due to traumatic or non-traumatic events, can cause a decrease in connectivity between affected areas of the brain, which is suggested to be the cause of altered states of consciousness in DOC patients (Scheeringa et al., 2009; Stipacek, Grabner, Neuper, Fink, & Neubauer, 2003). Alterations in connectivity measured with EEG between certain brain areas, as found for example in patients with Alzheimer's disease or mild

cognitive impairment (Babiloni et al., 2015), may reflect dysfunctional neuroplasticity (Babiloni et al., 2015). When UWS patients were presented with different types of stimuli in comparison with a resting condition, they did not show an increase in fronto-parietal coherence as a response to the stimuli as observed in MCS patients and controls (Cavinato et al., 2015). The fronto-parietal network has two main functions: On the one hand it is responsible for self-awareness (the 'internal' network) and on the other hand for awareness of one's environment ('external') (Noirhomme et al., 2010). Lesions in areas belonging to this network are described as the underlying cause of DOC (Davey et al., 2000).

Connectivity can also be expressed with wSMI, which describes the amount of information that is shared across different brain areas (King et al., 2013), whereas TE is a means to quantify the amount of directed information flow. Transfer entropy between electrode A and B is the amount of uncertainty which is reduced for the signal at electrode A when past voltages at electrodes A and B are known. Jordan, Paprotny, Kochs and Schneider (2011) found that propofol induced loss of consciousness in healthy participants was closely related with a decline in frontoparietal information transfer.

EEG microstate analysis is a widely-used tool (Khanna et al., 2015); however microstate analysis has not commonly been used in DOC research so far. They represent short intervals of unique field topographies (Koenig et al., 2002), which last approximately 80-120 ms (Lehmann, Ozaki, & Pal, 1987). The most frequently found topographies are (Michel & Koenig, 2017):

- A right-frontal to left-posterior
- B left-frontal to right-posterior
- C frontal to occipital

- D mostly frontal and medial to slightly less occipital activity than class C

Each of these microstates has been suggested to represent an underlying neurological function or specific process (Lehmann et al., 1987). Several studies found that in resting state EEG, these microstates vary across behavioural states and neuropsychiatric disorders (see Khanna, Pascual-Leone, Michel, & Farzan, 2015, for a review). The transition between different microstates has been interpreted as a switch between the activation of different neural networks (Khanna et al., 2015). The duration and frequency of microstates can characterize different behavioural or mental states. Cantero, Atienza and Salas (1999) found that the number of microstates in one second is higher in states of drowsiness than during REM sleep or relaxed wakefulness, whereas the duration of a single microstate is longer in relaxed wakefulness than in drowsy periods and REM sleep.

3 Aim of this thesis

The clinical work with DOC patients revolves around two topics:

Classification: What is the patient's current state? Is the behaviourally assessed diagnosis correct?

Prediction: What is the prognosis?

Clinicians and researchers are developing new methods and adjusting established methods from other fields of brain and behavioural research to meet their needs in the endeavour to better understand DOC. This thesis addresses the questions above in three studies using a routine clinical method: EEG. In addition, this thesis considers another important question: How **reliable** is the method used for diagnosis?

Clinical experience suggests that patients with severe DOC caused by brain injury do not have constant performance levels but show strong variance in their behavioural abilities (Beckinschtein et al., 2009; Cruse et al., 2013). This could result in patients displaying an ERP at certain times but not at others. **Study I** of this thesis examines whether these performance fluctuations are captured by ERP amplitudes and/or latency data in DOC patients (Study I: Schorr et al. 2014). It was expected that variability in ERP data would be closely correlated with variability in CRS-R scores.

Connectivity between different brain areas has been shown to indicate a patient's level of consciousness (Jordan et al., 2013). **Study II** aimed at identifying EEG connectivity patterns between certain brain areas (i.e., coherence) and EEG power (EEG power spectra) that are on the one hand characteristic for either UWS or MCS, and on the other hand, predictive for the recovery of patients with DOC (Schorr et al., 2016).

Finally, **Study III** explored the differential predictive value of different EEG markers in the same resting state EEG dataset of DOC patients (Stefan et al., 2018). The aim was consciousness indexing and predicting clinical outcome after 12 months. Besides connectivity and power spectra, the study explored microstates and entropy, and tested an automated classification scheme for outcome prediction.

4 Summary of studies

4.1 Study I: Stability of auditory event-related potentials in coma research

(Schorr B, et al., 2014)

Based on clinical experience and on the results of previous studies, it has been shown that patients' performance levels can fluctuate strongly during a day (Bekinschtein, Golombek, Simonetta, Coleman, & Manes, 2009; Cruse et al., 2013) or between days. However, diagnostic tests are often done only once. A patient might not show the expected reaction, (e.g. an ERP) at this particular time, but may do so at another time point. Hence, we tested in this study the retest reliability of ERPs in response to tones in addition to the behavioural rating assessed with the CRS-R.

Twelve age-matched DOC patients (8 UWS, 4 MCS; 6 with traumatic, and 6 with non-traumatic brain injury) and twelve healthy controls were tested with an auditory oddball task four times: twice per day (morning vs. afternoon) over two days. In addition, the patients' state of consciousness was assessed by two independent raters with the CRS-R. The CRS-R was correlated with the following EEG parameters: occurrence of the P300, P300 amplitudes, and P300 latencies.

Retest-reliability for CRS-R scores was high (all Krippendorff's $\alpha \geq .83$) across all sessions, as well as for within-day (.94) and between-day (.83) comparisons. The same is true when looking at the subscales of the CRS-R (all $\alpha \geq .73$). Retest-reliability for the occurrence of the P300 was relatively low in the patients, varying between $\alpha = .425$ for morning vs. afternoon and $\alpha = .245$ for day one vs. day two in the DOC patients. Retest-reliability for amplitudes and latencies was moderate to strong in both groups (all $\alpha \geq .43$). No correlation between total CRS-R scores, sub-scale scores, days since incidence and amplitudes and latencies was found. The results of the ERP

data are in accordance with circadian fluctuations found in DOC patients (Bekinschtein et al., 2009). The auditory oddball task, as used in this study, is not necessarily suited as a proof of consciousness. However, the results suggest that, for diagnostic purposes, diagnostic ERP protocols should be applied which include multiple testing sessions of the patients.

4.2 Study II: Coherence in resting-state EEG as a predictor for the recovery from unresponsive wakefulness syndrome

(Schorr, Schlee, Arndt, & Bender, 2016)

The EEG has been established as a useful and easily measurable tool to assess levels of DOC at the patient's bed side. ERPs were shown to differentiate between levels of consciousness and might be able to predict the clinical recovery from DOC. However, as we showed in Study I, performance levels of DOC patients can fluctuate and ERPs should be assessed in multiple testing sessions. Therefore, Study II aimed to examine the differences in resting-state EEG parameters, especially coherence and power spectra, between UWS and MCS and also their predictive value for the recovery from UWS. Previous studies found that lesions to subcortical structures in frontal and parietal regions may be the cause of the unconscious state of UWS patients and reduced consciousness in MCS patients (Davey, Victor, & Schiff, 2000). These regions belong to the so-called global neuronal workspace (Dehaene & Naccache, 2001); a disconnection between parts of this network can cause DOC (Schiff et al., 2005).

Seventy-three patients and 24 controls were included in the study. 5-minute resting-state EEG data was collected, and patients' CRS-R scores were assessed. CRS-R scores of UWS patients were collected after 12 months and patients were divided into two groups (improved or unimproved) for

further analysis. Frontal, parietal, fronto-parietal, fronto-temporal, and fronto-occipital coherence was analysed and compared between the two groups, as well as power spectra in the respective brain areas.

Results showed that patients, who recovered from UWS, initially presented higher parietal coherence in delta and theta frequencies and higher fronto-parietal coherence in delta, theta, alpha and beta frequencies. Furthermore, besides parietal delta and theta coherence, a high fronto-parietal theta and alpha coherence was associated with an improvement from UWS to MCS.

Coherence, especially between frontal and parietal areas, was suggested to have a high diagnostic value, differentiating MCS from UWS patients (Cavinato et al., 2015). Study II showed that coherence, specifically between frontal and parietal brain areas also has a predictive value for recovery among DOC patients. It is important to note here that the results cannot predict individual courses of the disorder. Nevertheless, they will help clinicians and also patients' relatives to better understand a patient's condition and constitute a solid basis for future research.

4.3 Study III: Consciousness Indexing and Outcome Prediction with Resting-State EEG in Severe Disorders of Consciousness

(Stefan, S. et al., 2018)

As in Study II, resting-state data of UWS and MCS patients was analysed (n=62). Using several EEG markers on the same dataset, their ability to index (n=62) and also predict (n=39) consciousness levels was explored. EEG microstates, entropy, power spectrums and connectivity were analysed and a complex network analysis was done. Lastly, the possibility of an automated system was explored, using a Sequential Floating Forward Selection (SFFS) to obtain a subset of features best at predicting a patient's outcome. As in Study II, EEG markers, which are normally used simply to index consciousness, were used for prediction.

In summary, the parameters tested were better at predicting clinical outcome than at discriminating the classification of the level of consciousness. Possibly the behavioral-based initial classification may not be precise enough to actually capture the patients' state (van Erp et al., 2015). Connectivity measures, coherence, wSMI and TE, were generally higher for patients in UWS who evolved to a minimally conscious state, which is in line with Study II. However, connectivity did not significantly differentiate between MCS and UWS patients, implying that connectivity is better at predicting outcome than indexing the level of consciousness. The clustering coefficient resulting from thresholding beta coherence successfully predicted outcome. Entropy was higher in improved UWS and MCS patients compared to UWS patients (as in Thul et al., 2016; Gosseries et al., 2011), who remained in an unconscious state, which suggests that these patients show a higher complexity of active neural networks. With respect to EEG power, as shown before in other studies (e.g. Lehembre et al., 2012), power in the alpha band was a greater in MCS than UWS patients, and power in the delta band was greater for UWS patients vs. MCS patients and in UWS patients who remained unresponsive. Microstate analysis revealed a high classification power (MCS vs. UWS) in relation to the amount of time spent in microstate D in the alpha frequency. Finally, the SFFS yielded "frequency of microstate A" in the 2-20 Hz frequency band, "path length" and "average path length" obtained by thresholding alpha coherence as having the greatest predictive power.

5 Discussion

5.1 The contribution of Studies I-III to the diagnostics of Disorders of Consciousness

Patients in an altered state of consciousness show consistent behaviour over time, as was suggested by the strong retest-reliability of the CRS-R scores found across different testing sessions in **Study I**, but are, at the same time, subject to variability in their performance to process external stimuli, here represented by the low retest-reliability in ERP markers. This variability may be due to fluctuations in circadian rhythms, as suggested by Bekinschtein (2009), and a general fluctuation of the patients' performance levels throughout a day or between days, caused by instabilities in their physical state. In contrast to previous studies, which only looked at intermediate time ranges (e.g. 1 month), **Study I** showed that these fluctuations of ERPs occur in rather short time intervals, even within several hours. The results suggest that, in order to avoid misdiagnoses, diagnostic tests using ERPs should be performed at multiple time points, and at short intervals, e.g. 1 to 2 days apart. The fact that the absence of an ERP may be mistaken as a sign of unawareness of the patient, and the variability of ERP findings depending on the daily or current state of condition in **Study I,** led us to move on to quantitative EEG parameters to index consciousness and to approach the question of prognosis in DOC patients.

Consciousness is argued to result from communication between two networks that work in synchrony, also called the global neuronal workspace (Dehaene & Naccache, 2001): the frontal (executive control) and retrolandic (cognitive) network (Leon-Carrion et al., 2012). In MCS patients, the synchrony between these networks was severely disrupted compared to patients with preserved alertness (Leon-Carrion et al., 2012). In **Study II**, coherence within and between frontal

and parietal regions in MCS and UWS patients were compared, and also between those patients who recovered from the UWS state and those who remained in the state of unresponsiveness for one year. **Study II** was the first to provide evidence that high parietal delta and theta, and high fronto-parietal theta and alpha coherence represents a marker for the recovery from UWS with high predictive sensitivity and specificity. The improved patients already showed early signs of a partly preserved connectivity in the regions belonging to the global neuronal workspace, before the patients even presented with behavioural signs of minimal consciousness.

Finally, in **Study III**, multiple quantitative EEG markers (EEG microstates, entropy, power spectrums, and connectivity) were compared with regard to their ability to categorize different consciousness levels and predict clinical recovery. Although already established as standard methods in EEG research, techniques such as microstate analysis are not commonly used in DOC patients to assess levels of consciousness. As in **Study III**, ApEn and permutation entropy already differentiated successfully between MCS and UWS in previous studies (Thul et al., 2016; Gosseries et al., 2011), as well as delta and alpha power, as was also shown by Lehembre et al. (2012). Moreover, ApEn and permutation entropy successfully predicted the recovery from UWS, which is in line with previous findings (Sara & Pistoia, 2010, Sara et al., 2011). Finally, EEG microstate presented as an important marker for the differentiation between levels of consciousness and also for the recovery of consciousness after 12 months.

5.2 Performance levels and retest-reliability in EEG

Data on the retest-reliability of EEG assessments consists mostly of studies investigating younger populations and only few with samples taken from older participants (for an overview see Walhovd, & Fjell, 2002) with none addressing the issue of varying performance levels in DOC patients. It is well-known that DOC patients do show fluctuations in their performance levels over time (Beckinschtein et al., 2009; Cruse et al., 2013). Studies by Cassidy, Robertson and O'Connell (2012) and Walhovd and Fjell (2002) investigated retest-reliability of ERPs in healthy participants, considering rather long time periods ranging from one month to one year. Cassidy et al. (2012) tested a battery of typical ERP paradigms eliciting a wide range of components (e.g. P1, N1, P300 etc.) on two different occasions, one month apart. They found strong test-retest-reliability of amplitudes for all paradigms, but only weak to moderate reliability for greater latencies (e.g. P300, P400), and components elicited by oddball tasks showed a change in magnitude across sessions. Walhovd and Fjell (2002) reported similar results. As for **Study I,** moderate to strong reliability for amplitudes and latencies was observed in both groups. However, the most important finding was that only one UWS patient showed a P300 component in all four sessions, while in the remaining patient sample the rate of occurrence varied between one and three times. Especially interesting was the observation that ERPs fluctuated across time-points but the behaviour observed with the CRS-R remained relatively stable.

ERPs are used for classification and even communication with DOC patients (Donchin et al., 1986; Risetti et al., 2013; Lulé et al., 2013). **Study I** showed that ERPs underlie strong short-term fluctuations. Only one patient actually showed variance in their P300 activity from one day to the next, together with a change in the CRS-R scores, with a P300 present. When the CRS-R score indicated MCS, also a P300 was detected. This case shows how important it is to be aware of the

variability of performance levels of the patients when testing them, and that it can be useful to rely on more than one assessment. Even though the P300 component is not established as a marker for the presence of consciousness, it is a marker for intact stimulus processing. The retest-reliability of active paradigms, e.g. where the patient is asked to follow commands, should be explored, since they have been shown to be useful in revealing traces of consciousness (Schnakers et al., 2009).

The results of **Study I** should be considered when using EEG in the clinical routine with DOC patients, especially when addressing the sensitive subject of consciousness indexing and prognosis, which can be particularly challenging and distressing for clinicians and relatives alike. Retest-reliability has yet to be tested for quantitative EEG features where no external stimuli are involved, but multiple testing sessions over a short period of time, i.e. within one week, can be effective when using EEG for diagnostic purposes in DOC.

5.3 What is the patient's current state? Is the behaviourally assessed diagnosis correct? Classification power of resting-state EEG analysis

The correct classification of the consciousness level is error-prone, as discussed above. When the neurological basis has been clinically assessed as precisely as possible, e.g. through computer tomography, the next step is usually the assessment of the patient's behaviour. As described in **Study I** and earlier in this synopsis, the CRS-R is a rather robust measure with high retest-reliability. Cortese et al. (2015), however, showed that scores vary between morning and afternoon assessments, leading to the question of whether treatment plans should be structured according to the patient's circadian rhythm. And although, as stated by Wade (2018), misdiagnoses are rare, they do occur and are disastrous for the individual. Cases continue to emerge of patients who were diagnosed as UWS but were found to be aware and could follow commands during fMRI and EEG assessments (Monti et al., 2010; Owen et al., 2006; Cruse et al., 2012). An overview of the most

important findings in fMRI and PET research in the area of DOC is provided in section 2.2, above. However, FDG-PET and fMRI are not available to a wide spectrum of clinicians and patients due to physical, technical and financial limitations. Various EEG parameters have been explored to overcome these restrictions. Results of **Study III** are in line with previous findings with entropy, ApEn and permutation entropy, both discriminating successfully between MCS and UWS. Higher entropy is commonly found for MCS patients in comparison to UWS patients (Thul et al., 2016; Gosseries et al., 2011). As entropy reflects the complexity of an EEG signal in response to stimulation, higher entropy in MCS patients, in comparison to UWS patients may reflect their preserved ability to consciously process incoming information.

Delta (MCS<UWS) and alpha (MCS>UWS) power also successfully distinguish between UWS and MCS (Lehembre et al., 2012). **Study II** showed lower alpha and beta power and higher delta power in DOC patients (both UWS and MCS) than healthy controls. Alpha activity is suggested to be the most basic form of information transmission (Klimesch, 1999), whereas beta activity reflects a great variety of different functions (working memory, object recognition, and also perception (Tallon-Baudry, Bertrand, & Fischer, 2010; Donner et al., 2007)). High delta power, highest here in the UWS patients, has also previously been associated with a high level of unresponsiveness (Bagnato et al., 2015). **Study II** confirmed that a reduction of alpha and beta power and an increase in delta power is characteristic for reduced levels of consciousness.

As described earlier, microstates are short-lasting stable states of specific brain topographies (Lehmann et al., 1987). **Study III** found microstates to be the best marker in the differentiation between MCS and UWS, with the percentage of time spent in microstate D as the key difference. Britz et al. (2010) used simultaneous EEG-fMRI to attribute EEG microstates to distinct neuronal networks found in the fMRI assessment, with which they correlated best: auditory network

(microstate A), visual network (microstate B), saliency network (microstate C), attention network (microstate D). Patients in the investigated population in **Study III** spent more (UWS) or less (MCS) time in the microstate D. One possible interpretation could be that the attention network in MCS patients is more activated. But seeing how multiple resting-state networks, identified with fMRI, may overlap, the interpretation of microstates remains difficult (Michel & Koenig, 2017). For example, Yuan, Zotev, Phillips, Drevets and Bodurka (2012) identified 13 microstates and 10 resting-state networks. Nevertheless, our results are in line with a study by Comsa, Bekinschtein and Chennu (2017), who let healthy participants perform an active task during which they were allowed to become drowsy and unresponsive. In this state, the duration of microstate D significantly increased. An increased duration was associated with an increased state of unresponsiveness (Comsa et al., 2017). To conclude, the results presented above add to the existing findings on the use of resting-state EEG analysis in the classification of DOC, and moreover suggest that microstate analysis is an important tool for judging the level of consciousness and predicting recovery from UWS.

5.4 What is the prognosis for the patient? Predictive power of EEG resting-state analysis

A variety of studies addressed this topic using a wide range of methods, CRS-R, fMRI, FDG-PET, and EEG. CRS-R scores have been proven to be a good predictor of a positive clinical course. Only recently, Portaccio et al. (2018) found, in a large cohort study of 137 patients, that higher scores at admission predicted improved responsiveness after 3-7 months. FDG-PET, and fMRI have also performed well at predicting outcome (Silva et al., 2015; Stender et al., 2014; Wang et al., 2015) as described in section 2.2 above.

The studies presented in this thesis focus on resting-state EEG analysis for prognosis of the clinical course. As shown in **Studies II** and **III**, connectivity can be used to predict the recovery of consciousness in UWS patients on a group level. Both studies showed that coherence is generally higher in patients who later improved in their level of consciousness. Previous studies had shown that coherence has a high diagnostic value for DOC patients (Cavinato et al., 2015), and that activity in the fronto-parietal network is impaired in UWS patients (Laureys, 2005). Lesions in the regions belonging to this network are argued to be the reason for altered states of consciousness in DOC patients (Davey et al., 2000). Chennu and colleagues (2017) found, in line with the findings of **Study II**, that connectivity hubs located in frontal and parietal areas are useful predictors of recovery. The high sensitivity and specificity of the coherence in parietal delta and theta, and fronto-parietal theta and alpha in **Study II** was indicative of their value as prognostic markers for a positive clinical course.

Study III also confirmed that ApEn and permutation entropy, in addition to their previously mentioned capacity to differentiate between UWS and MCS, successfully predict outcome. Previous studies found that relatively high ApEn in UWS was a predictor for a recovery (Sara & Pistoia, 2010, Sara et al., 2011). The increased entropy in patients who later recovered reflected intact neural networks, already at an early stage, when consciousness did not yet manifest itself in observable behaviour. The delta power was significantly smaller in patients who recovered consciousness, which is in line with studies by Bagnato et al. (2015), and Golkowksi et al. (2017) who could also associate smaller delta power with a positive outcome.

In **Study III**, microstate analysis proved to be very successful in the classification of levels of consciousness, and was particularly effective in predicting outcome. In particular, microstate A was in many aspects successful at predicting recovery. If we take into account the categorization

of Britz et al. (2010) and argue that microstate A is associated with the auditory network, one possible interpretation could be that patients with an intact auditory network are more likely to recover from an unresponsive state. In our cohort, it would thus be interesting to correlate this result with the auditory sub-scale of the CRS-R. As mentioned earlier, the attribution of specific underlying networks to the topographies of different microstates is difficult. Nevertheless, most studies connecting microstates to resting-state networks in essence argue that abnormalities in these networks manifest themselves as alterations in the syntax of the microstates, e.g. frequency and duration (Khanna et al., 2015).

The most noteworthy finding from **Study III** may be the fact that microstates, together with characteristic path lengths and average clustering coefficients obtained from thresholding alpha coherence, could be used for an automated outcome prediction in our cohort. No study did find a combination of EEG markers to have a similar strong predictive value, with an Area under the curve of 92 ± 4%, so far. Sitt et al. (2014) did aim to automatically classify patients as UWS or MCS based on different EEG markers, and 67% of UWS patients and 76% of MCS patients were indeed classified in the correct group; however they could not predict with certainty the regaining of signs of consciousness in their cohort.

5.5. Limitations

Working with DOC patients presents a number of obstacles to establishing diagnostic methods which yield reliable results. The common goal of all these studies is finding markers which can be applied easily to individual cases. Each patient's medical history is unique and the events preceding the DOC differ widely. While **Study II** took this into account to some degree, even computer tomography data may not show the complete extent of the injuries and hence a classification of

patients into, for example, TBI, subarachnoid hemorrhage (SBH) or anoxia neglects small differences. Almost all of the studies discussed in this thesis, including **Studies I-III**, were based on group comparisons of patients, who presented with a wide variety of lesions. Taking a closer look at the subgroups would be desirable. Depending on the location of the underlying lesion, certain EEG markers are more useful than others in the classification or prediction of consciousness.

The relative instability of the P300 in both patient and control groups in **Study I** may have been influenced by the paradigm itself. It is well established that the frequency of the target stimulus and the total number of trials is crucial (Fischer et al., 2010); the rarer the target, the higher the P300 amplitude and the more robust the occurrence of a P300 (Duncan-Johnson & Donchin, 1977). A trade-off exists between having a sufficient number of trials to obtain robust results, but at the same time the EEG-recording session should not exceed the patient's capacity. One idea could be to use a novelty P300 paradigm, in which three different types of, e.g., tones, are presented: an infrequent novel tone among target tones and distractors, which increases the chance of a P300 occurring. Morlet and Fischer (2014) suggest inserting at least 50 "novels" for an adequate signal-to-noise ratio. This paradigm can be combined with a more emotional stimulus like the patient's own name as a novel stimulus (Morlet & Fischer, 2014).

5.6 Conclusion & outlook

No doubt, the methods presented in this work are not as yet suitable for individual outcome prediction. Nonetheless, the thesis points towards potential EEG analysis techniques suitable for use on individual datasets. As **Study I** proposes, retest-reliability has to be considered when applying EEG analysis to patient data as a diagnostic tool and its applicability should be investigated not only for ERPs, but also for other analysis techniques. This is especially important

given that automated analysis schemes are currently being developed (Sitt et al., 2014; **Study III**). The clinical routine uses EEG on a daily basis and automated analysis techniques are attractive to maximize the information output of a single recording, with little effort needed on the part of the data analyst.

All methods used on resting-state EEG presented in this work can also be applied to active EEG measures of varying complexity, such as ERPs, as used in **Study I**, or event-related desynchronization, e.g. motor imagery (Cruse et al., 2006). To conclude, this thesis demonstrates that: (a) the appearance of ERPs underlies strong fluctuations which is represented by the rather low retest-reliability; a missing ERP could be misinterpreted as unconsciousness of the patient. This may be avoided by repeated assessments over a short period of time; furthermore, (b) coherence, power analysis, entropy, microstates and complex network analysis are all valuable markers in predicting recovery from an unresponsive state, and (c) an automatic classification scheme may be used to predict patient outcomes. Most notably, depending on the research question (classification vs. prognosis), different EEG parameters proved useful. This leads to the conclusion that detectable consciousness and the ability to regain consciousness are not necessarily linked, and that multiple techniques, such as active paradigms combined with quantitative EEG analyses, should be considered when assessing a patient. Measuring basic stimulus processing with an oddball task (e.g. **Study I**), in combination with a connectivity and microstate analysis to establish intact neural networks (**Studies II** & **III**), could provide a foundation for the prognosis of recovery of brain functionality and with it, consciousness, in a DOC patient.

EEG is already an established, cost effective and easy-to-use tool in everyday clinical practice. The analysis methods examined in this thesis, including automatic classification, e.g. with SFFS as applied in **Study III**, are simple to implement. Future research in this area should focus on

establishing methods that can be used for diagnosis and prognosis in individual patients to monitor a patient's progress early on in the rehabilitation process, and to assess how a patient responds to a certain treatment and therapy plan.

6 References

Adams, J.H., Graham, D.I., & Jennett, B. (2000). The neuropathology of the vegetative state after an acute brain insult. *Brain, 123*, 1327–1338.

Andrews, K., Murphy, L., Munday, R., & Littlewood, C. (1996). Misdiagnosis of the vegetative state: retrospective study in a rehabilitation unit. *British Medical Journal*, *313*, 13-16.

Babiloni, C., Lizio, R., Marzano, N., Capotosto, P., Soricelli, A., Triggiani, A.I., Cordone, S., Gesualdo, L., Del Percio, C. (2015). Brain neural synchronization and functional coupling in Alzheimer's disease as revealed by resting state EEG rhythms. *International journal of psychophysiology,* doi:10.1016/j.ijpsycho.2015.02.008

Bagnato, S., Boccagni, C., Sant'Angelo, A., Prestandrea, C., Mazzilli, R., & Galardi, G. (2015). EEG predictors of outcome in patients with disorders of consciousness admitted for intensive rehabilitation. *Clinical Neurophysiology, 126* (5), 959-966. doi:DOI 10.1016/j.clinph.2014.08.005

Bekinschtein, T.A., Golombek, D.A., Simonetta, S.H., Coleman, M.R., & Manes, F.F. (2009). Circadian rhythms in the vegetative state. *Brain Injury, 23* (11), 915-919. doi:10.1080/02699050903283197

Bekinschtein, T.A., Manes, F.F., Villarreal, M., Owen, A.M., & Della-Maggiore, V. (2011). Functional imaging reveals movement preparatory activity in the vegetative state. *Frontiers in human neuroscience, 5*, 5. doi:10.3389/fnhum.2011.00005

Bender, A., Jox, R.J., Grill, E., Straube, A., & Lulé, D. (2015). Persistent vegetative state and minimally conscious state: a systematic review and meta-analysis of diagnostic procedures. *Deutsches Ärzteblatt International, 112* (14), 235-242. doi:10.3238/arztebl.2015.0235

Bruno, M. A., Vanhaudenhuyse, A., Thibaut, A., Moonen, G. & Laureys, S. (2011). From unresponsive wakefulness to minimally conscious PLUS and functional locked-in syndromes: recent advances in our understanding of disorders of consciousness. *Journal of Head Trauma Rehabilitation*, *258*(7), 1373-1384.

Britz, J., Van De Ville, D., Michel, C.M. (2010). BOLD correlates of EEG topography reveal rapid resting-state network dynamics. *NeuroImage, 52*, 1162-1170.

Boly, M., Phillips, C., Balteau, E., Schnakers, C., Degueldre, C., Moonen, G., Luxen, A., Peigneux, P., Faymonville, M.E., Maquet, P., Laureys, S. (2008). Consciousness and cerebral baseline activity fluctuations. *Human brain mapping, 29* (7), 868-874. doi:10.1002/hbm.20602

Cantero, J.L., Atienza, M., & Salas, R.M. (2002). Human alpha oscillations in wakefulness, drowsiness period, and REM sleep: different electroencephalographic phenomena within the alpha band. *Clinical Neurophysiology, 32*(1), 54-71.

Cassidy, S.M., Robertson, I.H., & O'Connell, R.G. (2012). Retest reliability of event-related potentials: Evidence from a variety of paradigms. *Psychophysiology, 49* (5), 659-664. doi:DOI 10.1111/j.1469-8986.2011.01349.x

Cavinato, M., Volpato, C., Silvoni, S., Sacchetto, M., Merico, A., & Piccione, F. (2011). Event-related brain potential modulation in patients with severe brain damage. *Clinical Neurophysiology, 122* (4), 719-724. doi:DOI 10.1016/j.clinph.2010.08.024

Cavinato, M., Genna, C., Manganotti, P., Formaggio, E., Storti, S.F., Campostrini, S., Arcaro, C., Casanova, E., Petrone, V., Piperno, R., Piccione, F. (2015). Coherence and Consciousness:

Study of Fronto-Parietal Gamma Synchrony in Patients with Disorders of Consciousness. *Brain Topography, 28* (4), 570-579. doi:DOI 10.1007/s10548-014-0383-5

Chennu, S., Annen, J., Wannez, S., Thibaut, A., Chatelle, C., Cassol, H., Martens, G., Schnakers, C., Gosseries, O., Menon, D., Laureys, S. (2017). Brain networks predict metabolism, diagnosis and prognosis at the bedside in disorders of consciousness. *Brain, 140*(8), 2120–2132.

Comsa, J.M., Bekinschtein, T.A., & Chennu, S. (2017). Transient topographical dynamics of the electroencephalogram predict brain connectivity and behavioural responsiveness during drowsiness. *bioRxiv*, doi: https://doi.org/10.1101/231464

Cortese, M.D., Riganello, F., Arcuri, F., Pugliese, M.E., Lucca, L.F., & Sannita, W.G. (2015). Coma Recovery Scale R: variability in the disorder of consciousness. *BMC Neurology, 15*, 186.

Cruse, D., Chennu, S., Fernandez-Espejo, D., Payne, W.L., Young, G.B., & Owen, A.M. (2012). Detecting awareness in the vegetative state: electroencephalographic evidence for attempted movements to command. *PLoS One, 7*(11), e49933.

Cruse, D., Thibaut, A., Demertzi, A., Nantes, J.C., Bruno, M.A., Gosseries, O., Vanhaudenhuyse, A., Bekinschtein, T.A., Owen, A.M., Laureys, S. (2013). Actigraphy assessments of circadian sleep-wake cycles in the Vegetative and Minimally Conscious States. *BMC Medicine*, *11,* 18. doi:10.1186/1741-7015-11-18

Davey, M.P., Victor, J.D., & Schiff, N.D. (2000). Power spectra and coherence in the EEG of a vegetative patient with severe asymmetric brain damage. *Clinical Neurophysiology, 111* (11), 1949-1954. doi:Doi 10.1016/S1388-2457(00)00435-1

Dehaene, S., & Naccache, L. (2001). Towards a cognitive neuroscience of consciousness: Basic evidence and a workspace framework. *Cognition, 79*, 1–37.

Demertzi, A., Gomez, F., Crone, J.S., Vanhaudenhuyse, A., Tshibanda, L., Noirhomme, Q., Thonnard, M., Charland-Verville, V., Kirsch, M., Laureys, S., Soddu, A. (2014). Multiple fMRI system-level baseline connectivity is disrupted in patients with consciousness alterations. *Cortex, 52*, 35–46.

Demertzi, A., Antonopoulos, G., Heine, L., Voss, H.U., Crone, J.S., de Los Angeles, C., Bahri, M.A., Di Perri, C., Vanhaudenhuyse, A., Charland-Verville, V., Kronbichler, M., Trinka, E., Phillips, C., Gomez, F., Tshibanda, L., Soddu, A., Schiff, N.D., Whitfield-Gabrieli, S., Laureys, S. (2015). Intrinsic functional connectivity differentiates minimally conscious from unresponsive patients. *Brain, 138*, 2619–2631.

DeVolder, A.G., Goffinet, A.M., Bol, A., Michel, C., de Barsy, T., & Laterre, C. (1990). Brain glucose metabolism in postanoxic syndrome. Positron emission tomographic study. *Archives of Neurology, 47*,197–204.

Donchin, E., Karis, D., Bashore, T.R., Coles, M.G.H., & Gratton, G.(1986). Cognitivepsychophysiology and human information processing. In: Coles, M.G.H., Donchin, E., Porges, S.W.(eds), *Psychophysiology: Systems, Processes, and Applications* (pp 244-267). Guildford, New York.

Donner, T.H., Siegel, M., Oostenveld, R., Fries, P., Bauer, M., & Engel, A.K. (2007). Population activity in the human dorsal pathway predicts the accuracy of visual motion detection. *Journal of neurophysiology, 98*(1), 345-359. doi:10.1152/jn.01141.2006

Duncan-Johnson CC, Donchin E (1977) On quantifying surprise: the variation of event-related potentials with subjective probability. *Psychophysiology, 14* (5), 456-467.

Faymonville, M. E., Pantke, K. H., Berré, J., Sadzot, B., Ferring, M., De Tiege, X., Mavroudakis, N., van Bogaert, P., Lambermont, B., Damas, P., Franck, G., Lamy, M., Luxen, A., Moonen,

G., Maquet, P., Laureys, S. (2004). Zerebrale Funktionen bei hirngeschädigten Patienten. *Der Anaesthesist*, *53*(12), 1195-1202.

Fischer, C., Morlet, D., & Giard, M. (2000). Mismatch negativity and N100 in comatose patients. *Audiology and Neurotology, 5* (3-4),192-197. doi:13880

Fischer, C., Luauté, J., Nemoz, C., Morlet, D., Kirkorian, G., & Mauguiere, F. (2006). Improved prediction of awakening or nonawakening from severe anoxic coma using tree-based classification analysis. *Critical care medicine., 34* (5),1520-1524. doi:Doi 10.1097/01.Ccm.0000215823.36344.99

Fischer, C., Luauté, J., & Morlet, D. (2010). Event-related potentials (MMN and novelty P3) in permanent vegetative or minimally conscious states. *Clinical neurophysiology : official journal of the International Federation of Clinical Neurophysiology*, *121*(7), 1032-1042. doi:10.1016/j.clinph.2010.02.005

Giacino, J. T., Kezmarsky, M. A., DeLuca, J. & Cicerone, K. D. (1991). Monitoring rate of recovery to predict outcome in minimally responsive patients. *Archives of Physical Medicine and Rehabilitation, 72*(11), 897-901.

Giacino, J. T., & Kalmar, K. (1997). The vegetative and minimally conscious states: a comparison of clinical features and functional outcome. *The Journal of Head Trauma Rehabilitation, 12*(4), 36-51.

Giacino, J. T., Ashwal, S., Childs, N., Cranford, R., Jennett, B., Katz, D. I., Kelly J. P., Rosenberg, J. H., Whyte J., Zafonte R. D., Zalser, N. D. (2002). The minimally conscious state: Definition and diagnostic criteria. *Neurology, 58*, 349-353.

Giacino, J.T., Kalmar, K., & Whyte, J. (2004). The JFK Coma Recovery Scale-Revised: measurement characteristics and diagnostic utility. *Archives of physical medicine and rehabilitation, 85* (12), 2020-2029.

Gill, M. R., Reiley, D. G. & Green, S. M. (2004). Interrater reliability of Glasgow Coma Scale scores in the emergency department. *Annals of Emergency Medicine*, *43*(2), 215-223.

Golkowski, D., Merz, K., Mlynarcik, C., Kiel, T., Schorr, B., Lopez-Rolon, A., Lukas, M., Jordan, D., Bender, A., Ilg, R. (2017). Simultaneous EEG-PET-fMRI measurements in disorders of consciousness: an exploratory study on diagnosis and prognosis. *Journal of Neurology, 264*(9), 1986-1995. doi: 10.1007/s00415-017-8591-z

Grosseries, O., Schnakers, C., Ledoux, D. , Vanhaudenhuyse, A., Bruno, M.A., Demertzi, A., Noirhomme, Q., Lehembre, R., Damas, P., Goldman, S., Peeters, E., Moonen, G., Laureys, S. (2011). Automated EEG entropy measurements in coma, vegetative state/unresponsive wakefulness syndrome and minimally conscious state. *Functional Neurology, 26*(1):25–30.

Guldenmund, P., Stender, J., Heine, L., & Laureys, S.(2012). Mindsight: diagnostics in disorders of consciousness. *Critical care research and practice, 2012*, 624724. doi:10.1155/2012/624724

Jennett, B. (2002). The vegetative state. Journal of Neurology. *Neurosurgery & Psychiatry*, *73*(4), 355-357.

Johnson, R., Jr. (1986). A triarchic model of P300 amplitude. *Psychophysiology, 23*(4), 367-384.

Jordan, D., Paprotny, S., Kochs, E. F., & Schneider, G. (2011). Symbolic transfer entropy indicates changes of cortical flow of information between consciousness and propofol-induced unconsciousness: 7AP1-4. *European Journal of Anaesthesiology (EJA), 28*, 97.

Jordan, D., Ilg, R., Riedl, V., Schorer, A., Grimberg, S., Neufang, S., Omerovic, A., Berger, S., Untergehrer, G., Preibisch, C., Schulz, E., Schuster, T., Schroter, M., Spoormaker, V., Zimmer, C., Hemmer, B., Wohlschlager, A., Kochs, EF., Schneider, G. (2013). Simultaneous electroencephalographic and functional magnetic resonance imaging indicate impaired

cortical top-down processing in association with anesthetic-induced unconsciousness. *Anesthesiology, 119* (5), 1031-1042. doi:10.1097/ALN.0b013e3182a7ca92

Khanna, A., Pascual-Leone, A., Michel, C.M., & Farzan, F. (2015). Microstates in resting-state EEG: current status and future directions. *Neuroscience & Biobehavioural Reviews, 49*, 105-13. doi: 10.1016/j.neubiorev.2014.12.010

King, J.R., Sitt, J.D., Faugeras, F., Rohaut, B., El Karoui, I., Cohen, L., Naccache, L., Dehaene, S. (2013). Information sharing in the brain indexes consciousness in noncommunicative patients. *Current Biology*. *23*(19), 1914-9. doi: 10.1016/j.cub.2013.07.075

Klimesch, W. (1999). EEG alpha and theta oscillations reflect cognitive and memory performance: a review and analysis. *Brain research reviews, 29*(2-3), 169-195. doi:Doi 10.1016/S0165-0173(98)00056-3

Koenig, T., Prichep, L., Lehmann, D., Valdes Sosa, P., Braeker, E., Kleinlogel, H., Isenhart, R., Roy John, E. (2002). Millisecond by Millisecond, Year by Year: Normative EEG Microstates and Developmental Stages. *NeuroImage, 16*, 41–48. doi:10.1006/nimg.2002.1070

Kotchoubey, B. (2005). Event-related potential measures of consciousness: two equations with three unknowns. *Progress in brain research, 150*, 427-444. doi:Doi 10.1016/S0079-6123(05)50030-X

Laureys, S. (2005). The neural correlate of (un)awareness: lessons from the vegetative state. *Trends in Cognitive Sciences*, *9* (12), 556-559. doi:10.1016/j.tics.2005.10.010

Laureys, S., Perrin, F. & Brédart, S. (2007). Self-consciousness in non-communicative patients. *Consciousness and Cognition*, *16*(3), 722-741.

Laureys, S., Celesia, G.G., Cohadon, F., Lavrijsen, J., Leon-Carrion, J., Sannita, W.G., Sazbon, L., Schmutzhard, E., von Wild, K.R., Zeman, A., Dolce, G., European Task Force on Disorders

of Consciousness, (2010). Unresponsive wakefulness syndrome: a new name for the vegetative state or apallic syndrome. *BMC medicine*, *8*(68). doi:10.1186/1741-7015-8-68

Lehembre, R., Grosseries, O., Lugo, Z., Jedidi, Z., Chatelle, C., Sadzot, B., Laureys, S., Noirhomme, Q. (2012). Electrophysiological investigations of brain function in coma, vegetative and minimally conscious patients. *Archives Italiennes de Biologie, 150*(2-3), 122-39. doi: 10.4449/aib.v150i2.1374.

Lehembre, R., Marie-Aurlie, B., Vanhaudenhuyse, A. , Chatelle, C., Cologan, V., Leclercq, Y., Soddu, A., Macq, B., Laureys, S., Noirhomme, Q. (2012). Restingstate EEG study of comatose patients: a connectivity and frequency analysis to find differences between vegetative and minimally conscious states. *Functional Neurology, 27*(1), 41–47.

Lehmann, D., Ozaki, H., & Pal, I. (1987). EEG alpha map series: brain microstates by space-oriented adaptive segmentation. *Electroencephalography and Clinical Neurophysiology, 67*, 271–288.

Leon-Carrion, J., Leon-Dominguez, U., Pollonini, L., Wu, M.H., Frye, R.E., Dominguez-Morales, M.R., & Zouridakis, G. (2012). Synchronization between the anterior and posterior cortex determines consciousness level in patients with traumatic brain injury (TBI). *Brain research, 1476*, 22-30. doi:10.1016/j.brainres.2012.03.055

Lesko, M. M., Jenks, T., O'Brien, S. J., Childs, C., Bouamra, O., Woodford, M., & Lecky, F. (2013). Comparing Model Performance for Survival Prediction Using Total Glasgow Coma Scale and Its Components in Traumatic Brain Injury. *Journal of Neurotrauma*, *30*(1), 17-22.

Lücking, C. H. & Wallesch, C. W. (1992). Phänomenologie und Klinik der Bewusstseinsstörungen. In H. C. Hopf, K. Poeck & H. Schliack, (Hrsg.), *Neurologie in Praxis und Klinik Band 1* (2. überarbeitete Auflage, o. S.). Stuttgart: Georg Thieme Verlag

Lulé, D., Noirhomme, Q., Kleih, S.C., Chatelle, C., Halder, S., Demertzi, A., Bruno, M.A., Gosseries, O., Vanhaudenhuyse, A., Schnakers, C., Thonnard, M., Soddu, A., Kübler, A., Laureys, S. (2013). Probing command following in patients with disorders of consciousness using a brain-computer interface. *Clinical neurophysiology, 124* (1), 101-106.

Manganotti, P., Formaggio, E., Storti, S.F., Fiaschi, A., Battistin, L., Tonin, P., Piccione, F., Cavinato, M. (2013). Effect of high-frequency repetitive transcranial magnetic stimulation on brain excitability in severely brain-injured patients in minimally conscious or vegetative state. *Brain stimulation, 6*(6), 913-921. doi:10.1016/j.brs.2013.06.006

Michel, C.M., & Koenig, T. (2017). EEG microstates as a tool for studying the temporal dynamics of whole-brain neuronal networks: A review. *NeuroImage*, pii: S1053-8119(17)31008-X. doi: 10.1016/j.neuroimage.2017.11.062.

Monti, M.M., Vanhaudenhuyse, A., Coleman, M.R., Boly, M., Pickard, J.D., Tshibanda, L., Owen, A.M., Laureys, S. (2010). Willful modulation of brain activity in disorders of consciousness. *The New England Journal of Medicine, 362*, 579–589.

Morlet, D., & Fischer, C. (2014). MMN and Novelty P3 in Coma and Other Altered States of Consciousness: A Review. *Brain Topography, 27*(4), 467-479. doi: 10.1007/s10548-013-0335-5

Newcombe, V.F.J., Williams, G.B., Scoffings, D., Cross, J., Carpenter, T.A., Pickard, J.D., & Menon, D.K. (2010). Aetiological differences in neuroanatomy of the vegetative state: insights from diffusion tensor imaging and functional implications. *Journal of Neurology, Neurosurgery, and Psychiatry, 81*, 552–561.

Noirhomme, Q., Soddu, A., Lehembre, R., Vanhaudenhuyse, A., Boveroux, P., Boly, M., & Laureys, S. (2010). Brain connectivity in pathological and pharmacological coma. Frontiers in systems neuroscience, 4, 160. doi:10.3389/fnsys.2010.00160

O'Dell, M. W., Jasin, P., Stivers, M., Lyons, N., Schmidt, S., & Moore, D. E. (1996). Interrater reliability of the coma recovery scale. *The Journal of Head Trauma Rehabilitation*, *11*(3), 61-66.

Oder, W., & Wurzer, W. (2011). Das Schädel-Hirn-Trauma. In Lehrner, J., Pusswald, G., Fertl, E., Strubreither, W., & Kryspin-Exner, I. (Hrsg.), *Klinische Neuropsychologie: Grundlagen–Diagnostik–Rehabilitation.* 2. Auflage. (pp. 309-327). Berlin: Springer.

Owen, A.M., Coleman, M.R., Boly, M., Davis, M.H., Laureys, S., & Pickard, J.D. (2006). Detecting awareness in the vegetative state. *Science, 313*, 1402.

Pereda, E., Quiroga, R.Q., & Bhattacharya, J. (2005). Nonlinear multivariate analysis of neurophysiological signals. *Progress in Neurobiology, 77* (1-2), 1-37. doi:DOI 10.1016/j.pneurobio.2005.10.003

Perrin, F., Castro, M., Tillmann, B., & Luauté, J. (2015). Promoting the use of personally relevant stimuli for investigating patients with disorders of consciousness. *Frontiers in Psychology*. https://doi.org/10.3389/fpsyg.2015.01102

Plum, F., & Posner, J.B. (1966). The Diagnosis of Stupor and Coma. Philadelphia: F.A. Davis Company.

Plum, F. & Posner, J. B. (1982). *The diagnosis of stupor and coma (Vol. 19)*. Oxford University Press.

Poeck, H., & Hacke, W. (2001). *Neurologie.* 11. Auflage. Berlin: Springer

Portaccio, E., Morrocchesi,A., Romoli, A.M., Hakiki, B., Taglioli, M.P., Lippi, E., Di Renzone, M., Grippo, A., Macchi, C. (2017). Score on Coma Recovery Scale-Revised at admission predicts outcome at discharge in intensive rehabilitation after severe brain injury. *Brain injury, 32*(6), 730-734.

Pritchard, W.S. (1981). Psychophysiology of P300. *Psychological Bulletin, 89*(3), 506-540.

PVS TM-STFo (1994). Medical aspects of the persistent vegetative state (2).*The New England journal of medicine*, *330* (22), 1572-1579. doi:10.1056/NEJM199406023302206

PVS TM-STFo (1994). Medical aspects of the persistent vegetative state (1). *The New England journal of medicine*, *330* (21), 1499-1508. doi:10.1056/NEJM199405263302107

Rappaport, M., Hall, K. M., Hopkins, K., Belleza, T., & Cope, D. N. (1982). Disability rating scale for severe head trauma: coma to community. *Archives of Physical Medicine and Rehabilitation*, *63*(3), 118-123.

Risetti, M., Formisano, R., Toppi, J., Quitadamo, L.R., Bianchi, L., Astolfi, L., Cincotti, F., Mattia, D. (2013). On ERPs detection in disorders of consciousness rehabilitation. *Frontiers in Human Neuroscience*, *7*, 775.

Sara, M. & Pistoia, F. (2010). Complexity loss in physiological time series of patients in a vegetative state. *Nonlinear Dynamics, Psychology, and Life Sciences, 14* (1), 1-13.

Sara, M., Pistoia, F., Pasqualetti, P., Sebastiano, F., Onorati, P., & Rossini, P.M. (2011). Functional Isolation Within the Cerebral Cortex in the Vegetative State: A Nonlinear Method to Predict Clinical Outcomes. *Neurorehabilitation and Neural Repair. 25* (1), 35-42. doi:10.1177/1545968310378508

Scheeringa, R., Petersson, K.M., Oostenveld, R., Norris, D.G., Hagoort, P., & Bastiaansen, M.C.M.(2009). Trial-by-trial coupling between EEG and BOLD identifies networks related to alpha and theta EEG power increases during working memory maintenance. *NeuroImage, 44* (3), 1224-1238. doi:10.1016/j.neuroimage.2008.08.041

Schiff, N.D., Rodriguez-Moreno, D., Kamal, A., Kim, K. H., Giacino, J. T., Plum, F., & Hirsch, J. (2005). fMRI reveals large scale network activation in minimally conscious patients. *Neurology, 64*, 514–523. 10.1212/01.WNL.0000150883.10285.44

Schorr, B., Schlee, W., Arndt, M., Lulé, D., Kolassa, I.T., Lopez-Rolon, A., & Bender, A. (2014). Stability of auditory event-related potentials in coma research. *Journal of Neurology, 262* (2), 307-315. doi:10.1007/s00415-014-7561-y

Schorr, B., Schlee, W., Arndt, M., & Bender, A. (2016). Coherence in restingstate EEG as a predictor for the recovery from unresponsive wakefulness syndrome. *Journal of Neurology, 263*, 937–953. https ://doi.org/10.1007/ s0041 5-016-8084-5

Schnakers, C., Giacino, J., Kalmar, K., Piret, S., Lopez, E., Boly, M., Malone, R., Laureys, S. (2006). Does the FOUR score correctly diagnose the vegetative and minimally conscious states. *Annals of Neurololgy*, *60* (6), 744-745.

Schnakers, C., Perrin, F., Schabus, M., Majerus, S., Ledoux, D., Damas, P., Boly, M., Vanhaudenhuyse, A., Bruno, M.A., Moonen, G., Laureys, S. (2008). Voluntary brain processing in disorders of consciousness. *Neurology, 71*(20), 1614-1620. doi:10.1212/01.wnl.0000334754.15330.69

Schnakers, C., Giacino, J., & Laureys, S. (2010). Coma: Detecting signs of consciousness in severely brain injured patients recovering from coma. In: Stone JH, Blouin M (eds) *International Encyclopedia of Rehabilitation*. http://cirrie.buffalo.edu/encyclopedia/en/article/133/

Silva, S., de Pasquale, F., Vuillaume, C., Riu, B., Loubinoux, I., Geeraerts, T., Seguin, T., Bounes, V., Fourcade, O., Demonet, J.F., Peran, P. (2015). Disruption of posteromedial large-scale neural communication predicts recovery from coma. Neurology, 85, 2036–2044.

Sitt, J.D., King, J.R., El Karoui, I., Rohaut, B., Faugeras, F., Gramfort, A., Cohen, L., Sigman, M., Dehaene, S., Naccache, L. (2014). Large scale screening of neural signatures of consciousness in patients in a vegetative or minimally conscious state. *Brain, 137*, 2258-2270. doi:10.1093/brain/awu141

Stender, J., Gosseries, O., Bruno, M.A., Charland-Verville, V., Vanhaudenhuyse, A., Demertzi, A., Chatelle, C., Thonnard, M., Thibaut, A., Heine, L., Soddu, A., Boly, M., Schnakers, C., Gjedde, A., Laureys, S. (2014). Diagnostic precision of PET imaging and functional MRI in disorders of consciousness: a clinical validation study. *Lancet, 384*, 514–522.

Stender, J., Kupers, R., Rodell, A., Thibaut, A., Chatelle, C., Bruno, M.A., Gejl, M., Bernard, C., Hustinx, R., Laureys, S., Gjedde, A. (2015). Quantitative rates of brain glucose metabolism distinguish minimally conscious from vegetative state patients. *Journal of Cerebral Blood Flow and Metabolism, 35*, 58–65.

Stepan, C., Haidinger, G. & Binder H. (2004a). Die Problematik der klinischen Verlaufsbeurteilung von Patienten mit Apallischem Syndrom (AS) anhand von Rehabilitationsskalen - ein Überblick. *Journal für Neurologie, Neurochirurgie und Psychiatrie*, *5*(3), 14-22.

Stipacek, A., Grabner, R.H., Neuper, C., Fink, A., & Neubauer, A.C. (2003). Sensitivity of human EEG alpha band desynchronization to different working memory components and increasing levels of memory load. *Neuroscience letters*, *353* (3), 193-196.

Tallon-Baudry, C., Bertrand, O., & Fischer, C. (2001). Oscillatory synchrony between human extrastriate areas during visual short-term memory maintenance. *Journal of Neuroscience, 21*(20), art. no.-RC177.

Tommasino, C., Grana, C., Lucignani, G., Torri, G., & Fazio, F. (1995). Regional cerebral metabolism of glucose in comatose and vegetative state patients. *Journal of Neurosurgical Anesthesiology, 7*, 109–116.

Teasdale, G. & Jennett, B. (1974). Assessment of coma and impaired consciousness: a practical scale. *The Lancet*, *304*(7872), 81-84.

Thul, A., Lechinger, J., Donis, J., Michitsch, G., Pichler, G., Kochs, E.F., Jordan, D., Ilg, R., Schabus, M. (2016). EEG entropy measures indicate decrease of cortical information processing in disorders of consciousness. *Clinical Neurophysiology, 127*(2), 1419–1427.

van Erp, W.S., Lavrijsen, J.C.M., Vos, P.E. Bor, H., Laureys, S., & Koopmans, R.T. (2015). The vegetative state: prevalence, misdiagnosis, and treatment limitations. *Journal of the American Medical Directors Association, 16*(1),85.e9-85.e14. https ://doi.org/10.1016/j.jamda .2014.10.014

Vanhaudenhuyse, A., Noirhomme, Q., Tshibanda, L.J., Bruno, M.A., Boveroux, P., Schnakers, C., Soddu, A., Perlbarg, V., Ledoux, D., Brichant, J.F., Moonen, G., Maquet, P., Greicius, M.D., Laureys, S., Boly, M. (2010). Default network connectivity reflects the level of consciousness in non-communicative brain-damaged patients. *Brain : a journal of neurology, 133* (Pt 1),161-171. doi:10.1093/brain/awp313

Voss, A. (1993). Standards der neurologischen-neurochirurgischen Frührehabilitation. In: von Will K. & Janzik, H.H. (Hrsg). *Spektrum der Neurorehabilitation* (pp112-120). München, Bern, Wien, New York: Zuckschwerdt.

Wade, D.T. (2018). How often is the diagnosis of the permanent vegetative state incorrect? A review of the evidence. *European Journal of Neurology*, *25*(4), 619-625. doi: 10.1111/ene.13572

Walhovd, K.B., & Fjell, A.M. (2002). One-year test-retest reliability of auditory ERPs in young and old adults. *International Journal of Psychophysiology*, *46* (1), 29-40.

Wang, F., Di, H., Hu, X., Jing, S., Thibaut, A., Di Perri, C., Huang, W., Nie, Y., Schnakers, C., Laureys, S. (2015). Cerebral response to subject's own name showed high prognostic value in traumatic vegetative state. *BMC Medicine, 13,* 83.

Wu, X., Zou, Q., Hu, J., Tang, W., Mao, Y., Gao, L., Zhu, J., Jin, Y., Wu, X., Lu, L., Zhang, Y., Zhang, Y., Dai, Z., Gao, J.H., Weng, X., Zhou, L., Northoff, G., Giacino ,J.T., He, Y., Yang, Y. (2015). Intrinsic functional connectivity patterns predict consciousness level and recovery outcome in acquired brain injury. *Journal of Neuroscience, 35*, 12932–12946.

Yuan, H., Zotev, V., Phillips, R., Drevets, W.C., Bodurka, J. (2012). Spatiotemporal dynamics of the brain at rest — Exploring EEG microstates as electrophysiological signatures of BOLD resting state networks. *NeuroImage, 60*, 2062–2072.

Zeman, A. (2008). Consciousness: concepts, neurobiology, terminology of impairments, theoretical models and philosophical background. *Handbook of Clinical Neurology*, *90*, 3-31. doi: 10.1016/S0072-9752(07)01701-0.

Part II Original Research Articles

I Stability of auditory event-related potentials in coma research

Reference: Schorr, B., Schlee, W., Arndt, M., Lulé, D., Kolassa, I.T., Lopez-Rolon, A., & Bender, A. (2014). Stability of auditory event-related potentials in coma research. *Journal of Neurology, 262* (2), 307-315. doi:10.1007/s00415-014-7561-y

J Neurol (2015) 262:307–315
DOI 10.1007/s00415-014-7561-y

ORIGINAL COMMUNICATION

Stability of auditory event-related potentials in coma research

Barbara Schorr · Winfried Schlee · Marion Arndt · Dorothée Lulé · Iris-Tatjana Kolassa · Alexander Lopez-Rolon · Andreas Bender

Received: 25 July 2014 / Revised: 16 October 2014 / Accepted: 24 October 2014 / Published online: 9 November 2014

Abstract Patients with unresponsive wakefulness syndrome (UWS) or in minimally conscious state (MCS) after brain injury show significant fluctuations in their behavioural abilities over time. As the importance of event-related potentials (ERPs) in the detection of traces of consciousness increases, we investigated the retest reliability of ERPs with repeated tests at four different time points. Twelve healthy controls and 12 inpatients (8 UWS, 4 MCS; 6 traumatic, 6 non-traumatic) were tested twice a day (morning, afternoon) for 2 days with an auditory oddball task. ERPs were recorded with a 256-channel-EEG system, and correlated with behavioural test scores in the Coma Recovery Scale-revised (CRS-R). The number of identifiable P300 responses varied between zero and four in both groups. Reliabilities varied between Krippendorff's $\alpha = 0.43$ for within-day comparison, and $\alpha = 0.25$ for between-day comparison in the patient group. Retest reliability was strong for the CRS-R scores for all comparisons ($\alpha = 0.83$–0.95). The stability of auditory information processing in patients with disorders of consciousness is the basis for other, even more demanding tasks and cognitive potentials. The relatively low ERP-retest reliability suggests that it is necessary to perform repeated tests, especially when probing for consciousness with ERPs. A single negative ERP test result may be mistaken for proof that a UWS patient truly is unresponsive.

Keywords Disorders of consciousness · Minimally conscious state · Unresponsive wakefulness syndrome · P300 · ERPs · EEG

Introduction

Patients with severe acute brain injury may suffer from disorders of consciousness (DOC), i.e., they may be in a coma, vegetative state (VS, also referred to as unresponsive wakefulness syndrome, UWS), or minimally conscious state (MCS) [1, 2]. The behavioural difference between VS/UWS and MCS is that MCS patients show non-reflexive and reproducible behaviour such as command following, visual fixation or pursuit indicative of consciousness. Yet, they are unable to communicate [3].

The rate of misdiagnosis is high in patients with DOC and is estimated around 40 % [4]. Thus, MCS patients are frequently mistakenly classified as VS/UWS; however, they might indeed be aware of what is, for example, being said at their bedside. Currently, the most widely accepted tool for a clinical diagnosis and distinction between the different DOC states is the Coma Recovery Scale-revised (CRS-R) [5–7]. However, the CRS-R as well is a purely

B. Schorr · M. Arndt · A. Bender
Therapiezentrum Burgau, Kapuzinerstraße 34, 89331 Burgau, Germany

B. Schorr (✉) · I.-T. Kolassa
Clinical and Biological Psychology, Institute of Psychology and Education, University of Ulm, Albert-Einstein-Allee 47, 89069 Ulm, Germany
e-mail: barbara.schorr@uni-ulm.de

W. Schlee
Institute for Psychiatry and Psychotherapy, University of Regensburg, Universitätsstraße 84, 93053 Regensburg, Germany

D. Lulé
Department of Neurology, University of Ulm, Oberer Eselsberg 45, 89081 Ulm, Germany

A. Lopez-Rolon · A. Bender
Department of Neurology, Klinikum Grosshadern, University of Munich, Marchioninistraße 15, 81377 Munich, Germany

behaviour-based scale. Restrictions due to visual, auditory or motor impairments in the patient due to brain injury may lead to misdiagnoses [1]. Therefore, novel diagnostic approaches such as functional magnet resonance imaging (fMRI) or EEG-based measures attempt to detect traces of consciousness, even if clinical ratings imply VS/UWS [8–11].

Electrophysiological approaches such as event-related potentials (ERPs) are more easily available for these severely affected patients at bedside and have better temporal resolution than for example fMRI. Therefore, ERPs with auditory paradigms have been suggested to distinguish different DOC states, but also as prognostic tools for the course of the disorder [12–15]. More recently, ERPs were used in brain computer interfaces (BCI) to serve as communication tools in DOC patients or locked-in-syndrome patients [16].

A widely used auditory ERP paradigm used in DOC research is the so-called oddball paradigm: participants are presented with a rare target among frequent distractors, usually in a ratio of 20 % targets vs. 80 % distractors [11]. The task can be a passive task, e.g., listening to sine tones [11, 17], or an active task, e.g., counting one's own name among unfamiliar names [18]. The ERP elicited in response to the rare target stimulus independent of the task is a parietal positive deflection around 300 ms after stimulus onset—the P300. The amplitude of the P300 depends on stimulus saliency, but also on participant's attentiveness [19, 20]. The passive form of this paradigm can yield information about intact stimulus processing for which consciousness is not necessarily needed, i.e., the basic capacity of differentiating between two stimuli. The active form, e.g., the counting of one's own name among unfamiliar names vs. not counting and listening passively [18], can yield information about the attentiveness in the participant and, therefore, conscious processing when comparing the amplitudes from both active and passive sessions. The amplitude is usually higher in the active compared to the passive condition. In the case of patients with DOC this difference may reflect the level of conscious processing in the patients [18].

Clinical experience suggests that patients with severe DOC due to brain injury do not have constant performance levels but show strong variance in their behavioural abilities [21, 22]. This could result in the fact that a patient may not show a P300 at one time point, but may do so if tested at the different time or on a different day.

As the use of auditory ERPs for diagnostic, prognostic, or even communication purposes attracts growing interest in coma science, it is important to establish the robustness of electrophysiological measures, in this case ERPs. We have, therefore, studied the stability of ERPs at four different time points [twice a day (within day) on two different days (between day)] in DOC patients as well as in healthy control as a proof of principle of P300 paradigms in DOC.

Table 1 Patient information, including CRS-R scores for each testing session

ID	Age	Sex	DOC state	Diagnosis	Days since incident
P1	33	M	UWS	GCI	709
P3	38	F	UWS	GCI	94
P5	62	M	UWS	GCI	386
P2	51	F	MCS/ UWS	SAH	210
P4	33	F	UWS	SAH	52
P7	54	F	UWS	SAH	39
P9	17	M	UWS	SAH	33
P6	69	F	MCS	TBI	60
P8	47	M	UWS	TBI	998
P10	21	M	UWS	TBI	2,359
P11	26	F	MCS	TBI	323
P12	51	F	UWS/ MCS	TBI	2,187
Mean (SD)	41 (16)				620.83 (827.72)

GCI global cerebral ischemia, *SAH* subarachnoid haemorrhage, *CRS-R* Coma Recovery Scale-revised, *TBI* traumatic brain injury

Hypotheses

Seeing that performance levels in DOC patients vary also across short time periods, we expect variability in the P300 component concerning the occurrence, as well as the amplitudes and latencies observed in DOC patients across all four measurements. Furthermore, we expect this variability to be associated with the variability of the CRS-R scores. For healthy controls, we expect the P300 to be stable across all four measurements.

Methods

Participants

Twelve DOC inpatients [41.8 ± 16.4 years, mean ± standard deviation (SD)] were recruited in the Therapiezentrum Burgau, a specialized neurorehabilitation centre for patients after severe brain injury. Eight patients were diagnosed with VS/UWS (3 female) and 4 with MCS (4 female) (see Table 1). All DOC patients were additionally enrolled in a large multicentre cohort study [23]. Patients were only included in this study when their

medication was identical throughout the four measurements to avoid possible confounds in the data.

Twelve healthy controls (42.8 ± 15.9 years) were recruited among the clinic employees. Patients and controls did not differ significantly with respect to age ($p = 0.88$) or gender ($p = 0.41$).

The study was approved by the institutional review board of the University of Munich. Healthy controls gave written informed consent prior to participating in the experiment. For patients written informed consent was provided by the appointed legal surrogates prior to participation.

Procedure

Individuals in both groups underwent 4 testing sessions, each lasting around 20–30 min. We tested controls and patients twice per day at 9 am and 1 pm (within day) on two separate days (between day), which were 4 days apart. Prior to each session, the patients' state of consciousness was assessed by two experienced raters independently, using the CRS-R.

Paradigm

We presented 4 blocks with 50 sounds each, including 10 targets and 40 standards in randomized order (200 stimuli in total). Targets were high-pitch tones (1,500 Hz); standards were low-pitch tones (1,000 Hz). Each sound was presented for 500 ms with an inter-stimulus interval of 500 ms. Prior to the main experiment, 10 example tones (2 targets and 8 standards) were presented.

We instructed both controls and patients to pay attention to the high-pitch tones and count along silently in their minds. Stimuli were programmed in e-Prime 2.0 (Psychology Software Tools, Pittsburgh, PA, USA) and presented via speakers positioned on both sides in about 30 cm distance of the participants' head.

EEG acquisition and processing

EEG data were recorded at a sampling rate of 250 Hz with a 256 channel high-density geodesic sensor net with Net Amps 300 amplifier and Net Station 4.5. Software (Electrical Geodesic Inc., Eugene, OR, USA). During recording, electrodes were referenced to the vertex and impedances were kept under 50 μV.

Trials were band-pass filtered (4–35 Hz) and segmented into windows starting −100 ms before to +900 ms after stimulus onset. A baseline correction was performed using the interval (−100 ms; 0 ms) before stimulus onset. The data were inspected manually for artefacts and trials or channels with excessive noise were excluded. Next we re-referenced the electrodes to the common average. Trials were time locked to the stimulus onset and averaged.

For the detection of P300 peaks in each participant, we defined a region of interest with 73 electrodes over central and parietal brain areas (Fig. 1) [11].

Difference waves (target—standard) were calculated and visually inspected to find the strongest P300 for each participant. Visual identification of the P300 in one electrode was performed by taking into account the activity in the 4–5 surrounding electrodes. Amplitude and latency of the P300 were extracted for further analysis. Global mean field power (GMFP) was taken as measure of global brain activation following the tones [24]. Amplitudes and latencies were extracted for further analysis as well. Additionally, we conducted a cluster-based nonparametric permutation analysis to identify the electrode clusters among all electrodes showing the strongest response related to the P300 [25, 26]. This was done to statistically support our choice of electrodes. Similar to our visual inspection, clusters included 5–6 channels, depending on their position on the scalp. The time window of interest was set to 250 ms until 800 ms after the trial onset, since we expected the P300 occurrence during this time period. A cluster was identified as significant if the Monte Carlo significance probability (p) was lower than the set critical alpha level, in our case 0.05. The complete methodological approach can be found in Maris and Oostenwald [27]. All processing steps were done using Fieldtrip, a toolbox in MATLAB for EEG analysis (Mathworks, Natick, MA, USA; [28]).

Statistical analysis

Group statistics were performed by computing multilevel models using the *nlme* package in R (R Development Core Team, 2008; [29]). For group comparisons between healthy controls and patients, group (control vs. patients) and session (measurements M1–4) were entered as fixed effects to predict amplitudes and latencies. Furthermore, level of consciousness (VS/UWS vs. MCS) and diagnosis (non-traumatic vs. traumatic) were used as fixed effects in a separate analysis in the patient group. We also compared the frequency of the occurrence of the P300 between both groups using a Chi-square test. Further correlation analyses of the P300 (general occurrence, amplitudes and latencies) with days since incidence and CRS-R scores were calculated with SPSS version 21 (SPSS Inc., Chicago, IL, USA).

For the retest-reliability analysis, the *irr* package in R was used to compute Krippendorff's alpha (α) [30, 31]. Krippendorff's alpha (α) is a reliability coefficient first developed for the analysis of content data, but is generally applicable where two or more data sets are generated by the same object, i.e., here we have the same participants over four different testing sessions. The coefficient can vary

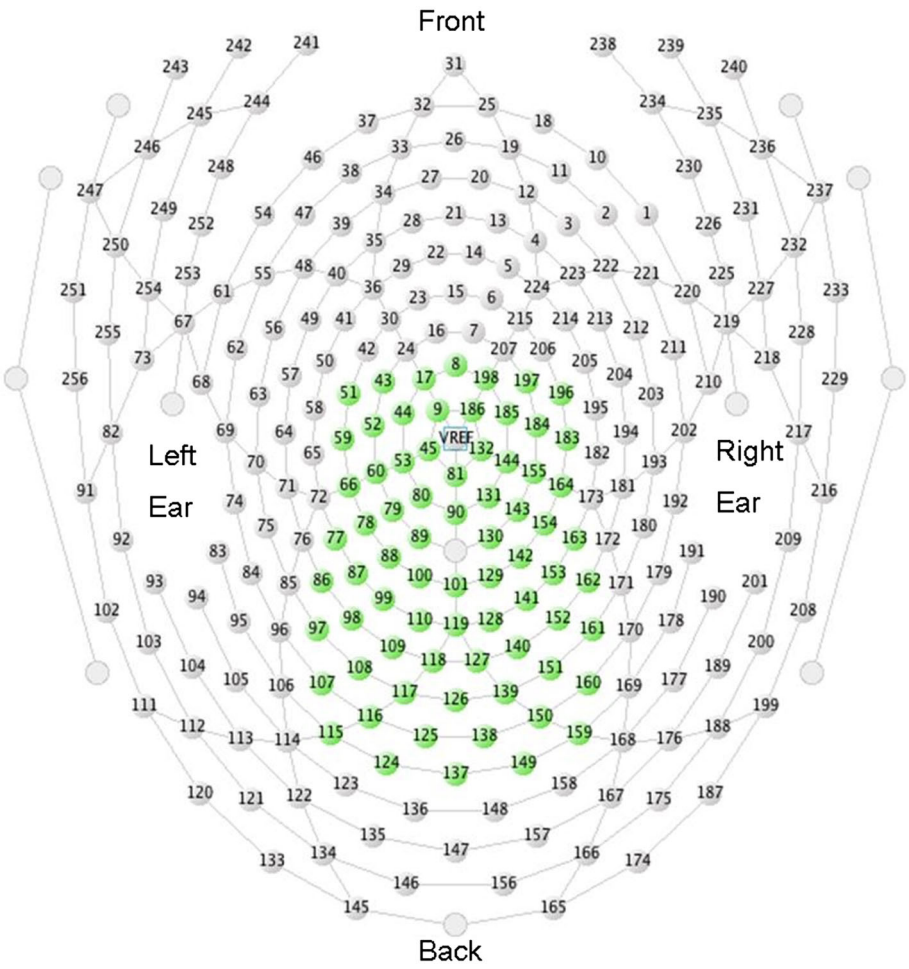

Fig. 1 Region of Interest with 73 electrodes (*green*) used for analysis

Table 2 Elicited P300 responses in both groups (patients on the left) for all the sessions including CRS-R scores for the patients

Patients						Healthy controls				
ID	M1 CRS-R	M2 CRS-R	M3 CRS-R	M4 CRS-R	Diagnosis	ID	M1	M2	M3	M4
P1	5	5	5	5	GCI	C1		a	a	a
P3	5	5[a]	5	5	GCI	C2				
P5	4	4	4	4	GCI	C3				
P2	10[a]	10[a]	6	6	SAH	C4		a	a	
P4	1[a]	1[a]	3	3[a]	SAH	C5	a	a	a	a
P7	3	3	2[a]	2	SAH	C6		a		
P9	6[a]	6[a]	6[a]	6[a]	SAH	C7	a	a	a	a
P6	9	9	9	9	TBI	C8			a	
P8	7[a]	7	7	7	TBI	C9	a	a	a	a
P10	7	7[a]	7[a]	7[a]	TBI	C10				a
P11	11[a]	11	11	11	TBI	C11	a	a	a	a
P12	7	11[a]	11	15	TBI	C12		a	a	a
Mean	6.25	6.58	6.33	6.66						

GCI global cerebral ischemia, *SAH* subarachnoid haemorrhage, *CRS-R* Coma Recovery Scale-revised, *TBI* traumatic brain injury

[a] A positive P300 response

between 0 and 1, with 1 representing perfect reliability. For the comparisons between morning and evening sessions and between day one and day two, the mean was calculated for each constellation, e.g., (CRS-R morning on day 1 + CRS-R morning on day 2)/2 = CRS-R morning, (CRS-R morning day 1 + CRS-R afternoon day 1)/

2 = CRS-R day 1, etc., and then the α coefficient was computed. All analyses mentioned above were done on both the single electrode data and the GMFP data.

Results

In ten controls (84 %) and nine patients (75 %) at least one P300 could be identified. Three UWS patients (37.5 %) did not show a P300 response.

Controls showed in 56.25 % (27 out of 48 testing sessions) and patients in 35.42 % (17/48) of the sessions a clear P300. In four controls and one UWS patient we detected a P300 in all testing sessions; For the rest of the cohort, the amount of identifiable P300 responses varied between one and three times (Table 2). Interestingly, patient P2 varied in her CRS-R scores from MCS on day 1, i.e., M1 and M2, to UWS on day 2, i.e., M3 and M4. In both sessions on day one a P300 could be identified, but not on day two. CRS-R total scores and subscale scores can be found in Tables 2 and 3, respectively.

Cluster-based permutation confirmed significant clusters only in those areas that were also identified by visual inspection.

Group comparisons

We found a significant association between group and whether or not a P300 would occur ($\chi^2(1) = 4.196$, $p = 0.04$), i.e., the occurrence of the P300 was significantly higher in the control group compared to the patient group. The mean amplitude and mean latency of the P300 in the single electrode analysis did not differ significantly between patients and controls [P300 amplitude (M ± SD): 4.99 ± 2.43 vs. 2.84 ± 1.82 μV; P300 latency (M ± SD): 510 ± 187 vs. 611 ± 152 ms]. This was true also for the GMFP analysis [patients vs. controls: amplitude (M ± SD): 1.83 ± 1.70 vs. 2.81 ± 0.57 μV; latency (M ± SD): 410 ± 156.20 ms; 354 ± 113.91 ms].

When contrasting the P300 of UWS and MCS patients, neither mean amplitudes (3.25 ± 2.15 vs. 2.03 ± 0.47 μV) nor mean latencies (624 ± 145 vs. 587 ± 196 ms) did show a significant difference. This was again also true for the GMFP analysis (UWS vs. MCS: amplitudes: 1.87 ± 0.55 vs. 1.77 ± 0.67 μV; latency: 366 ± 111 vs. 487 ± 210 ms). Example plots of the activity at a single electrode of patient data from all four measurements can be found in Fig. 2.

CRS-R and ERPs

There was no correlation between total CRS-R scores, subscale scores, days since incidence, and amplitudes and

Table 3 CRS-R subscales and CRS-R-based diagnosis for each testing session (1–4)

	Au1	Au2	Au3	Au4	Vi1	Vi2	Vi3	Vi4	Mo1	Mo2	Mo3	Mo4	Ve1	Ve2	Ve3	Ve4	Co1	Co2	Co3	Co4	Ar1	Ar2	Ar3	Ar4	D1	D2	D3	D4
P1	1	1	1	1	0	0	0	0	1	1	1	1	1	1	1	1	0	0	0	0	2	2	2	2	UWS	UWS	UWS	UWS
P2	1[a]	1[a]	1	1	1[a]	1[a]	0	0	5[a]	5[a]	2	2	2[a]	2[a]	2	2	0[a]	0[a]	0	0	1[a]	1[a]	1	1	MCS[a]	MCS[a]	UWS	UWS
P3	1	1[a]	1	1	0	0[a]	0	0	0	0[a]	0	0	2	2[a]	2	2	0	0[a]	0	0	2	2[a]	2	2	UWS	UWS[a]	UWS	UWS
P4	0[a]	0[a]	0	0[a]	0[a]	0[a]	0	0[a]	0[a]	0[a]	1	1[a]	1[a]	1[a]	1	1[a]	0[a]	0[a]	0	0[a]	0[a]	0[a]	0	1[a]	UWS[a]	UWS[a]	UWS	UWS[a]
P5	0	0	0	0	0	0	0	0	2	2	2	2	1	1	1	1	0	0	0	0	1	1	1	1	UWS	UWS	UWS	UWS
P6	2	2	2	2	2	2	2	2	2	2	2	2	1	1	1	1	0	0	0	0	2	2	2	2	MCS	MCS	MCS	MCS
P7	1	1	1[a]	1	1	1	1[a]	1	0	0	0[a]	0	0	0	0[a]	0	0	0	0[a]	0	1	1	1[a]	1	UWS	UWS	UWS[a]	UWS
P8	1[a]	1	1	1	0[a]	0	0	0	2[a]	2	2	2	2[a]	2	2	2	0[a]	0	0	0	2[a]	2	2	2	UWS[a]	UWS	UWS	UWS
P9	1[a]	1[a]	1[a]	1[a]	1[a]	1[a]	1[a]	1[a]	1[a]	1[a]	1[a]	1[a]	1[a]	1[a]	1[a]	1[a]	0[a]	0[a]	0[a]	0[a]	2[a]	2[a]	2[a]	2[a]	UWS[a]	UWS[a]	UWS[a]	UWS[a]
P10	1	1[a]	1[a]	1[a]	1	1[a]	1[a]	1[a]	1	1[a]	1[a]	1[a]	2	2[a]	2[a]	2[a]	0	0[a]	0[a]	0[a]	2	2[a]	2[a]	2[a]	UWS	UWS[a]	UWS[a]	UWS[a]
P11	2[a]	2	2	2	3[a]	3	3	3	2[a]	2	2	2	2[a]	2	2	2	0[a]	0	0	0	2[a]	2	2	2	MCS[a]	MCS	MCS	MCS
P12	0	1[a]	1	2	1	1[a]	1	4	2	5[a]	5	5	2	2[a]	2	2	0	0[a]	0	0	2	2[a]	2	2	UWS	MCS[a]	MCS	MCS

Au Auditory Function Scale, *Vi* Visual Function Scale, *Mo* Motor Function Scale, *Ve* Oromotor/Verbal Function Scale, *Co* Communication Scale, *Ar* Arousal Scale, *D* level of consciousness based on the CRS-R, *CRS-R* Coma Recovery Scale-revised, *UWS* unresponsive wakefulness syndrome, *MCS* minimally conscious state

[a] A positive P300 response

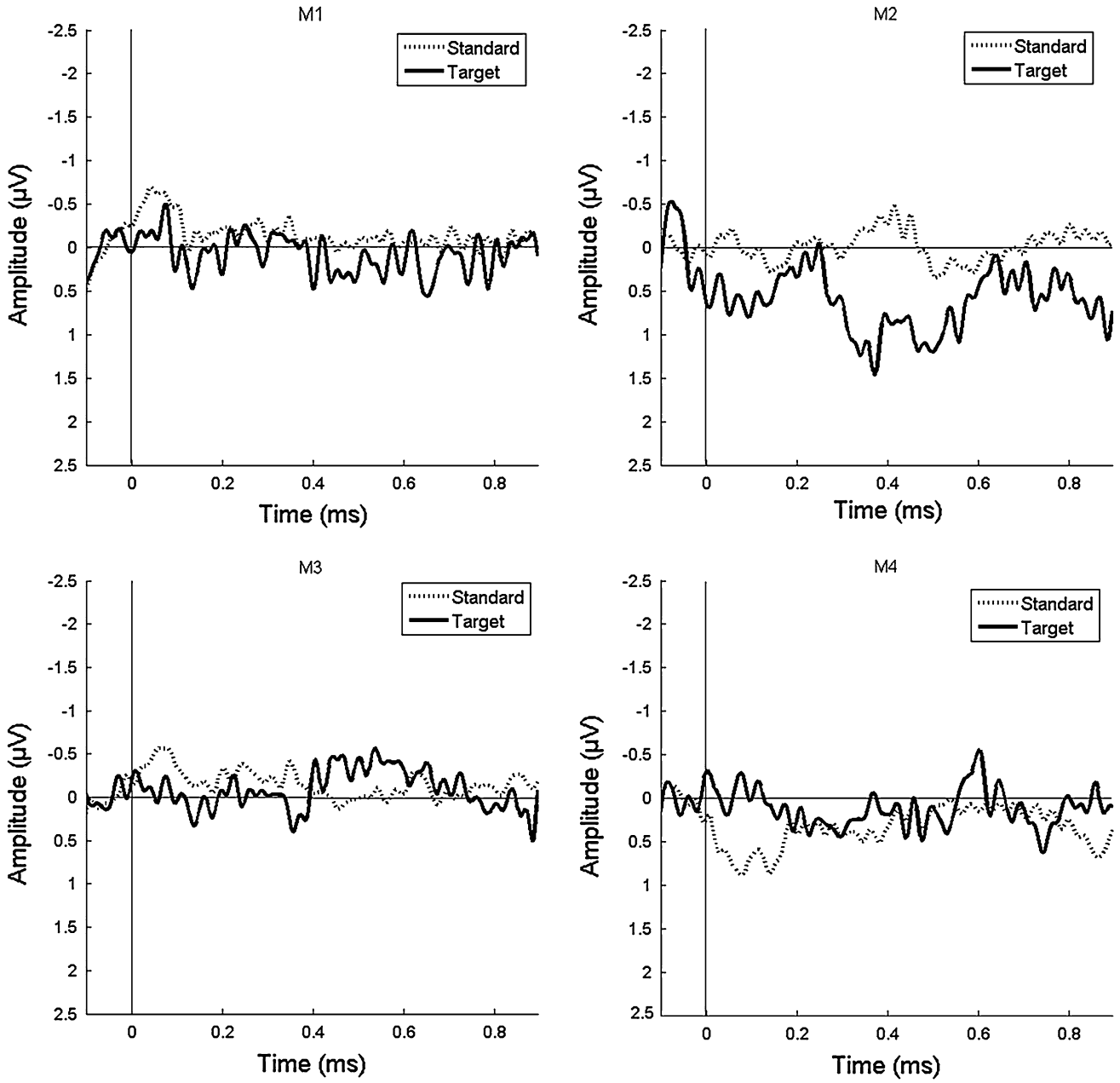

Fig. 2 Example data from one patient. The patient only showed P300 in one session (M2). Depicted is the target (*solid line*) vs. standard (*dashed line*) activity at the same electrode for all four measurements

latencies, for both single electrode and GMFP analyses (all $r \leq 0.55$, no correlation measures survived the Bonferroni correction for multiple comparisons, all $p \geq 0.006$).

Retest reliability

The reliability coefficients for behavioural and electrophysiological data can be found in Table 4. CRS-R scores showed a high retest reliability (all $\alpha \geq 0.83$) across all sessions, as well as for within-day and between-day comparisons. The same is true when looking at the subscales of the CRS-R (all $\alpha \geq 0.73$).

When looking at each session separately, the retest reliability for the general occurrence of the P300 was weak to moderate in both groups. When comparing morning vs. afternoon and day one vs. day two, we found strong reliabilities for both sessions in controls but weaker ones for patients.

When a P300 was observed, retest reliabilities for both amplitudes and latencies were moderate to strong in both groups when analysed on the single electrode basis (all

Table 4 Krippendorff's α for behavioural and electrophysiological data

	Krippendorff's α
CRS-R	
Subscales (over all four sessions)	
Auditory function scale	0.85
Visual function scale	0.79
Motor function scale	0.75
Verbal function scale	1
Communication scale	1
Arousal scale	0.91
Within day (morning vs. afternoon)	
Auditory function scale	0.88
Visual function scale	0.90
Motor function scale	0.94
Verbal function scale	1
Communication scale	1
Arousal scale	1
Between day (day 1 vs. day 2)	
Auditory function scale	0.88
Visual function scale	0.86
Motor function scale	0.73
Verbal function scale	1
Communication scale	1
Arousal scale	0.87
Total score (over all four sessions)	0.83
Within day (morning vs. afternoon)	0.94
Between day (day 1 vs. day 2)	0.83
P300 occurrence in general	
Over all four sessions	
Controls	0.47
Patients	0.25
Within day (morning vs. afternoon)	
Controls	0.72
Patients	0.42
Between day (day 1 vs. day 2)	
Controls	0.72
Patients	0.24
Single electrode data	
Amplitudes	
Over all four sessions	
Controls	0.43
Patients	0.67
Within day (morning vs. afternoon)	
Controls	0.54
Patients	0.90
Between day (day 1 vs. day 2)	
Controls	0.62
Patients	0.63
Latencies	
Over all four sessions	
Controls	0.42
Patients	0.51
Within day (morning vs. afternoon)	
Controls	0.43
Patients	0.51
Between day (day 1 vs. day 2)	
Controls	0.72
Patients	0.70

Krippendorff's alpha (α) is a reliability coefficient. It can vary between 0 and 1, with 1 representing perfect reliability

$\alpha \geq 0.43$). The retest reliabilities for the GMFP amplitudes were strong in the control group for all comparisons (all $\alpha \geq 0.77$) and weaker for the patient group (all $\alpha \leq 0.13$). Retest reliabilities for the latencies were weak in both groups (all $\alpha \leq 0.29$; see Table 4 amplitude and latency sections).

Discussion

As expected, we observed a general instability of the occurrence of the P300 component in patients. For clinical purposes it is especially interesting, that the retest reliability is weak in the patient group in the within-day comparison, and even weaker for the between-day comparison, even though the clinical appearance does not change, i.e., the retest reliability is strong for the CRS-R scores.

These results are in line with studies investigating circadian rhythms in DOC patients. Only 40–84 % of the patients show intact sleep–wake cycles when monitoring temperature [21] or movements via actigraphy [22]. These fluctuations may also be the cause of the strong variability in the occurrence of the P300 in our patient cohort.

Our results are partially in concordance with the finding by Cassidy et al. [32] who tested a battery of typical ERP paradigms eliciting a wide range of components (e.g., P1, N1, P300, etc.) on two different occasions, 1 month apart, in healthy participants. They found strong test–retest reliabilities for amplitudes for all paradigms, but only weak to moderate reliabilities for longer latencies (e.g., P300, P400), and components elicited by oddball tasks showed a change in magnitude across sessions. As for our results, we found moderate to strong reliabilities for both parameters in both groups, when a P300 was observed.

Furthermore, Cassidy et al. [32] reported that 3 % of the participants did not show late ERP components, such as the P300. In our study, 16 % of the healthy controls did not show a P300 in any session and only 33 % in all of the sessions.

Fatigue, work-related stress or the like throughout the day and between the sessions may have influenced the results in our control group. Previous studies investigating retest reliability of the P300 component, or also other ERP components, usually consider longer time periods (1 month [32] or even 1 year [31]). To our knowledge, no study investigated short-term fluctuations in the appearance of ERP.

Fluctuations in both groups may also be related to the paradigm itself. It is well established that the lower the frequency of the attended stimulus, the larger the amplitude [33]. Furthermore, a high trial count results in stronger effects [11]. In our case, 200 trials in total may have been too few to reliably elicit the P300. However, concerning especially DOC patient studies, the duration of the experimental sessions should be kept as short as possible to take into account circadian fluctuations and possible distorted sleep–wake cycles, as mentioned earlier.

Since the topic of retest reliability in clinical studies is important, larger cohorts would be necessary. Possible differences between early VS/UWS and MCS and also between different aetiologies could be of interest.

We are aware that the auditory oddball paradigm we used is far from being a proof for the presence of subclinical consciousness. Other paradigms such as the analysis of event-related desynchronization upon motor imagery tasks are much better suited for this purpose [34]. Yet, the stability of auditory information processing in DOC patients is the basis for other, even more demanding tasks and cognitive potentials, such as motor imagery or spelling devices by BCI. Therefore, it is important to be aware of the relative instability of the P300 ERPs in such patients. The importance of novel electrophysiological methods in DOC diagnostics is growing. The objective to use them as indicators for individual treatment planning in the future can only be reached when we gain an increased understanding of the underlying mechanisms. Therefore, a first step should be to increase the amount of available data by running the experiments not only on 1 day but rather on separate days to increase the sensitivity of eliciting an ERP, as is suggested by our data.

Conflicts of interest On behalf of all authors, the corresponding author states that there is no conflict of interest.

Ethical standard This study has been approved by the ethics committee of the University of Munich and has, therefore, been performed in the accordance with the ethical standards laid down in the 1964 Declaration of Helsinki.

References

1. Guldenmund P, Stender J, Heine L, Laureys S (2012) Mindsight: diagnostics in disorders of consciousness. Crit Care Res Pract 2012:624724. doi:10.1155/2012/624724
2. Giacino JT, Fins JJ, Laureys S, Schiff ND (2014) Disorders of consciousness after acquired brain injury: the state of the science. Nat Rev Neurol 10(2):99–114. doi:10.1038/nrneurol.2013.279
3. Giacino JT, Ashwal S, Childs N, Cranford R, Jennett B, Katz DI, Kelly JP, Rosenberg JH, Whyte J, Zafonte RD, Zasler ND (2002) The minimally conscious state: definition and diagnostic criteria. Neurology 58(3):349–353
4. Andrews K, Murphy L, Munday R, Littlewood C (1996) Misdiagnosis of the vegetative state: retrospective study in a rehabilitation unit. Br Med J 313:13–16
5. Giacino JT, Kalmar K, Whyte J (2004) The JFK coma recovery scale-revised: measurement characteristics and diagnostic utility. Arch Phys Med Rehabil 85(12):2020–2029
6. Schnakers C, Giacino J, Kalmar K, Piret S, Lopez E, Boly M, Malone R, Laureys S (2006) Does the FOUR score correctly diagnose the vegetative and minimally conscious states. Ann Neurol 60(6):744–745
7. Schnakers C, Majerus S, Giacino J, Vanhaudenhuyse A, Bruno MA, Boly M, Moonen G, Damas P, Lambermont B, Lamy M, Damas F, Ventura M, Laureys S (2008) A French validation study of the coma recovery scale-revised (CRSR). Brain Inj 22(10):786–792
8. Vanhaudenhuyse A, Noirhomme Q, Tshibanda LJ, Bruno MA, Boveroux P, Schnakers C, Soddu A, Perlbarg V, Ledoux D, Brichant JF, Moonen G, Maquet P, Greicius MD, Laureys S, Boly M (2010) Default network connectivity reflects the level of consciousness in non-communicative brain-damaged patients. Brain 133(Pt 1):161–171. doi:10.1093/brain/awp313
9. Qin P, Di H, Liu Y, Yu S, Gong Q, Duncan N, Weng X, Laureys S, Northoff G (2010) Anterior cingulate activity and the self in disorders of consciousness. Hum Brain Mapp 31(12):1993–2002. doi:10.1002/hbm.20989
10. Bekinschtein TA, Manes FF, Villarreal M, Owen AM, Della-Maggiore V (2011) Functional imaging reveals movement preparatory activity in the vegetative state. Front Hum Neurosci 5:5. doi:10.3389/fnhum.2011.00005
11. Fischer C, Luaute J, Morlet D (2010) Event-related potentials (MMN and novelty P3) in permanent vegetative or minimally conscious states. Clin Neurophysiol 121(7):1032–1042. doi:10.1016/j.clinph.2010.02.005
12. Donchin E, Karis D, Bashore TR, Coles MGH, Gratton G (1986) Cognitivepsychophysiology and human information processing. In: Coles MGH, Donchin E, Porges SW (eds) Psychophysiology: systems, processes, and applications. Guildford, New York, pp 244–267
13. Luauté J, Fischer C, Adeleine P, Morlet D, Tell L, Boisson D (2005) Late auditory and event-related potentials can be useful to predict good functional outcome after coma. Arch Phys Med Rehabil 86:917–923
14. Cavinato M, Freo U, Ori C, Zorzi M, Tonin P, Piccione F, Merico A (2009) Post-acute P300 predicts recovery of consciousness from traumatic vegetative state. Brain 23:973–980
15. Risetti M, Formisano R, Toppi J, Quitadamo LR, Bianchi L, Astolfi L, Cincotti F, Mattia D (2013) On ERPs detection in disorders of consciousness rehabilitation. Front Hum Neurosci 7:775
16. Lulé D, Noirhomme Q, Kleih SC, Chatelle C, Halder S, Demertzi A, Bruno MA, Gosseries O, Vanhaudenhuyse A, Schnakers C, Thonnard M, Soddu A, Kübler A, Laureys S (2013) Probing command following in patients with disorders of consciousness using a brain-computer interface. Clin Neurophysiol 124(1):101–106
17. Cavinato M, Volpato C, Silvoni S, Sacchetto M, Merico A, Piccione F (2011) Event-related brain potential modulation in patients with severe brain damage. Clin Neurophysiol 122(4):719–724. doi:10.1016/j.clinph.2010.08.024

18. Schnakers C, Perrin F, Schabus M, Majerus S, Ledoux D, Damas P, Boly M, Vanhaudenhuyse A, Bruno MA, Moonen G, Laureys S (2008) Voluntary brain processing in disorders of consciousness. Neurology 71(20):1614–1620. doi:10.1212/01.wnl.0000334754.15330.69
19. Pritchard WS (1981) Psychophysiology of P300. Psychol Bull 89(3):506–540
20. Johnson R Jr (1986) A triarchic model of P300 amplitude. Psychophysiology 23(4):367–384
21. Bekinschtein TA, Golombek DA, Simonetta SH, Coleman MR, Manes FF (2009) Circadian rhythms in the vegetative state. Brain Inj 23(11):915–919. doi:10.1080/02699050903283197
22. Cruse D, Thibaut A, Demertzi A, Nantes JC, Bruno MA, Gosseries O, Vanhaudenhuyse A, Bekinschtein TA, Owen AM, Laureys S (2013) Actigraphy assessments of circadian sleep-wake cycles in the vegetative and minimally conscious states. BMC Med 11:18. doi:10.1186/1741-7015-11-18
23. Grill E, Klein AM, Howell K, Arndt M, Bodrozic L, Herzog J, Jox R, Koenig E, Mansmann U, Müller F, Müller T, Dennis N, Schaupp M, Straube A, Bender A (2013) Design of the prospective german registry of outcome in patients with severe disorders of consciousness after acute brain injury. Arch Phys Med Rehabil 94(10):1870–1876
24. Lehmann D, Skrandies W (1980) Reference-free identification of components of checkerboard-evoked multichannel potential fields. Electroencephalogr Clin Neurophysiol 48(6):609–621
25. Esser SK, Huber R, Massimini M, Peterson MJ, Ferrarelli F, Tononi G (2006) A direct demonstration of cortical LTP in humans: a combined TMS/EEG study. Brain Res Bull 69(1):86–94. doi:10.1016/j.brainresbull.2005.11.003
26. Nichols TE, Holmes AP (2002) Nonparametric permutation tests for functional neuroimaging: a primer with examples. Hum Brain Mapp 15(1):1–25
27. Maris E, Oostenveld R (2007) Nonparametric statistical testing of EEG- and MEG-data. J Neurosci Methods 164(1):177–190. doi:10.1016/j.jneumeth.2007.03.024
28. Oostenveld R, Fries P, Maris E, Schoffelen JM (2011) FieldTrip: open source software for advanced analysis of MEG, EEG, and invasive electrophysiological data. Comput Intell Neurosci 2011:9
29. Pinheiro J, Bates D, DebRoy S, Sarker D, R Development Core Team (2013) nlme: linear and nonlinear mixed effects models. R package version 3.1–111
30. Krippendorff K (2011) Computing Krippendorff's alpha-reliability. Retrieved from http://repository.upenn.edu/asc_papers/43
31. Walhovd KB, Fjell AM (2002) One-year test-retest reliability of auditory ERPs in young and old adults. Int J Psychophysiol 46(1):29–40
32. Cassidy SM, Robertson IH, O'Connell RG (2012) Retest reliability of event-related potentials: evidence from a variety of paradigms. Psychophysiology 49(5):659–664. doi:10.1111/j.1469-8986.2011.01349.x
33. Duncan-Johnson CC, Donchin E (1977) On quantifying surprise: the variation of event-related potentials with subjective probability. Psychophysiology 14(5):456–467
34. Cruse D, Chennu S, Chatelle C, Bekinschtein TA, Fernandez-Espejo D, Pickard JD, Laureys S, Owen AM (2011) Bedside detection of awareness in the vegetative state: a cohort study. Lancet 378(9809):2088–2094. doi:10.1016/S0140-6736(11)61224-5

II Coherence in resting-state EEG as a predictor for the recovery from unresponsive wakefulness syndrome

Schorr, B., Schlee, W., Arndt, M., & Bender, A. (2016). Coherence in restingstate EEG as a predictor for the recovery from unresponsive wakefulness syndrome. *Journal of Neurology, 263*, 937–953. https ://doi.org/10.1007/ s0041 5-016-8084-5

J Neurol (2016) 263:937–953
DOI 10.1007/s00415-016-8084-5

ORIGINAL COMMUNICATION

Coherence in resting-state EEG as a predictor for the recovery from unresponsive wakefulness syndrome

Barbara Schorr[1,2] · Winfried Schlee[3] · Marion Arndt[1] · Andreas Bender[1,4]

Received: 17 November 2015 / Revised: 18 February 2016 / Accepted: 28 February 2016 / Published online: 16 March 2016

Abstract We investigated differences of EEG coherence within (short-range), and between (long-range) specified brain areas as diagnostic markers for different states in disorders of consciousness (DOC), and their predictive value for recovery from unresponsive wakefulness syndrome (UWS). EEGs of 73 patients and 24 controls were recorded and coma recovery scale- revised (CRS-R) scores were assessed. CRS-R of UWS patients was collected after 12 months and divided into two groups (improved/unimproved). Frontal, parietal, fronto-parietal, fronto-temporal, and fronto-occipital coherence was computed, as well as EEG power over frontal, parietal, occipital, and temporal areas. Minimally conscious patients (MCS) and UWS patients could not be differentiated based on their coherence patterns or on EEG power. Fronto-parietal and parietal coherence could positively predict improvement of UWS patients, i.e. recovery from UWS to MCS. Parietal coherence was significantly higher in delta and theta frequencies in the improved group, as well as the coherence between frontal and parietal regions in delta, theta, alpha, and beta frequencies. High parietal delta and theta, and high fronto-parietal theta and alpha coherence appear to provide strong early evidence for recovery from UWS with high predictive sensitivity and specificity. Short and long-range coherence can have a diagnostic value in the prognosis of recovery from UWS.

Keywords EEG coherence · Resting-state · Unresponsive wakefulness syndrome · Fronto-parietal network · Prognosis · Recovery

Electronic supplementary material The online version of this article (doi:10.1007/s00415-016-8084-5) contains supplementary material, which is available to authorized users.

✉ Barbara Schorr
barbara.schorr@uni-ulm.de

Winfried Schlee
winfried.schlee@gmail.com

Marion Arndt
m.arndt@therapiezentrum-burgau.de

Andreas Bender
andreas.bender@med.uni-muenchen.de

[1] Therapiezentrum Burgau, Kapuzinerstraße 34, 89331 Burgau, Germany

[2] Clinical and Biological Psychology, Institute of Psychology and Education, Ulm University, Albert-Einstein-Allee 47, 89069 Ulm, Germany

[3] Institute for Psychiatry and Psychotherapy, University of Regensburg, Universitätsstraße 84, 93053 Regensburg, Germany

[4] Department of Neurology, Klinikum Grosshadern, University of Munich, Marchioninistraße 15, 81377 Munich, Germany

Introduction

Improved medical care of brain injuries caused by anoxic, hemorrhagic, or traumatic events leads to an increasing number of patients remaining in altered states of consciousness. Severe brain injuries can result in a wide spectrum of disorders of consciousness (DOC). The unresponsive wakefulness syndrome (UWS), formally also known as vegetative state (VS), is a state in which the patient does not show reproducible behaviour or any behavioural response to the environment [1]. This state may be permanent without apparent recovery. The minimally conscious state (MCS) is characterized by the ability to follow commands, fixate objects with the eyes, or visual pursuit [2–5].

A widely accepted clinical tool for the differentiation between UWS and MCS is the coma recovery scale-revised (CRS-R) [6–8]. However, purely behaviour-based diagnostic tools can lead to misdiagnoses due to auditory, visual, or motor impairments of the patient [2, 9]. Imaging and electrophysiological techniques are therefore widely tested for their ability to discriminate UWS from MCS as additional diagnostic tools [10–13]. A recent systematic meta-analysis suggested, that quantitative electroencephalography (EEG) measures had the highest sensitivity and specificity for the detection of minimal consciousness, followed by functional magnetic resonance imaging (fMRI), and event-related potentials (ERP) [14].

EEG has proved to be a practical and yet powerful bedside method to examine patients in altered states of consciousness. Event-related potentials (ERP) have been shown to not only distinguish between different states of DOC [15, 16], but may eventually also be helpful in establishing means of communication for these patients [17]. Furthermore, the occurrence of ERPs is discussed to be a positive predictor for recovery from DOC [18–21]. For example, the auditory Mismatch Negativity (MMN) presumably predicts the recovery from unresponsive wakefulness [20]. However, DOC patients' performance levels fluctuate strongly during the course of a day or between different days [22]. The absence of such an ERP component may be misinterpreted and may lead to false diagnoses. In recent years, the combination of transcranial magnetic stimulation (TMS) with EEG has been proven to be superior to the traditional approach of using ERPs or somatosensory evoked potentials in the identification of minimal consciousness [23, 24]. Grosseries and colleagues used TMS in 17 patients [UWS, MCS, and Locked-in-Syndrome (LIS)]. A strong initial cortical activation resulting in a large low-frequency wave was triggered in the UWS patients when frontal and parietal regions were stimulated. This activation did however not propagate to adjacent brain areas. MCS patients showed a series of lower amplitude waves with higher frequencies, travelling to distant cortical areas, ipsi- and contralateral to the stimulated area [25].

Besides these active approaches, EEG resting-state activity has been of major interest. The default mode of brain function is characterized by consistently correlated spontaneous activity fluctuations in widely distributed brain areas [26–29]. Quantitative EEG analyses such as power spectra [30, 31] and connectivity indices are used to examine resting-state EEG of healthy and patient populations. Interaction between brain regions, i.e. connectivity, has also been shown to be an indicator for the level of consciousness [32]. The analysis of entropy in patients in sub-acute phase shortly after injury may help to differentiate between coma, MCS, or UWS [33]. Sitt and colleagues identified spectral power analysis, EEG complexity (spectral entropy, permutation entropy, algorithmic complexity), and functional connectivity to be most promising in differentiating UWS from MCS [34]. Additionally, entropy may serve as a predictor for clinical outcomes of UWS patients [35, 36]. In their studies, Sarà and colleagues found that patients with relatively low approximate entropy (ApEn) either remained in an unresponsive state or even died, whereas patients with higher ApEn regained consciousness or even made a full recovery [35, 36].

Apart from entropy analysis, coherence can be used to estimate neuronal connectivity. Coherence describes the coupling of frequencies between two different time series and can be used to measure synchrony of brain activity within or across different brain areas [37, 38]. For example, it has been shown that long- and short-range correlations of the alpha rhythm depend on age, the subject's condition and the performance of a cognitive task [39–42]. Patients with Alzheimer's disease and mild cognitive impairment have altered functional and effective EEG connectivity within fronto-parietal and fronto-temporal networks [43]. These alterations may reflect dysfunctional neuroplasticity of the neural transmission in long range cortical networks. Cavinato et al. [37] examined the coherence in frontal and parietal regions of DOC patients in response to a variety of stimuli and found increased coherence in comparison to resting state activity in the gamma frequency range after stimulation for controls as well as MCS patients but not for UWS patients.

Although several tools, such as fMRI or ERPs, might be able to detect traces of consciousness, even when clinical ratings imply UWS, the mechanisms underlying the recovery from UWS still remain unknown [44]. For relatives and physicians alike, the prognosis of whether a patient recovers from a state of unconsciousness is challenging and distressing.

This prospective study aimed at identifying differences in functional connectivity, i.e. the coupling of neural signals within (i.e. short-range) and between (i.e. long-range) different brain areas in MCS and UWS patients and healthy controls. Furthermore, we examined whether coherence has a prognostic value for recovery in UWS patients. To do so, we compared coherence patterns in patients that remained in UWS and those, who had at least regained minimal consciousness, at the 12 months follow-up.

Methods

Procedure

For each participant, a 5 min high-density resting state EEG was recorded. Prior to recording, the patients' state of consciousness was assessed independently by two

experienced raters with the CRS-R. Patients were positioned in bed, with eyes closed. The standard CRS-R arousal facilitation protocol was used to maintain the patient in a state of arousal during the whole recording period. The controls and were asked to sit relaxed, awake, with closed eyes, and not to engage in any specific mental activity. A follow-up clinical assessment (CRS-R) of the patients' state of consciousness was conducted 12 months after the initial EEG recording.

Participants

Seventy-three DOC inpatients (15 MCS patients: *Mean* age 50.3 ± *standard deviation* 10 years, 8 males; 58 UWS patients: 50.2 ± 17.1 years, 36 males) were recruited in the Therapiezentrum Burgau, a specialized neurorehabilitation centre for patients after severe brain injury (Table 1). It was ensured that patients were not under sedation for the EEG recording. 24 healthy controls (45.0 ± 16.2, 10 males) were matched with patients for age and sex.

EEG acquisition and processing

EEG data was recorded at a sampling rate of 250 Hz with a 256 channel high-density geodesic sensor net with Net Amps 300 amplifier and Net Station 4.5. Software (Electrical Geodesic Inc., Eugene, OR, USA). During recording, electrodes were referenced to the vertex and impedances were kept under 50 k Ohm.

Preprocessing and connectivity analysis was done with the Fieldtrip toolbox for EEG analyses in MATLAB (Mathworks, Natick, MA, USA; [45]) and the bsmart implementation [46]. A 1 Hz high-pass filter and a 100 Hz low-pass filter were applied, as well as a 50 Hz notch filter to remove line noise. Data were rereferenced to the average of all electrodes and then segmented into epochs of 2 seconds. Epochs were inspected manually after an in-house MATLAB script identified possible artefacts (e.g. eye-movements exceeding 70 μV, eye-blinks exceeding 140 μV and muscle artefacts exceeding 200 μV) and bad trials were rejected. A mean of 137 (±8) epochs per person were analysed.

For further analyses, 30 frontal electrodes, 32 parietal electrodes, 31 occipital and 16 temporal electrodes were identified as regions of interest (ROI) and used for further analysis of connectivity (Fig. 1). To depict functional interaction between brain regions, we performed a coherence analysis. Coherence is the measure of synchrony of brain activity across different brain regions and is calculated between pairs of signals as a function of frequency [47]. A multivariate autoregressive model was fitted to each individual dataset. Different model orders between 3 and 15 were tested with the bsmart toolbox [46] which provides functions to calculate the multivariate Akaike information criterion (AIC) [48]. A model order of five was found to be the best fit. This means, each data point in the EEG time series was modelled as a weighted linear sum of its five preceding data points. This resulted in a matrix (channel × channel × frequency) of coefficients. From here we computed the spectral transfer matrix. It contains the pairwise transfer function between all channels. In the last step, we finally computed the coherence coefficients for each pair of electrodes for each frequency. Coherence coefficients differing three standard deviations (SD) from the mean were marked as outliers and excluded from the analysis.

To analyse the connectivity within and between specific brain regions, we extracted the coherence coefficients of specific electrode pairs from frontal, parietal, temporal, and occipital regions. Computed tomography scans of the patients were inspected and locations of brain lesions identified (Table 1). Studies have shown that the EEG activity over lesions can be significantly different from the activity over intact brain regions [49, 50]. In order to avoid the influence of the lesion on EEG power or coherence results, we only chose electrodes above intact brain regions for the analysis in patients with brain lesions ('lesion electrode set'). However, since DOC patients often have rather diffuse lesions, we controlled our results by also analysing the complete set of electrodes in each patient, resulting in a purely data driven approach ('complete electrode set'). A mean coherence value between and within certain brain regions was calculated for each frequency bin (connectivity within frontal cortex, connectivity within parietal cortex, connectivity between frontal and parietal, temporal, and occipital cortex). Finally, a mean coherence value for each frequency band (1–4 Hz delta, 5–8 Hz theta, 9–13 Hz alpha, 14–30 Hz beta, 30–100 Hz gamma) was calculated.

Additionally, we performed a power spectra analysis of the ROI. Preprocessed data were normalized and a Fast Fourier Transformation was performed. The percentage of each frequency band from the total power was calculated for each inspected brain region (frontal, parietal, occipital, and temporal).

Statistical analysis

Coherence values of both electrode sets (lesion and complete) were compared with a paired-sample student's *t* test. Multilevel models were computed for the group comparisons for all connectivity analyses and the power spectra analysis, using the nlme package in R [51, 52]. For the comparison between MCS patients, UWS patients, and the control group, group (MCS vs. UWS vs. controls) and frequency band (Delta, Theta, Alpha, Beta, Gamma) were

Table 1 Demographic details for the patients

ID	Gender	Age	Etiology	Antiepileptic/ neuroleptic medication	Location of lesion	Time since brain injury (days)	Baseline DOC category	Baseline CRS-R	For UWS: recovery of consciousness (at least MCS) yes/no	Follow-up CRS-R 5	Follow-up diagnosis
P1	M	37	Hypoxia	Levetiracetam		772	UWS	6	No		UWS
P2	F	26	Hypoxia	Levetiracetam		1043	UWS	7	No	7	UWS
P3	M	54	ICH		Left frontal lobe	50	MCS	4			
P4	F	51	Ischemic stroke	Levetiracetam	Right thalamus	58	UWS	8	yes	18	MCS
P5	M	49	TBI	Levetiracetam	Left frontal lobe	30	UWS	1	No	7	UWS
P6	F	29	Hypoxia	Melperon, Quetiapin		1183	MCS	10			
P7	F	50	ICH	Levetiracetam	Right basal ganglia	63	MCS	10			
P8	F	58	Hypoxia	Levetiracetam		63	UWS	2	No	5	UWS
P9	M	66	Hypoxia	Levetiracetam		49	UWS	4	No	6	UWS
P10	M	24	TBI	Levetiracetam	Global atrophy	1062	UWS	7	No	7	UWS
P11	M	63	Hypoxia	Levetiracetam, Valproat		48	UWS	2	No	5	UWS
P12	M	28	Hypoxia	Levetiracetam		947	UWS	5	No	5	MCS
P13	M	50	TBI		Right hemisphere	40	MCS	9			
P14	F	33	SAH	Levetiracetam	Left thalamus	52	UWS	1	No	8	UWS
P15	F	54	SAH		Left frontal lobe	197	UWS	6	No	6	UWS
P16	M	61	Hypoxia	Levetiracetam		28	UWS	4	No	4	UWS
P17	M	24	TBI	Levetiracetam	Brainstem	34	UWS	6	yes	22	MCS+
P18	M	56	TBI		Right frontal lobe	678	UWS	5	No	5	UWS
P19	M	66	TBI	Levetiracetam	Right frontal lobe	38	UWS	4	Yes	21	MCS+
P20	M	59	Ischemic stroke	Levetiracetam	Left frontal lobe	9	UWS	5	No	5	UWS
P21	F	74	Brain tumor	Levetiracetam, Quetiapin	Right frontal lobe	34	MCS	16			
P22	M	32	Hypoxia			56	UWS	6	No	6	UWS
P23	F	54	SDH	Levetiracetam	Left frontal lobe	138	UWS	3	No	6	UWS
P24	M	32	Hypoxia			790	UWS	3	Yes	8	MCS
P25	M	68	ICH	Levetiracetam	Left temporo-occipital area	34	UWS	3	Yes	9	MCS
P26	F	68	Hypoxia			442	UWS	3	No	3	UWS
P27	M	37	TBI	Levetiracetam	Left hemisphere	69	UWS	5	No	5	UWS
P28	F	62	SAH		Right temporal lobe	45	UWS	3	No	3	UWS
P29	M	48	TBI		Right parietal lobe	89	UWS	5	No	5	UWS
P30	F	53	Hypoxia			5316	UWS	7	No	7	UWS
P31	M	42	TBI		Right frontal lobe	53	UWS	8	No	8	UWS
P32	M	64	TBI	Levetiracetam	Right temporal lobe	185	UWS	1	No	1	UWS
P33	M	38	TBI	Levetiracetam	Left temporal lobe	4669	UWS	6	No	6	UWS
P34	M	59	ICH	Levetiracetam	Right frontal lobe	69	MCS	8			

Table 1 continued

ID	Gender	Age	Etiology	Antiepileptic/ neuroleptic medication	Location of lesion	Time since brain injury (days)	Baseline DOC category	Baseline CRS-R	For UWS: recovery of consciousness (at least MCS) yes/no	Follow-up CRS-R 5	Follow-up diagnosis
P35	F	45	SAH	Levetiracetam	Communicans anterior	120	MCS	13			
P36	F	66	Hypoxia	Levetiracetam		415	UWS	7	No	7	UWS
P37	M	69	Hypoxia			414	UWS	6	No	6	UWS
P38	M	17	TBI	Levetiracetam	Right temporal lobe	33	UWS	6	Yes	23	MCS+
P39	F	55	Hypoxia			34	UWS	3	No	3	UWS
P40	F	72	Hypoxia	Levetiracetam		58	UWS	4	No	4	UWS
P41	M	21	TBI	Levetiracetam, Vimpat	Right hemisphere	2363	UWS	7	No	7	UWS
P42	M	65	Hypoxia	Levetiracetam		37	UWS	2	No	6	UWS
P43	M	50	TBI		Right hemisphere	2187	UWS	7	No	7	UWS
P44	M	62	ICH		Right parietal lobe	1096	UWS	3	No	3	UWS
P45	F	45	SAH	Levetiracetam	Right hemisphere	513	UWS	7	Yes	9	MCS
P46	F	75	Hypoxia	Levetiracetam		79	UWS	3	No	3	UWS
P47	F	70	Hypoxia			50	UWS	5	Yes	9	MCS
P48	M	50	SAH		Right frontal lobe	142	MCS	11			
P49	M	73	Hypoxia			1900	UWS	3	No	4	UWS
P50	M	67	Hypoxia			33	UWS	3	No	3	UWS
P51	M	20	Hypoxia	Levetiracetam		25	UWS	6	No	7	MCS
P52	M	47	SAH	Levetiracetam	Right fronto-parietal area	63	MCS	12			
P53	M	40	Hypoxia	Levetiracetam		1684	MCS	10			
P54	M	20	TBI		Right hemisphere	1241	UWS	8	No	8	UWS
P55	F	64	Ischemic stroke		Left hemisphere	55	UWS	2	Yes	20	MCS+
P56	M	54	Hypoxia			25	UWS	3	No	3	UWS
P57	F	52	TBI	Levetiracetam	Left hemisphere	120	MCS	14			
P58	M	42	Hypoxia			3256	UWS	4	No	4	UWS
P59	M	19	TBI	Levetiracetam	Right frontal lobe	1205	UWS	6	No	6	UWS
P60	F	47	SAH	Levetiracetam, Vimpat	Right hemisphere	51	UWS	5	No	5	UWS
P61	F	50	Hypoxia	Levetiracetam		73	UWS	6	No	6	UWS
P62	M	49	SAH	Levetiracetam		744	MCS	9			
P63	F	58	Central pontine myelinolysis			355	UWS	6	Yes	7	MCS
P64	M	75	Hypoxia	Levetiracetam		36	UWS	4	No	4	UWS
P65	M	76	Ischemia		Cerebellum	47	UWS	5	No	5	UWS
P66	M	62	ICH	Levetiracetam, Melperon	Basal ganglia	76	MCS	8			
P67	F	47	TBI		Left frontal lobe	29	MCS	6			

Table 1 continued

ID	Gender	Age	Etiology	Antiepileptic/ neuroleptic medication	Location of lesion	Time since brain injury (days)	Baseline DOC category	Baseline CRS-R	For UWS: recovery of consciousness (at least MCS) yes/no	Follow-up CRS-R 5	Follow-up diagnosis
P68	F	26	TBI	Levetiracetam	Right hemisphere	2365	UWS	6	No	6	UWS
P69	F	68	Hypoxia			1109	UWS	6	No	6	UWS
P70	M	52	Hypoxia	Levetiracetam		25	UWS	3	No	3	UWS
P71	F	47	Hypoxia	Levetiracetam, Seroquel, Ergenyl		66	MCS	10			
P72	M	46	Hypoxia	Levetiracetam, Vimpat		1794	UWS	6	No	6	UWS
P73	F	37	ICH		Nucleus caudatus	362	UWS	6	Yes	10	MCS

CRS-R scores from the day of the EEG acquisition and the follow-up CRS-R scores after 12 months after the EEG

ICH intra cranial haemorrhage, *TBI* traumatic brain injury, *SAH* subarachnoid haemorrhage, *CRS-R* Coma recovery scale-revised

entered as fixed effects to predict coherence or power and subject identity and group affiliation were entered as random effects. Contrasts were set to compare UWS and controls, and MCS patients and controls, and the patient groups in each frequency band. Furthermore, we compared UWS patients who evolved to a higher consciousness level (MCS or better) after 12 months after the original EEG recording (I; Improved), with patients who did not show any sign of consciousness after the same amount of time (U; Unimproved). Group (I vs. U), frequency band (delta, theta, alpha, beta, and gamma), and etiology were entered as fixed effects, and subject identity and group affiliation were entered as random effects to predict coherence or power. For the connectivity this was done for frontal, parietal, fronto-parietal, fronto-temporal and fronto-occipital connectivity separately. For the power analysis, this was done for spectral power above frontal, parietal, occipital and temporal areas separately.

Two-sided Student's t tests were computed for further analyses of the differences in coherence between the patient groups (MCS vs. UWS; U vs. I; traumatic vs. non-traumatic). Since this study is exploratory in nature, we refrained from an adjustment for multiple comparisons [53–55]. Additionally, we correlated (Pearson's r) CRS-R scores and sub-scores with coherence and power spectra values, and coherence with the power spectra values of the corresponding brain areas. The prognostic power of the coherence was calculated using receiver-operating characteristic (ROC) curve analysis (SPSS version 21, Inc., Chicago, IL, USA). Optimal cut-off points were calculated using the Youden's index J = sensitivity + specificity−1 [56], where the highest J indicates the optimal cut-off.

Results

Coherence analysis of the lesion set of electrodes

Correlation between CRS-R and coherence

No significant correlations were found between CRS-R total scores, the sub-scores and the coherence values in the different brain areas.

MCS vs. UWS vs. controls

Coherence values (mean and SD) for all three groups (MCS, UWS, controls) for frontal, parietal, fronto-parietal, fronto-temporal, and fronto-occipital connectivity, as well as statistics and p values of main and interaction effects can be found in the online resource 1.

UWS patients had significantly lower alpha [t (80) = 4.376, $p < .001$] and beta [t (75.7) = 3.689,

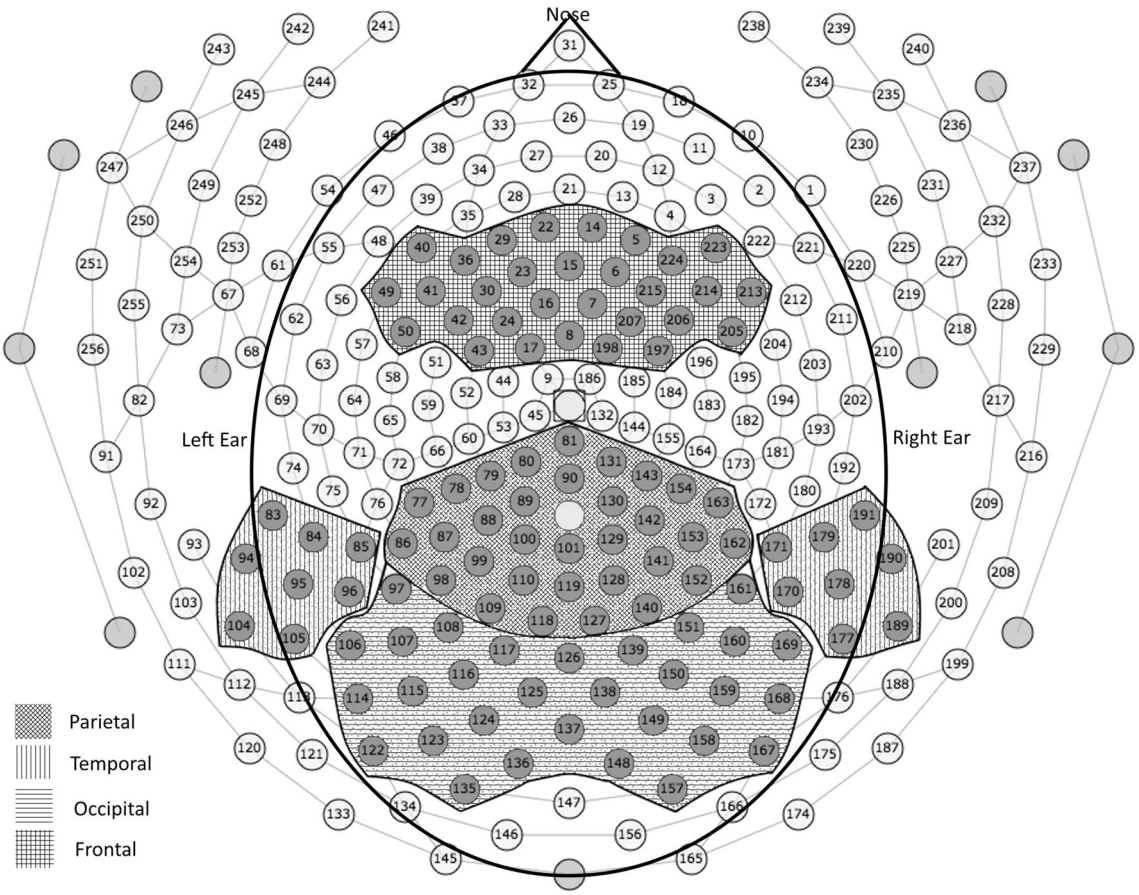

Fig. 1 Electrode layout of the ROI electrodes chosen for analysis

$p < .001$] coherence between frontal and parietal regions, and lower coherence in alpha frequency within parietal regions [t (80) = 2.591, $p = .011$] than controls. Furthermore, coherence in fronto-temporal and fronto-occipital connections was significantly lower in theta [*fronto-temporal*: t (37) = 3.418, $p = .002$; *fronto-occipital*: t (37) = 4.007, $p < .001$], alpha [t (37) = 4.856, $p < .001$; t (37) = 4.968, $p < .001$], and beta [t (37) = 3.011, $p = .005$, t (37) = 3.193, $p = .003$] bands in the MCS patients compared to controls (all $p < .005$) (Fig. 2a–e). We did not find any significant differences between UWS patients and MCS patients in specific frequency bands (all $p > .2$) in any networks.

Comparison between UWS long-term outcome groups (improved vs. unimproved)

From the UWS patients, 11 patients (19 %) had regained consciousness after 12 months, 48 (81 %) remained in a state of unresponsive wakefulness (see Table 2 in the online resource 2 for baseline and follow-up total CRS-R scores and sub-scale scores). Table 2 shows coherence values for UWS patients who improved (I) and UWS patients who did not (U) for frontal, parietal, fronto-parietal, fronto-temporal, and fronto-occipital connectivity, as well as student's t test results and p values for the significant effects.

Contrasts revealed significant group differences in parietal and fronto-parietal coherence [main effect of group parietal: $b = -.104$, t (55) = −2.782, $p = .007$; main effect of group fronto-parietal: $b = -.098$, t (55) = −2.704, $p = .009$]. More specifically, parietal coherence was significantly higher in delta ($p = .046$) and theta ($p = .018$) frequencies in the improved group [interaction effect frequency × group: $b = .017$, t (230) = 2.174, $p = .030$]. Fronto-parietal coherence was higher as well in delta ($p = .044$), theta ($p = .009$), alpha ($p = .016$), and beta ($p = .034$) frequencies in the improved group [interaction effect frequency × group: $b = .088$, t (228) = 3.086, $p = .002$].

When taking into account the etiology of the brain damage (traumatic vs. non-traumatic), patients who recovered after a non-traumatic brain injury (9 patients) had higher fronto-parietal coherence in theta [t (40) = 2.698, $p = .010$; *Mi:* .53, *SDi:* .09, *Mu:* .43, *SDu:* .09], alpha [t (40) = 2.176, $p = .035$; *Mi:* .50, *SDi:* .09,

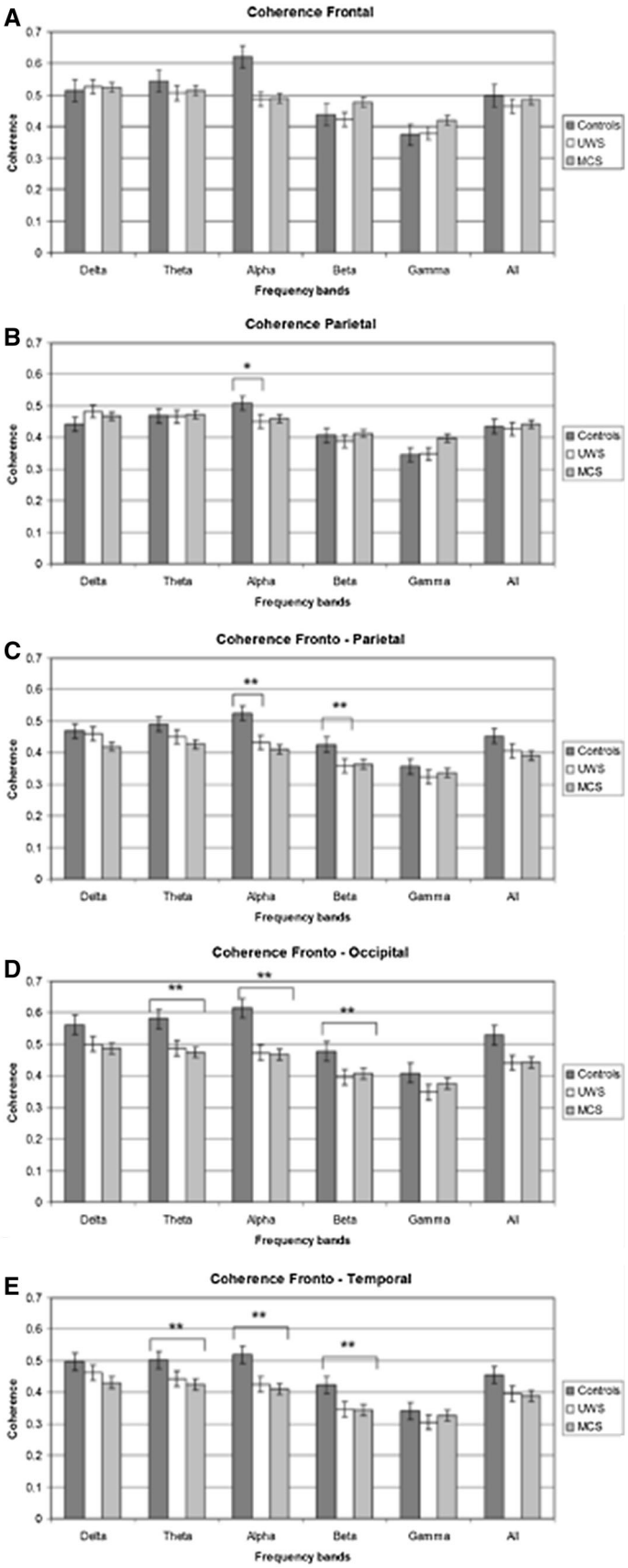

Fig. 2 Mean coherence values for UWS patients, MCS patients, and controls. *Error bars* depict standard error mean. Depicted are: Coherence within frontal electrodes (**a**); Coherence within parietal electrodes (**b**); Coherence between frontal and parietal electrodes (**c**); coherence between frontal and temporal electrodes (**d**); Coherence between frontal and occipital electrodes (**e**). $*p < .05$; $**p < .01$

Table 2 Coherence values (mean and standard deviation) for unresponsive patients, who regained a level of minimal consciousness (I), and patients who remained in an unresponsive state of consciousness (U)

	Group "I" = improved "U" = unimproved	Mean	Standard deviation	Significant differences in the coherence between improved and unimproved UWS patients (t and p values)
Frontal				
Delta	I	.59	.12	
	U	.51	.12	
Theta	I	.55	.07	
	U	.49	.09	
Alpha	I	.51	.09	
	U	.48	.10	
Beta	I	.45	.12	
	U	.41	.12	
Gamma	I	.34	.11	
	U	.38	.14	
Parietal				
Delta	I	.54	.08	t (56) = 2.043, p = .046
	U	.46	.11	
Theta	I	.52	.08	t (56) = 2.444, p = .018
	U	.45	.09	
Alpha	I	.50	.08	
	U	.43	.09	
Beta	I	.43	.13	
	U	.37	.10	
Gamma	I	.34	.14	
	U	.34	.12	
Frontal-Parietal				
Delta	I	.52	.12	t (56) = 2.064, p = .044
	U	.44	.11	
Theta	I	.51	.09	t (56) = 2.725, p = .009
	U	.43	.09	
Alpha	I	.49	.09	t (56) = 2.489, p = .016
	U	.41	.08	
Beta	I	.42	.13	t (56) = 2.179, p = .034
	U	.34	.09	
Gamma	I	.34	.15	
	U	.31	.12	
Frontal-Occipital				
Delta	I	.54	.15	
	U	.49	.11	
Theta	I	.51	.14	
	U	.48	.10	
Alpha	I	.48	.12	
	U	.46	.10	
Beta	I	.44	.12	
	U	.38	.10	
Gamma	I	.33	.14	
	U	.35	.13	
Frontal-Temporal				
Delta	I	.50	.12	
	U	.45	.12	
Theta	I	.47	.09	
	U	.43	.10	
Alpha	I	.45	.10	
	U	.41	.10	
Beta	I	.40	.12	
	U	.33	.11	
Gamma	I	.31	.14	
	U	.30	.13	

t and p values for significant differences in the coherence in specific frequency bands are displayed. Significance level was set at $p < .05$

Mu: .42, *SDu:* .09], and beta [t (40) = 2.160, p = .037; *Mi:* .43, *SDi:* .13, *Mu:* .35, *SDu:* .10] frequencies than patients who did not recover (33 patients). With only 2 (improved) vs. 14 (unimproved) patients with TBI, the statistical results have to be interpreted with caution. Patients who did not recover after a TBI (14 patients) showed significantly higher fronto-parietal coherence in the gamma band [interaction effect *Frequency* × *Group* × *Etiology:* b = .088, t (228) = 3.086, p = .002; t (14) = −2.788, p = .015; *mean improved (Mi):* .12, *standard deviation (SDi):* .08, *M unimproved (Mu):* .32, *SDu:* .09], and higher fronto-occipital coherence [t (14) = −2.543, p = .023; *Mi:* .14, *SDi:* .11, *Mu:* .37, *SDu:* 12] in the gamma band, than patients who did recover from a TBI (2 patients).

ROC curve analysis revealed parietal coherence in the theta band to be most powerful in the early discrimination between patients who will eventually improve and those patients who remain unresponsive. Sensitivity was at 73 % and specificity at 79 % with a cut-off value of .50 (*AUC*: .75, *95 % confidence interval (CI)*: .58–.93, p = .01). Furthermore, parietal coherence in the delta frequency (cut-off: .50), and fronto-parietal coherence in the theta (cut-off: .50) and alpha (cut-off: .46) frequencies significantly (all $p < .03$) showed strong discriminative performance for the differentiation of the two patient groups (Fig. 3a–d).

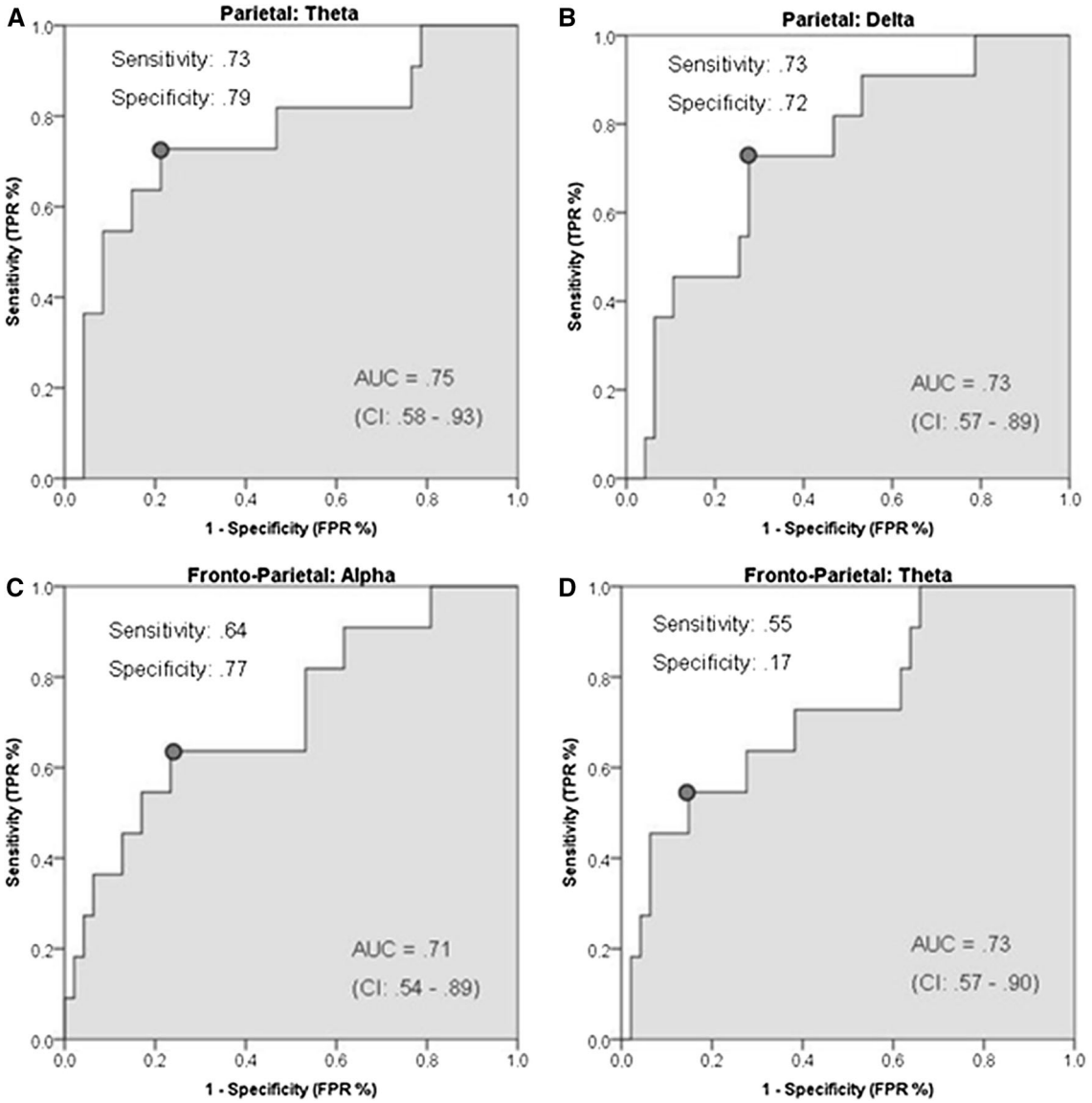

Fig. 3 ROC curve analysis for parietal theta (**a**) and delta (**b**), and fronto-parietal alpha (**c**) and theta (**d**): *x* axis: 1-specificity (*FPR* false positive rate), *y*-axis: sensitivity (*TPR* true positive rate), *AUC* area under the curve, *CI* confidence interval

In general, UWS patients who regained consciousness had higher coherence values in all frequency bands across all brain regions (Fig. 4a–e). Complete main and interaction effects are listed in the online resource 2.

Complementary analysis of complete set of electrodes

Coherence calculated from the complete set of electrodes was significantly higher than the coherence from the lesion set (all $p \leq .026$, except parietal gamma, fronto-parietal beta, fronto-occipital delta and gamma which were not significantly different), but the group comparison confirmed our previous results. Coherence could still not differentiate between UWS and MCS patients (all $p \geq .172$), but could predict improvement in the UWS patients (all $p \leq .044$).

Power spectra analysis

Correlation between CRS-R and power spectra

Frontal delta power correlated positively with follow-up motor ($r = .295$, $p = .011$) and auditory ($r = .243$, $p = .038$) subscale scores. Furthermore, temporal delta correlated positively ($r = 283$, $p = .015$), and occipital ($r = -.260$, $p = .026$) and temporal ($r = -.270$, $p = .021$) theta correlated negatively with the follow-up motor subscale scores.

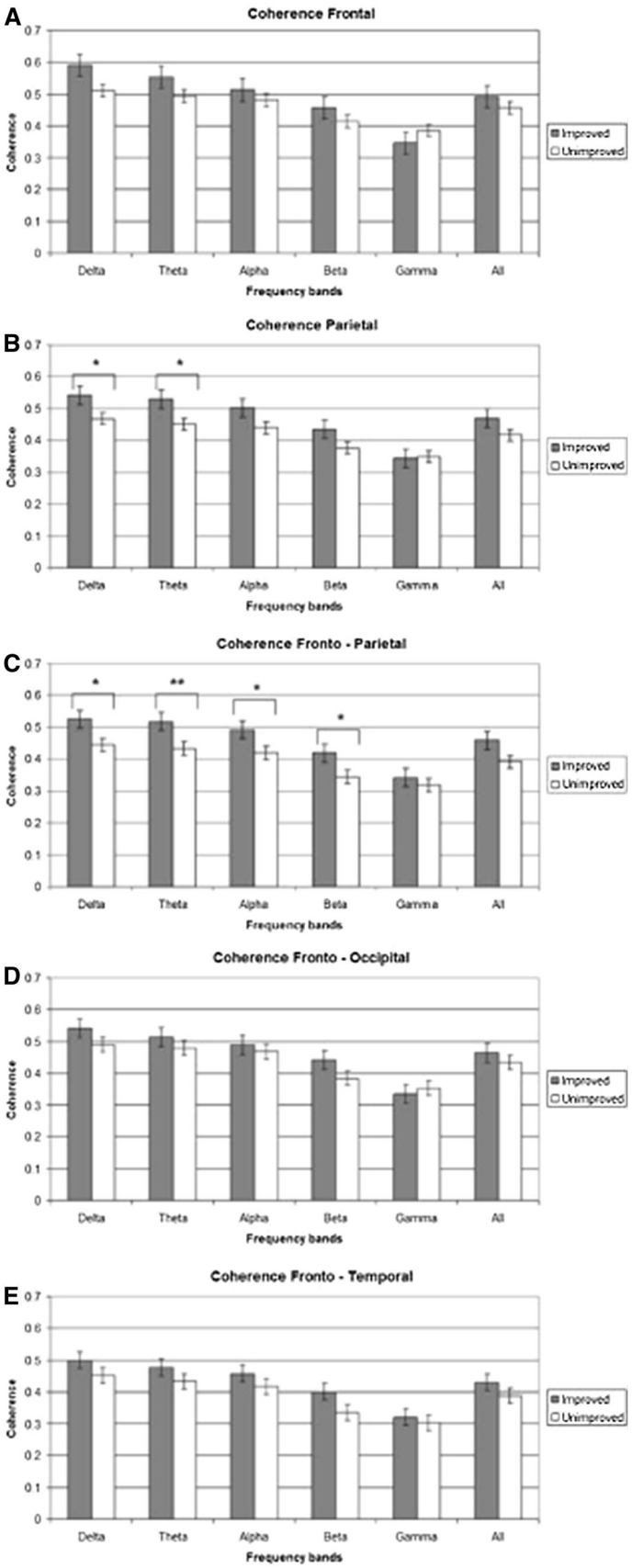

Fig. 4 Mean coherence values for UWS patients who did regain consciousness (improved) and patients who remained unconscious (unimproved). *Error bars* depict standard error mean. Depicted are: coherence within frontal electrodes (**a**); coherence within parietal electrodes (**b**); Coherence between frontal and parietal electrodes (**c**); coherence between frontal and temporal electrodes (**d**); coherence between frontal and occipital electrodes (**e**). $^{*}p < .05$; $^{**}p < .01$

MCS vs. UWS vs. controls

Power values (mean and SD) for all three groups (MCS, UWS, controls) for frontal, parietal, temporal and occipital power spectra, as well as statistics and p values can be found in the online resource 1. Patient groups had overall significantly lower percentage of alpha and beta power than the control group (all $p \leq .015$), and a significantly higher percentage of delta power (all $p \leq .001$).

Comparison between UWS long-term outcome groups (improved vs. unimproved)

Power values (mean and SD) for both groups (U and I) for frontal, parietal, temporal and occipital power spectra, as well as statistics and p values can be found in the online resource 2. Overall, power of different frequencies did not differ significantly between the two groups (all $p \geq .05$).

Correlation analysis between coherence and power spectra

Significant correlations can be found in Table 3.

Table 3 Significant correlations between the coherence values and the EEG power percentages of the different frequency bands over each investigated brain area

Coherence and power spectra	Pearson's r	P
Frontal and Frontal		
Delta	.292	.004
Alpha	.631	<.001
Parietal and Parietal		
Delta	.305	.002
Alpha	.377	<.001
Gamma	.220	.030
Fronto-parietal and Frontal		
Theta	.206	.043
Alpha	.528	<.001
Fronto-parietal and Parietal		
Alpha	.534	<.001
Beta	.258	.011
Gamma	.263	.009
Fronto-occipital and Frontal		
Alpha	.611	<.001
Fronto-occipital and Occipital		
Alpha	.636	<.001
Beta	.334	.001
Gamma	.218	.032
Fronto-temporal and Frontal		
no significant correlations		
Fronto-temporal and Temporal		
Alpha	.458	<.001
Beta	.226	.026

Significance level was set at $p < .05$

Discussion

In the present study, we investigated differences in short- and long-range connectivity between DOC patients in different states of consciousness and compared these to a healthy population. UWS patients in our study had significantly lower coherence in alpha frequency in parietal areas, and lower beta and alpha coherence in fronto-parietal connectivity than the control group. MCS patients had significantly lower coherence in the theta, beta and alpha frequencies in fronto-temporal and fronto-occipital connections. Additionally, the patient groups were found to show significantly lower alpha and beta power, and higher delta power over all brain regions than the control group. Alpha is hypothesized to be a basic form of information transmission in the brain [57]. Beta oscillations are associated with a great number of brain functions such as selective attention [58], working memory [59], object recognition [60], and perception [61]. Alterations in both rhythms, here a decrease in power in the patient groups, can be interpreted as markers for altered—and potentially reduced—cortical functioning. Increased delta power is in line with previous studies finding delta to be associated with unawareness in patients with DOC [62]. The differences in coherence within and between frontal and parietal regions between the patient groups and controls are in accordance with the theory, that long and short-range communication in the brain is hypothesized to be based, among others, on alpha phase-synchronization or phase-coherence [63, 64]. Therefore, the level of alpha synchronization may be directly linked to the level of attention and consciousness [65, 66]. The reduction in beta frequency may reflect the reduction (in MCS patients) or the total loss (in UWS patients) of awareness in patients with DOC. Reduced theta coherence and high delta power in the MCS patient group compared to the healthy controls is in line with previous studies reporting a connection between increased slow wave activity and a reduced level of consciousness in patients with severe brain injury [67, 68]. However, coherence and EEG power did not differentiate between UWS and MCS in our sample.

Additionally, we aimed at identifying markers in the connectivity patterns with prognostic value for the recovery from UWS. To the best of our knowledge, this is the first demonstration that high parietal delta and theta, and high fronto-parietal theta and alpha coherence appear to provide strong early evidence for recovery from UWS with high predictive sensitivity and specificity. Parietal

coherence, i.e. short-range connectivity within the parietal region, was significantly higher in delta and theta frequencies in the recovered group, as well as the coherence between frontal and parietal regions in delta, theta, alpha, and beta frequencies (long-range connectivity). The EEG power did not differ between the two groups. Delta waves are most prominent in early development and during slow-wave sleep. However, there is also evidence for their involvement in motivational processes [65]. Furthermore, an increase in delta oscillations during mental tasks [69] is suggested to represent a type of inhibition suppressing irrelevant neural activity during a mental task [70, 71].

High delta and theta coherence, as we found in the improved patients, is usually associated with lower levels of consciousness [67, 68]. However, Bagnato and colleagues examined the prognostic value of standard EEG in 106 UWS and MCS patients retrospectively and correlated the amplitudes, frequencies, and reactivity to stimuli with the 3 months outcome according to the CRS-R. Normal amplitudes, higher alpha frequency and reactivity to stimuli were associated with improvements in CRS-R scores after 3 months in contrast to lower amplitudes and delta and theta frequencies, but also patients with dominant delta power showed improvements [62]. An increase in alpha power has been shown to be correlated with recovery in UWS patients [72].

In our sample, coherence in different frequency bands predicted outcome, even when EEG power in these frequencies did not differ significantly between the groups. In this case this may indicate that not the mere percentage of the power of a certain frequency band in the brain activity is a marker for the state of a patient, but the coordinated information processing, i.e. here the phase-sychnrony within these frequency bands, yields important information about the status of the patient. Coherence, especially between frontal and parietal areas, is suggested to have a high diagnostic value for patients with DOC [37]. The activity in the fronto-parietal network comprising bilateral frontal and temporo-parietal cortices is commonly impaired in altered states of consciousness [73, 74]. The fronto-parietal network can be divided into two distinct sub-networks, the 'internal' and the 'external' network [75]. The first is involved mainly in the awareness of the self (precuneus/posterior cingulated, mesas-frontal/anterior cingulated, temporo-parietal cortices) [76, 77]. The latter, encompassing lateral and dorsal fronto-parietal areas, is responsible for awareness of the external world [78]. Damage of subcortical structures in frontal and parietal regions leads to decreased connectivity between these regions. This is argued to underlie the state of unconsciousness in UWS patients, and the severely reduced state of consciousness in MCS patients [79]. Light sedation can already lead to a decreased cortico-cortical connectivity in both 'internal' and 'external' networks in healthy volunteers [80]. FMRI studies showed a decrease in cortico-cortical connectivity in DOC patients in this network [13, 81]. Furthermore, functional connectivity in key nodes of both networks shows a linear correlation with decreasing consciousness [80]. Despite the fact, that we could not differentiate between MCS and UWS based on coherence patterns, i.e. we could not prove coherence to be a true neural correlate of consciousness in our sample, our findings still suggest, that the synchrony between frontal and parietal regions in patients, who will eventually improve from an unresponsive state of consciousness to an at least minimally conscious state is higher than in unfavourable clinical courses. Complete hypometabolism in the fronto-parietal network measured with 18-F-Fluorodeoxyglucose (FDG) Positron Emission Tomography (PET) has been associated with UWS, whereas partial preservation of the activity and incomplete hypometabolism in this area can be a marker for the MCS [82]. 69 % of the patients who were diagnosed UWS based on their CRS-R scores, but showed the activity pattern associated with MCS in the FDG-PET, recovered consciousness [82].

An increase in delta oscillations can be found in a wide range of pathological states, including structural lesions. Increased cortical delta activity was found over white matter lesions [49], in chronic aphasia patients with damages in left cortical-subcortical perisylvian areas [83], and can also be caused by a reduction of cortical blood flow caused by cerebral ischemia [84]. Brain lesions can cause focal attenuation of the EEG activity over the lesion site [50]. Because of these alterations we excluded electrodes over these sites from our analysis and examined the activity over the intact regions. However, since DOC patients often have diffuse lesions we also analyzed the complete set of electrodes. Coherence was generally higher with the complete electrode set; however, the analysis confirmed our findings. UWS patients who improved showed higher parietal (delta, theta) and fronto-parietal coherence (delta, theta, alpha, and beta).

Coherence also differed depending on the etiology of the brain damage. If the cause of the DOC is non-traumatic, patients who will eventually recover show high theta, alpha, and beta coherence between frontal and parietal areas. Again, intact communication between frontal and parietal brain areas seems to be a marker for a more positive clinical course. In case of TBI, high fronto-parietal and fronto-occipital gamma coherence after a TBI reflected a persisting UWS in our patient group. Spontaneous gamma oscillations are thought to be associated with thalamocortical synaptic interactions, possibly subserving the

integrative functions of consciousness [85, 86]. High gamma coherence in MCS patients and healthy controls is suggested to represent the high level of ongoing information gathering and the preserved representation of one self and the external [37, 87]. However, increased gamma amplitudes are also found during hallucinations in schizophrenic patients, and are suggested to reflect perceptual distortions in epilepsy [85]. Hyper-connectivity in this frequency band may reflect a dysfunctional communication between anterior and posterior brain regions in our UWS patient group. Nonetheless, this result would have to be tested in a larger sample of TBI patients.

The high sensitivity and specificity of the coherence we found for certain frequency bands is indicative of their value as prognostic markers for a positive clinical course. To be able to predict the outcome of one individual patient, cut-off values are needed which clearly separate coherence values, which predict a negative outcome, from those which predict a more positive clinical course. It is known, that local lesions can have an impact on the global connectivity pattern in the brain [88]. Our sample and its subgroups (UWS vs. MCS, improved vs. unimproved) featured a wide range of lesions which makes their influence on the results hard to determine. For predictions on the single subject basis, EEG characteristics of the specific lesion (ICH, SAH, TBI, etc.) would have to be considered.

The sensitivity, specificity, and cut-off values we provided here suggest that coherence analysis may become a useful prognostic tool in the future, even though they are currently far from being suitable for individual prognostication. Resting-state EEG is a standard procedure in the treatment of DOC patients. In contrasts to ERP analysis, no additional equipment is needed for the recordings. Therefore, the analysis of coherence could be a useful extension to the diagnostic routine in clinical settings.

Acknowledgments This study was conducted in the framework of the KOPFregister, supported by the ZNS-Hannelore Kohl Stiftung, Germany (Grant No. 2011013 awarded to Andreas Bender), and the Deutsche Stiftung Neurologie, Germany.

Compliance with ethical standards

Conflicts of interest None of the authors have potential conflicts of interest to be disclosed.

Ethical standards This study has been approved by the ethics committee of the University of Munich and has, therefore, been performed in the accordance with the ethical standards laid down in the 1964 Declaration of Helsinki.
The study was approved by the institutional review board of the University of Munich. Healthy controls gave written informed consent prior to participating in the experiment. For patients, written informed consent was provided by the appointed legal surrogates prior to participation.

References

1. Laureys S, Celesia GG, Cohadon F, Lavrijsen J, Leon-Carrion J, Sannita WG, Sazbon L, Schmutzhard E, von Wild KR, Zeman A, Dolce G, European Task Force on Disorders of C (2010) Unresponsive wakefulness syndrome: a new name for the vegetative state or apallic syndrome. BMC Med 8:68. doi:10.1186/1741-7015-8-68
2. Guldenmund P, Stender J, Heine L, Laureys S (2012) Mindsight: diagnostics in disorders of consciousness. Crit Care Res Pract 2012:624724. doi:10.1155/2012/624724
3. PVS TM-STFo (1994) Medical aspects of the persistent vegetative state (2). N Engl J Med 330(22):1572–1579. doi:10.1056/NEJM199406023302206
4. PVS TM-STFo (1994) Medical aspects of the persistent vegetative state (1). N Engl J Med 330(21):1499–1508. doi:10.1056/NEJM199405263302107
5. Giacino JT, Fins JJ, Laureys S, Schiff ND (2014) Disorders of consciousness after acquired brain injury: the state of the science. Nat Rev Neurol 10(2):99–114. doi:10.1038/nrneurol.2013.279
6. Giacino JT, Kalmar K, Whyte J (2004) The JFK Coma Recovery Scale-Revised: measurement characteristics and diagnostic utility. Arch Phys Med Rehabil 85(12):2020–2029
7. Schnakers C, Giacino J, Kalmar K, Piret S, Lopez E, Boly M, Malone R, Laureys S (2006) Does the FOUR score correctly diagnose the vegetative and minimally conscious states. Ann Neurol 60(6):744–745
8. Schnakers C, Giacino J, Laureys S (2010) Coma: detecting signs of consciousness in severely brain injured patients recovering from coma. In: Stone JH, Blouin M (eds) International Encyclopedia of Rehabilitation. http://cirrie.buffalo.edu/encyclopedia/en/article/133/
9. Giacino JT, Schnakers C, Rodriguez-Moreno D, Kalmar K, Schiff N, Hirsch J (2009) Behavioral assessment in patients with disorders of consciousness: gold standard or fool's gold? Prog Brain Res 177:33–48. doi:10.1016/S0079-6123(09)17704-X
10. Bekinschtein TA, Manes FF, Villarreal M, Owen AM, Della-Maggiore V (2011) Functional imaging reveals movement preparatory activity in the vegetative state. Front Hum Neurosci 5:5. doi:10.3389/fnhum.2011.00005
11. Fischer C, Luaute J, Morlet D (2010) Event-related potentials (MMN and novelty P3) in permanent vegetative or minimally conscious states. Clinical Neurophysiol 121(7):1032–1042. doi:10.1016/j.clinph.2010.02.005
12. Qin P, Di H, Liu Y, Yu S, Gong Q, Duncan N, Weng X, Laureys S, Northoff G (2010) Anterior cingulate activity and the self in disorders of consciousness. Hum Brain Mapp 31(12):1993–2002. doi:10.1002/hbm.20989
13. Vanhaudenhuyse A, Noirhomme Q, Tshibanda LJ, Bruno MA, Boveroux P, Schnakers C, Soddu A, Perlbarg V, Ledoux D, Brichant JF, Moonen G, Maquet P, Greicius MD, Laureys S, Boly M (2010) Default network connectivity reflects the level of consciousness in non-communicative brain-damaged patients. Brain 133(Pt 1):161–171. doi:10.1093/brain/awp313
14. Bender A, Jox RJ, Grill E, Straube A, Lule D (2015) Persistent vegetative state and minimally conscious state: a systematic review and meta-analysis of diagnostic procedures. Dtsch Arztebl Int 112(14):235–242. doi:10.3238/arztebl.2015.0235
15. Donchin E, Karis D, Bashore TR, Coles MGH, Gratton G (1986) Cognitivepsychophysiology and human information processing. In: Coles MGH, Donchin E, Porges SW (eds) Psychophysiology: systems, processes, and applications. Guildford, New York, pp 244–267
16. Risetti M, Formisano R, Toppi J, Quitadamo LR, Bianchi L, Astolfi L, Cincotti F, Mattia D (2013) On ERPs detection in

disorders of consciousness rehabilitation. Front Hum Neurosci 7:775
17. Lulé D, Noirhomme Q, Kleih SC, Chatelle C, Halder S, Demertzi A, Bruno MA, Gosseries O, Vanhaudenhuyse A, Schnakers C, Thonnard M, Soddu A, Kübler A, Laureys S (2013) Probing command following in patients with disorders of consciousness using a brain-computer interface. Clin Neurophysiol 124(1):101–106
18. Cavinato M, Volpato C, Silvoni S, Sacchetto M, Merico A, Piccione F (2011) Event-related brain potential modulation in patients with severe brain damage. Clin Neurophysiol 122(4):719–724. doi:10.1016/j.clinph.2010.08.024
19. Fischer C, Luaute J, Nemoz C, Morlet D, Kirkorian G, Mauguiere F (2006) Improved prediction of awakening or nonawakening from severe anoxic coma using tree-based classification analysis. Crit Care Med 34(5):1520–1524. doi:10.1097/01.Ccm.0000215823.36344.99
20. Fischer C, Morlet D, Giard M (2000) Mismatch negativity and N100 in comatose patients. Audiol Neurootol 5(3–4):192–197. doi:10.1159/000013880
21. Kotchoubey B (2005) Event-related potential measures of consciousness: two equations with three unknowns. Prog Brain Res 150:427–444. doi:10.1016/S0079-6123(05)50030-X
22. Schorr B, Schlee W, Arndt M, Lule D, Kolassa IT, Lopez-Rolon A, Bender A (2014) Stability of auditory event-related potentials in coma research. J Neurol 262(2):307–315. doi:10.1007/s00415-014-7561-y
23. Ragazzoni A, Pirulli C, Veniero D, Feurra M, Cincotta M, Giovannelli F, Chiaramonti R, Lino M, Rossi S, Miniussi C (2013) Vegetative versus Minimally Conscious States: a study using TMS-EEG, sensory and event-related potentials. PLoS One 8(2):ARTN e57069. doi:10.1371/journal.pone.0057069
24. Massimini M, Boly M, Casali A, Rosanova M, Tononi G (2009) A perturbational approach for evaluating the brain's capacity for consciousness. Prog Brain Res 177:201–214. doi:10.1016/S0079-6123(09)17714-2
25. Gosseries O, Thibaut A, Boly M, Rosanova M, Massimini M, Laureys S (2014) Assessing consciousness in coma and related states using transcranial magnetic stimulation combined with electroencephalography. Ann Fr Anesth 33(2):65–71. doi:10.1016/j.annfar.2013.11.002
26. Greicius MD, Krasnow B, Reiss AL, Menon V (2003) Functional connectivity in the resting brain: a network analysis of the default mode hypothesis. Proc Natl Acad Sci USA 100(1):253–258. doi:10.1073/pnas.0135058100
27. Raichle ME (2015) The brain's default mode network. Annu Rev Neurosci 38:433–447. doi:10.1146/annurev-neuro-071013-014030
28. Raichle ME, MacLeod AM, Snyder AZ, Powers WJ, Gusnard DA, Shulman GL (2001) A default mode of brain function. Proc Natl Acad Sci USA 98(2):676–682. doi:10.1073/pnas.98.2.676
29. Vincent JL, Kahn I, Snyder AZ, Raichle ME, Buckner RL (2008) Evidence for a frontoparietal control system revealed by intrinsic functional connectivity. J Neurophysiol 100(6):3328–3342. doi:10.1152/jn.90355.2008
30. Manganotti P, Formaggio E, Storti SF, Fiaschi A, Battistin L, Tonin P, Piccione F, Cavinato M (2013) Effect of high-frequency repetitive transcranial magnetic stimulation on brain excitability in severely brain-injured patients in minimally conscious or vegetative state. Brain Stimul 6(6):913–921. doi:10.1016/j.brs.2013.06.006
31. Piccione F, Cavinato M, Manganotti P, Formaggio E, Storti SF, Battistin L, Cagnin A, Tonin P, Dam M (2011) Behavioral and neurophysiological effects of repetitive transcranial magnetic stimulation on the minimally conscious state: a case study. Neurorehabil Neural Repair 25(1):98–102. doi:10.1177/1545968310369802
32. Jordan D, Ilg R, Riedl V, Schorer A, Grimberg S, Neufang S, Omerovic A, Berger S, Untergehrer G, Preibisch C, Schulz E, Schuster T, Schroter M, Spoormaker V, Zimmer C, Hemmer B, Wohlschlager A, Kochs EF, Schneider G (2013) Simultaneous electroencephalographic and functional magnetic resonance imaging indicate impaired cortical top-down processing in association with anesthetic-induced unconsciousness. Anesthesiology 119(5):1031–1042. doi:10.1097/ALN.0b013e3182a7ca92
33. Gosseries O, Schnakers C, Ledoux D, Vanhaudenhuyse A, Bruno MA, Demertzi A, Noirhomme Q, Lehembre R, Damas P, Goldman S, Peeters E, Moonen G, Laureys S (2011) Automated EEG entropy measurements in coma, vegetative state/unresponsive wakefulness syndrome and minimally conscious state. Funct Neurol 26(1):25–30
34. Sitt JD, King JR, El Karoui I, Rohaut B, Faugeras F, Gramfort A, Cohen L, Sigman M, Dehaene S, Naccache L (2014) Large scale screening of neural signatures of consciousness in patients in a vegetative or minimally conscious state. Brain 137:2258–2270. doi:10.1093/brain/awu141
35. Sara M, Pistoia F (2010) Complexity loss in physiological time series of patients in a vegetative state. Nonlinear Dynamics Psychol Life Sci 14(1):1–13
36. Sara M, Pistoia F, Pasqualetti P, Sebastiano F, Onorati P, Rossini PM (2011) Functional Isolation Within the Cerebral Cortex in the Vegetative State: a Nonlinear Method to Predict Clinical Outcomes. Neurorehabil Neural Repair 25(1):35–42. doi:10.1177/1545968310378508
37. Cavinato M, Genna C, Manganotti P, Formaggio E, Storti SF, Campostrini S, Arcaro C, Casanova E, Petrone V, Piperno R, Piccione F (2015) Coherence and Consciousness: study of Fronto-Parietal Gamma Synchrony in Patients with Disorders of Consciousness. Brain Topogr 28(4):570–579. doi:10.1007/s10548-014-0383-5
38. Pereda E, Quiroga RQ, Bhattacharya J (2005) Nonlinear multivariate analysis of neurophysiological signals. Prog Neurobiol 77(1–2):1–37. doi:10.1016/j.pneurobio.2005.10.003
39. Babiloni C, Binetti G, Cassetta E, Cerboneschi D, Dal Forno G, Del Percio C, Ferreri F, Ferri R, Lanuzza B, Miniussi C, Moretti DV, Nobili F, Pascual-Marqui RD, Rodriguez G, Romani GL, Salinari S, Tecchio F, Vitali P, Zanetti O, Zappasodi F, Rossini PM (2004) Mapping distributed sources of cortical rhythms in mild Alzheimer's disease. A multicentric EEG study. Neuroimage 22(1):57–67. doi:10.1016/j.neuroimage.2003.09.028
40. Nunez PL, Wingeier BM, Silberstein RB (2001) Spatial-temporal structures of human alpha rhythms: theory, microcurrent sources, multiscale measurements, and global binding of local networks. Hum Brain Mapp 13(3):125–164
41. Salenius S, Kajola M, Thompson WL, Kosslyn S, Hari R (1995) Reactivity of magnetic parieto-occipital alpha rhythm during visual imagery. Electroencephalogr Clin Neurophysiol 95(6):453–462
42. Salmelin R, Hari R, Lounasmaa OV, Sams M (1994) Dynamics of brain activation during picture naming. Nature 368(6470):463–465. doi:10.1038/368463a0
43. Babiloni C, Lizio R, Marzano N, Capotosto P, Soricelli A, Triggiani AI, Cordone S, Gesualdo L, Del Percio C (2015) Brain neural synchronization and functional coupling in Alzheimer's disease as revealed by resting state EEG rhythms. Int J Psychophysiol. doi:10.1016/j.ijpsycho.2015.02.008
44. Bagnato S, Boccagni C, St'Angelo A, Fingelkurts AA, Fingelkurts AA, Galardi G (2013) Emerging from an unresponsive wakefulness syndrome: brain plasticity has to cross a threshold level. Neurosci Biobehav Rev 37(10):2721–2736. doi:10.1016/j.neubiorev.2013.09.007
45. Oostenveld R, Fries P, Maris E, Schoffelen JM (2011) FieldTrip: open Source Software for Advanced Analysis of MEG, EEG, and

Invasive Electrophysiological Data. Comput Intell Neurosci 2011:9
46. Cui J, Xu L, Bressler SL, Ding M, Liang H (2008) BSMART: a Matlab/C toolbox for analysis of multichannel neural time series. Neural Netw 21(8):1094–1104. doi:10.1016/j.neunet.2008.05.007
47. Walter DO (1968) Coherence as a measure of relationship between EEG records. Electroencephalogr Clin Neurophysiol 24(3):282
48. Box G, Jenkins GM, Reinsel GC (1994) Time series analysis: forecasting and control, 3rd edn. Prentice Hall, Englewood Cliffs
49. Gloor P, Ball G, Schaul N (1977) Brain lesions that produce delta waves in the EEG. Neurology 27(4):326–333
50. Andraus ME, Alves-Leon SV (2011) Non-epileptiform EEG abnormalities: an overview. Arq Neuropsiquiatr 69(5):829–835
51. Pinheiro J, Bates D, De Roy S, Sarker D, Team RDC (2013) nlme: linear and nonlinear mixed effects models
52. Team RDC (2008) R: a language and environment for statistical computing
53. Noble WS (2009) How does multiple testing correction work? Nat Biotechnol 27(12):1135–1137. doi:10.1038/nbt1209-1135
54. Roback P, Askins RA (2005) Judicious use of multiple hypothesis tests. Conserv Biol 19(1):261–267. doi:10.1111/j.1523-1739.2005.00269.x
55. Shaffer J (1995) multiple hypothesis testing. Annu Rev Psychol 46:561–584
56. Youden WJ (1950) Index for rating diagnostic tests. Cancer 3(1):32–35
57. Klimesch W (1999) EEG alpha and theta oscillations reflect cognitive and memory performance: a review and analysis. Brain Res Rev 29(2–3):169–195. doi:10.1016/S0165-0173(98)00056-3
58. Gross J, Pollok B, Dirks A, Timmermann L, Butz A, Schnitzler A (2005) Task-dependent oscillations during unimanual and bimanual movements in the human primary motor cortex and SMA studied with magnetoencephalography. Neuroimage 26(1):91–98. doi:10.1016/j.neuroimage.2005.01.025
59. Tallon-Baudry C, Bertrand O, Fischer C (2001) Oscillatory synchrony between human extrastriate areas during visual short-term memory maintenance. J Neurosci 21(20):RC177
60. Sehatpour P, Molholm S, Schwartz TH, Mahoney JR, Mehta AD, Javitt DC, Stanton PK, Foxe JJ (2008) A human intracranial study of long-range oscillatory coherence across a frontal-occipital-hippocampal brain network during visual object processing. Proc Natl Acad Sci USA 105(11):4399–4404. doi:10.1073/pnas.0708418105
61. Donner TH, Siegel M, Oostenveld R, Fries P, Bauer M, Engel AK (2007) Population activity in the human dorsal pathway predicts the accuracy of visual motion detection. J Neurophysiol 98(1):345–359. doi:10.1152/jn.01141.2006
62. Bagnato S, Boccagni C, Sant'Angelo A, Prestandrea C, Mazzilli R, Galardi G (2015) EEG predictors of outcome in patients with disorders of consciousness admitted for intensive rehabilitation. Clin Neurophysiol 126(5):959–966. doi:10.1016/j.clinph.2014.08.005
63. Fries P (2005) A mechanism for cognitive dynamics: neuronal communication through neuronal coherence. Trends Cogn Sci 9(10):474–480. doi:10.1016/j.tics.2005.08.011
64. Lachaux JP, Rodriguez E, Martinerie J, Varela FJ (1999) Measuring phase synchrony in brain signals. Hum Brain Mapp 8(4):194–208
65. Knyazev GG (2013) EEG correlates of self-referential processing. Front Hum Neurosci 7:264. doi:10.3389/fnhum.2013.00264
66. Palva S, Palva JM (2007) New vistas for alpha-frequency band oscillations. Trends Neurosci 30(4):150–158. doi:10.1016/j.tins.2007.02.001
67. Fingelkurts AA, Fingelkurts AA, Bagnato S, Boccagni C, Galardi G (2012) DMN operational synchrony relates to self-consciousness: evidence from patients in vegetative and minimally conscious states. Open Neuroimag J 6:55–68. doi:10.2174/1874440001206010055
68. Leon-Carrion J, Martin-Rodriguez JF, Damas-Lopez J, Martin JMBY, Dominguez-Morales MR (2008) Brain function in the minimally conscious state: a quantitative neurophysiological study. Clin Neurophysiol 119(7):1506–1514. doi:10.1016/j.clinph.2008.03.030
69. Srinivasan R, Winter WR, Nunez PL (2006) Source analysis of EEG oscillations using high-resolution EEG and MEG. Prog Brain Res 159:29–42. doi:10.1016/S0079-6123(06)59003-X
70. Vogel W, Broverman DM, Klaiber EL (1968) EEG and mental abilities. Electroencephalogr Clin Neurophysiol 24(2):166–175
71. Harmony T (2013) The functional significance of delta oscillations in cognitive processing. Front Integr Neurosci 7:83. doi:10.3389/fnint.2013.00083
72. Babiloni C, Sara M, Vecchio F, Pistoia F, Sebastiano F, Onorati P, Albertini G, Pasqualetti P, Cibelli G, Buffo P, Rossini PM (2009) Cortical sources of resting-state alpha rhythms are abnormal in persistent vegetative state patients. Clin Neurophysiol 120(4):719–729. doi:10.1016/j.clinph.2009.02.157
73. Alkire MT, Miller J (2005) General anesthesia and the neural correlates of consciousness. Prog Brain Res 150:229–244. doi:10.1016/S0079-6123(05)50017-7
74. Laureys S (2005) The neural correlate of (un)awareness: lessons from the vegetative state. Trends Cogn Sci 9(12):556–559. doi:10.1016/j.tics.2005.10.010
75. Noirhomme Q, Soddu A, Lehembre R, Vanhaudenhuyse A, Boveroux P, Boly M, Laureys S (2010) Brain connectivity in pathological and pharmacological coma. Front Syst Neurosci 4:160. doi:10.3389/fnsys.2010.00160
76. Gusnard DA, Raichle ME, Raichle ME (2001) Searching for a baseline: functional imaging and the resting human brain. Nat Rev Neurosci 2(10):685–694. doi:10.1038/35094500
77. Greicius MD, Supekar K, Menon V, Dougherty RF (2009) Resting-State Functional Connectivity Reflects Structural Connectivity in the Default Mode Network. Cereb Cortex 19(1):72–78. doi:10.1093/cercor/bhn059
78. Boly M, Phillips C, Balteau E, Schnakers C, Degueldre C, Moonen G, Luxen A, Peigneux P, Faymonville ME, Maquet P, Laureys S (2008) Consciousness and cerebral baseline activity fluctuations. Hum Brain Mapp 29(7):868–874. doi:10.1002/hbm.20602
79. Davey MP, Victor JD, Schiff ND (2000) Power spectra and coherence in the EEG of a vegetative patient with severe asymmetric brain damage. Clin Neurophysiol 111(11):1949–1954. doi:10.1016/S1388-2457(00)00435-1
80. Boveroux P, Bonhomme V, Boly M, Vanhaudenhuyse A, Maquet P, Laureys S (2008) Brain function in physiologically, pharmacologically, and pathologically altered states of consciousness. Int Anesthesiol Clin 46(3):131–146. doi:10.1097/AIA.0b013e318181a8b3
81. Cauda F, Micon BM, Sacco K, Duca S, D'Agata F, Geminiani G, Canavero S (2009) Disrupted intrinsic functional connectivity in the vegetative state. J Neurol Neurosurg Psychiatry 80(4):429–431. doi:10.1136/jnnp.2007.142349
82. Stender J, Gosseries O, Bruno MA (2014) Diagnostic precision of PET imaging and functional MRI in disorders of consciousness: a clinical validation study (vol 384, pg 514, 2014). Lancet 384(9942):494
83. Spironelli C, Angrilli A (2009) EEG delta band as a marker of brain damage in aphasic patients after recovery of language. Neuropsychologia 47(4):988–994. doi:10.1016/j.neuropsychologia.2008.10.019
84. Nagata K, Tagawa K, Hiroi S, Shishido F, Uemura K (1989) Electroencephalographic correlates of blood flow and oxygen metabolism provided by positron emission tomography in patients with cerebral infarction. Electroencephalogr Clin Neurophysiol 72(1):16–30

85. Herrmann CS, Demiralp T (2005) Human EEG gamma oscillations in neuropsychiatric disorders. Clin Neurophysiol 116(12):2719–2733. doi:10.1016/j.clinph.2005.07.007
86. Llinas RRRU (1992) Rostrocaudal scan in human bra a global characteristic of the 40 Hz response during sensory input. In: Basar THB (ed) Induced rhythms in the brain. Birkhauser, Boston, pp 147–154
87. Fries P (2009) Neuronal gamma-band synchronization as a fundamental process in cortical computation. Annu Rev Neurosci 32:209–224. doi:10.1146/annurev.neuro.051508.135603
88. van Dellen E, Hillebrand A, Douw L, Heimans JJ, Reijneveld JC, Stam CJ (2013) Local polymorphic delta activity in cortical lesions causes global decreases in functional connectivity. Neuroimage 83:524–532. doi:10.1016/j.neuroimage.2013.06.009

Electronic Supplementary Material: Part 1 (Online Resource 1)

1. Coherence values and group statistics for the comparison between MCS patients, UWS patients, and the control group

1.1 Frontal

Supplementary Table 1.1: Mean coherence values and standard deviation for all three groups

	Group	Mean	Standard Deviation
Delta	UWS	.52	.12
	MCS	.52	.10
	Controls	.51	.11
Theta	UWS	.50	.09
	MCS	.51	.11
	Controls	.54	.08
Alpha	UWS	.48	.10
	MCS	.49	.08
	Controls	.62	.13
Beta	UWS	.42	.12
	MCS	.47	.13
	Controls	.43	.05
Gamma	UWS	.37	.14
	MCS	.42	.12
	Controls	.37	.08

Main and interaction effects of group affiliation (MCS, UWS, controls) and frequency band (delta, theta, alpha, beta, gamma) as predictors of the coherence within frontal areas:

Main effects:
Frequency: $x^2(5) = 116.876$, $p < .0001$
Group: $x^2(7) = 11.778$, $p = .002$

Interaction effects:
Frequency × Group: $x^2(9) = 16.577$, $p < .001$

We found following main and interaction effects for the comparison between the patient groups:

Main effects:
Frequency: $x^2(5) = 96.112$, $p < .0001$
Group: $x^2(6) = 5.140$, $p = .023$

Interaction effects:
Frequency × Group: $x^2(7) = 6.155$, $p = .013$

1.2 Parietal

Supplementary Table 1.2: Mean coherence values and standard deviation for all three groups

	Group	Mean	Standard

			Deviation
Delta	UWS	.48	.11
	MCS	.46	.12
	Controls	.44	.07
Theta	UWS	.46	.09
	MCS	.47	.13
	Controls	.46	.04
Alpha	UWS	.45	.09
	MCS	.45	.10
	Controls	.50	.06
Beta	UWS	.38	.11
	MCS	.41	.06
	Controls	.40	.04
Gamma	UWS	.34	.12
	MCS	.39	.13
	Controls	.34	.05

Main and interaction effects of group affiliation (MCS, UWS, controls) and frequency band (delta, theta, alpha, beta, gamma) as predictors of the coherence within parietal areas:

Main effects:
Frequency: $x^2(5) = 97.503$, $p < .0001$
Group: $x^2(7) = 13.697$, $p = .001$

Interaction effects:
Frequency × Group: $x^2(9) = 14.176$, $p < .001$

Contrasting the patient groups against the control group, we found an interaction effect for UWS vs. controls:

UWS/Controls × Frequency: $b = 0.007$, $t(385) = 2.079$, $p = .038$

We found following main and interaction effects for the comparison between the patient groups:

Main effects:
Frequency: $x^2(5) = 73.125$, $p < .0001$
Group: $x^2(6) = 5.403$, $p = .020$

Interaction effects:
Frequency × Group: $x^2(7) = 4.776$, $p < .028$

1.3 Fronto-Parietal

Supplementary Table 1.3: Mean coherence values and standard deviation for all three groups

	Group	Mean	Standard Deviation
Delta	UWS	.46	.11
	MCS	.41	.08
	Controls	.46	.08
Theta	UWS	.44	.09

	MCS	.42	.08
	Controls	.49	.06
Alpha	UWS	.43	.09
	MCS	.41	.07
	Controls	.52	.07
Beta	UWS	.35	.10
	MCS	.36	.08
	Controls	.42	.05
Gamma	UWS	.32	.12
	MCS	.33	.12
	Controls	.35	.06

Main and interaction effects of group affiliation (MCS, UWS, controls) and frequency band (delta, theta, alpha, beta, gamma) as predictors of the coherence between frontal and parietal areas:

Main effects:
Frequency: $x^2(5) = 124.567$, $p < .0001$

Group: not significant ($p = 0.07$)

Interaction effects:
Frequency × Group: $x^2(9) = 14.245$, $p < .001$

Contrasting the patient groups against the control group, we found a main effect of group for UWS vs. controls, and an interaction effect for UWS vs. controls:

UWS vs. Controls: $b = 0.050$, $t(94) = 2.402$, $p = .014$

UWS/Controls × Frequency: $b = 0.007$, $t(385) = 2.109$, $p = .035$

We found following main and interaction effects for the comparison between the patient groups:

Main effects:
Frequency: $x^2(5) = 94.826$, $p < .0001$
Group: $x^2(6) = 4.608$, $p < .031$

Interaction effects:
Frequency × Group: $x^2(7) = 4.531$, $p < .033$

1.4 Fronto-occipital

Supplementary Table 1.3: Mean coherence values and standard deviation for all three groups

	Group	**Mean**	**Standard Deviation**
Delta	UWS	.50	.12
	MCS	.46	.08
	Controls	.56	.12
Theta	UWS	.48	.10
	MCS	.47	.06
	Controls	.58	.08
Alpha	UWS	.47	.10

	MCS	.46	.06
	Controls	.61	.10
Beta	UWS	.39	.10
	MCS	.40	.07
	Controls	.47	.06
Gamma	UWS	.34	.13
	MCS	.37	.10
	Controls	.40	.07

Main and interaction effects of group affiliation (MCS, UWS, controls) and frequency band (delta, theta, alpha, beta, gamma) as predictors of the coherence between frontal and occipital areas:

Main effects:
Frequency: $x^2(5) = 110.577$, $p < .0001$
Group: $x^2(7) = 8.229$, $p = .016$

Interaction effects:
Frequency × Group: $x^2(9) = 16.824$, $p < .001$

Contrasting the patient groups against the control group, we found a main effect of group for MCS vs. Controls:

MCS vs. Controls: $b = 0.048$, $t(94) = 2.245$, $p = .027$

We found following main and interaction effects for the comparison between the patient groups:

Main effects:
Frequency: $x^2(5) = 80.862$, $p < .0001$
Group: $x^2(6) = 5.746$, $p < .016$

Interaction effects:
Frequency × Group: $x^2(7) = 6.641$, $p < .010$

1.5 Fronto-temporal

Supplementary Table 1.3: Mean coherence values and standard deviation for all three groups

	Group	**Mean**	**Standard Deviation**
Delta	UWS	.46	.12
	MCS	.43	.08
	Controls	.49	.10
Theta	UWS	.44	.10
	MCS	.42	.08
	Controls	.50	.05
Alpha	UWS	.42	.10
	MCS	.41	.08
	Controls	.51	.05
Beta	UWS	.34	.11
	MCS	.34	.09

	Controls	.42	.06
Gamma	UWS	.30	.13
	MCS	.32	.13
	Controls	.34	.07

Main and interaction effects of group affiliation (MCS, UWS, controls) and frequency band (delta, theta, alpha, beta, gamma) as predictors of the coherence between frontal and temporal areas:

Main effects:
Frequency: $x^2(5) = 148.391$, $p < .0001$
Group: not significant ($p = .118$)

Interaction effects:
Frequency × Group: $x^2(9) = 17.734$, $p < .001$

Contrasting the patient groups against the control group, we found a main effect of group for MCS vs. Controls:

MCS vs. Controls: $b = 0.048$, $t(94) = 2.187$, $p = .031$

We found following main and interaction effects for the comparison between the patient groups:

Main effects:
Frequency: $x^2(5) = 111.143$, $p < .0001$
Group: $x^2(6) = 4.606$, $p < .031$

Interaction effects:
Frequency × Group: $x^2(7) = 7.107$, $p < .010$

2. EEG power values and group statistics fort he comparison between MCS patients, UWS patients, and the control group

2.1 Frontal

Supplementary Table 2.1: Mean power values (percent of the individual overall power for each frequency band) and standard deviation for all three groups

	Group	**Mean**	**Standard Deviation**
Delta	UWS	71.66	13.64
	MCS	74.42	12.70
	Controls	45.94	19.08
Theta	UWS	19.29	8.66
	MCS	17.56	11.20
	Controls	18.26	4.55
Alpha	UWS	5.93	7.66
	MCS	4.75	3.42

	Controls	30.86	18.43
Beta	UWS	1.99	3.70
	MCS	1.75	2.27
	Controls	4.03	2.44
Gamma	UWS	1.11	2.42
	MCS	1.50	2.83
	Controls	.88	.73

Main and interaction effects of group affiliation (MCS, UWS, controls) and frequency band (delta, theta, alpha, beta, gamma) as predictors of the EEG power in frontal areas:

Interaction effects:
Frequency ×Group: x^2 (9) = 22.685, $p < .0001$

Contrasting the patient groups against the control group, we found following main and interaction effects:

UWS vs. Controls: $b = -5.080$, $t(94) = -2.114$, $p = .037$

UWS/Controls ×Frequency: $b = 1.693$, $t(385) = 2.337$, $p = .019$

MCS/Controls ×Frequency: $b = 2.018$, $t(385) = 2.056$, $p = .040$

We found following main effect for the comparison between the patient groups:

Frequency: $x^2(5) = 374.928$, $p < .0001$

Student's *t*-test:

UWS vs controls:
Delta: $t(33) = 5.997$, $p < .001$
Alpha: $t(26) = -6.401$, $p < .001$
Beta: $t(80) = -2.937$, $p = .015$

MCS vs controls:
Delta: $t(37) = 5.104$, $p < .001$
Alpha: $t(25) = -6.755$, $p < .001$
Beta: $t(37) = -2.219$, $p = .006$

2.2 Parietal

Supplementary Table 2.2: Mean power values (percent of the individual overall power for each frequency band) and standard deviation for all three groups

	Group	Mean	Standard Deviation
Delta	UWS	69.19	15.33
	MCS	69.25	15.45
	Controls	40.77	17.64
Theta	UWS	21.06	9.75
	MCS	20.33	12.94
	Controls	16.72	4.57
Alpha	UWS	7.34	9.35
	MCS	6.91	6.66
	Controls	36.32	18.54
Beta	UWS	1.603	1.80
	MCS	2.04	2.32
	Controls	5.16	2.73
Gamma	UWS	.79	1.46
	MCS	1.44	2.75
	Controls	1.00	1.20

Main and interaction effects of group affiliation (MCS, UWS, controls) and frequency band (delta, theta, alpha, beta, gamma) as predictors of EEG power in parietal areas:

Interaction effects:
Frequency × Group: $x^2(9) = 31.948$, $p < .0001$

Contrasting the patient groups against the control group, we found following main and interaction effects:

UWS vs. Controls: $b = -6.753$, $t(94) = -2.899$, $p = .004$

UWS/Controls × Frequency: $b = 2.251$, $t(385) = 3.205$, $p = .001$

MCS/Controls × Frequency: $b = 2.013$, $t(385) = 2.115$, $p = .035$

We found following main and interaction effects for the comparison between the patient groups:

Main effects:
Frequency: $x^2(5) = 388.553$, $p < .0001$

Student's *t*-test:

UWS vs controls:
Delta: $t(80) = 7.303$, $p < .001$
Theta: $t(78) = 2.739$, $p = .008$
Alpha: $t(27) = -7.283$, $p < .001$
Beta: $t(31) = -5.874$, $p < .001$

MCS vs controls:
Delta: $t(37) = 5.134$, $p < .001$
Alpha: $t(31) = -7.074$, $p < .001$
Beta: $t(37) = -3.661$, $p = .001$

2.3 Occipital

Supplementary Table 2.3: Mean power values (percent of the individual overall power for each frequency band) and standard deviation for all three groups

	Group	Mean	Standard Deviation
Delta	UWS	67.51	15.25
	MCS	68.83	13.31
	Controls	36.90	19.90
Theta	UWS	21.75	9.42
	MCS	19.86	11.30
	Controls	16.14	3.74
Alpha	UWS	7.79	10.48
	MCS	7.39	5.96
	Controls	41.25	21.43
Beta	UWS	1.95	2.05
	MCS	2.36	2.65
	Controls	4.71	2.64
Gamma	UWS	.98	1.54
	MCS	1.54	2.73
	Controls	.98	1.07

Main and interaction effects of group affiliation (MCS, UWS, controls) and frequency band (delta, theta, alpha, beta, gamma) as predictors of the EEG power in occipital areas:

Interaction effects:
Frequency × Group: $x^2(9) = 35.454$, $p < .0001$

Contrasting the patient groups against the control group, we found following main and interaction effects:

UWS vs. Controls: $b = -7.037$, $t(94) = -2.981$, $p = .003$

MCS vs. Controls: $b = 6.804$, $t(94) = -2.126$, $p = .036$

UWS/Controls × Frequency: $b = 2.345$, $t(385) = 3.295$, $p = .001$

MCS/Controls × Frequency: $b = 2.268$, $t(385) = 2.251$, $p = .019$

We found following main and interaction effects for the comparison between the patient groups:

Main effects:
Frequency: $x^2(5) = 394.484$, $p < .0001$

Student's *t*-test:

UWS vs controls:
Delta: $t(80) = 7.643$, $p < .001$
Theta: $t(79) = 3.856$, $p < .001$
Alpha: $t(27) = -7.296$, $p < .001$
Beta: $t(80) = -5.076$, $p < .001$

MCS vs controls:
Delta: $t(37) = 5.481$, $p < .001$
Alpha: $t(28) = -7.301$, $p < .001$
Beta: $t(37) = -2.695$, $p = .001$

2.4 Temporal

Supplementary Table 2.4: Mean power values (percent of the individual overall power for each frequency band) and standard deviation for all three groups

	Group	Mean	Standard Deviation
Delta	UWS	67.13	14.64
	MCS	67.54	15.54
	Controls	38.36	17.54
Theta	UWS	22.14	9.58
	MCS	20.18	12.59
	Controls	19.31	5.69
Alpha	UWS	7.26	8.97
	MCS	7.74	7.15
	Controls	35.37	17.25
Beta	UWS	2.20	2.63
	MCS	2.58	3.23
	Controls	5.44	2.84
Gamma	UWS	1.24	2.02
	MCS	1.93	3.43
	Controls	1.51	1.66

Main and interaction effects of group affiliation (MCS, UWS, controls) and frequency band (delta, theta, alpha, beta, gamma) as predictors of the EEG power in temporal areas:

Interaction effects:
Frequency ×Group: $x^2(9) = 33.517$, $p < .0001$

Contrasting the patient groups against the control group, we found following main and interaction effects:

UWS vs. Controls: $b = -6.701$, $t(94) = -3.016$, $p = .003$

UWS/Controls ×Frequency: $b = 2.233$, $t(385) = 3.334$, $p < .001$

MCS/Controls ×Frequency: $b = 1.945$, $t(385) = 2.143$, $p = .032$

We found following main and interaction effects for the comparison between the patient groups:

Main effects:
Frequency: $x^2(5) = 394.389$, $p < .0001$

Student's *t*-test:

UWS vs controls:
Delta: $t(80) = 7.630$, $p < .001$
Alpha: $t(28) = -7.570$, $p < .001$
Beta: $t(80) = -4.940$, $p < .001$

MCS vs controls:
Delta: $t(37) = 5.273$, $p < .001$
Alpha: $t(33) = -6.949$, $p < .001$
Beta: $t(37) = -2.886$, $p = .006$

Electronic Supplementary material: Part 2 (Online Resource 2)

3.1 Baseline and follow-up CRS-R scores for UWS patients

Supplementary Table 3.1: Baseline CRS-R scores from the baseline EEG assessment and 12 months follow-up CRS-R scores from the UWS patients.

ID	RE-COVERY	CRS-R TOTAL BASELINE	AUDI-TORY	VISUAL	MOTOR	VERBAL	COMMUNI-CATION	AROU-SAL	CRS-R FOLLOW-UP	AUDI-TORY	VIUSAL	MOTOR	VERBAL	COMMUNI-CATION	AROU-SAL
P1	no	6	1	0	1	2	0	2	**5**	1	0	1	2	0	1
P2	no	7	1	1	2	1	0	2	**7**	1	1	2	1	0	2
P3	yes	8	1	1	2	2	0	2	**18**	4	4	5	2	0	3
P5	no	1	0	0	0	1	0	0	**7**	1	1	2	1	0	2
P6	no	2	0	0	1	0	0	1	**5**	0	0	2	2	0	1
P9	no	4	0	0	2	0	0	2	**6**	1	0	2	1	0	2
P10	no	7	1	0	2	2	0	2	**7**	1	0	2	2	0	2
P11	no	2	1	0	0	1	0	1	**5**	1	0	2	1	0	1
P12	no	5	1	0	1	2	0	1	**5**	1	0	2	1	0	1
P13	no	1	0	0	0	1	0	0	**8**	2	1	2	1	0	2
P15	no	6	1	0	2	2	0	1	**6**	1	0	2	2	0	1
P16	no	4	0	0	2	1	0	1	**4**	0	0	2	1	0	1
P17	yes	6	1	0	2	1	0	2	**22**	4	5	6	3	1	3
P18	no	5	0	0	2	1	0	2	**5**	0	0	2	1	0	2
P19	yes	4	1	1	0	0	0	2	**21**	4	5	6	2	1	3
P20	no	5	1	0	2	1	0	1	**5**	1	0	2	1	0	1
P21	no	6	1	0	2	1	0	2	**6**	1	0	2	1	0	2
P23	no	3	1	1	0	0	0	1	**6**	1	1	2	1	0	1
P24	yes	3	0	0	1	0	0	2	**8**	1	1	3	1	0	2
P25	yes	3	0	0	2	1	0	0	**9**	1	2	3	1	0	2
P26	no	3	1	1	0	0	0	1	**3**	1	1	0	0	0	1
P27	no	5	1	0	2	1	0	1	**5**	1	0	2	1	0	1
P28	no	3	1	0	1	1	0	0	**3**	0	0	2	1	0	0
P29	no	5	1	0	2	1	0	1	**5**	1	0	1	0	0	2

P30	no	7	1	0	2	2	0	2	**7**	1	0	2	2	0	2
P31	no	8	1	1	3	1	0	2	**8**	1	1	3	1	0	2
P32	no	1	0	0	0	1	0	0	**1**	0	0	0	1	0	0
P33	no	6	1	0	2	2	0	1	**6**	1	0	2	2	0	1
P34	no	7	1	1	2	2	0	1	**7**	1	1	2	2	0	1
P37	no	6	1	0	2	1	0	2	**6**	1	0	2	1	0	2
P38	yes	6	1	1	1	1	0	3	**23**	4	5	6	3	2	3
P39	no	3	0	0	0	1	0	2	**3**	0	0	0	1	0	2
P40	no	4	0	0	2	1	0	1	**4**	0	0	2	1	0	1
P41	no	7	1	1	1	2	0	2	**7**	1	1	1	2	0	2
P42	no	2	0	0	0	1	0	1	**6**	1	0	2	1	0	2
P43	no	7	0	1	2	2	0	2	**7**	0	1	2	2	0	2
P44	no	3	0	0	0	1	0	2	**3**	0	0	0	1	0	2
P45	yes	7	2	0	2	2	0	1	**9**	3	0	2	2	0	2
P46	no	3	1	0	2	1	0	0	**3**	1	0	2	1	0	0
P47	yes	5	0	0	2	1	0	2	**9**	1	0	5	1	0	2
P48	no	3	1	0	1	1	0	0	**4**	1	0	1	1	0	1
P50	no	3	0	0	2	0	0	1	**3**	0	0	2	0	0	1
P51	no	6	1	1	2	0	0	2	**7**	2	2	1	0	0	2
P52	no	8	1	1	2	2	0	2	**8**	1	1	2	2	0	2
P55	yes	2	0	0	0	1	0	1	**20**	3	5	6	3	1	2
P56	no	3	0	0	2	1	0	0	**3**	0	0	2	1	0	0
P57	no	4	1	0	0	1	0	2	**4**	1	0	0	1	0	2
P59	no	6	1	0	1	2	0	2	**6**	1	0	1	2	0	2
P60	no	5	1	0	2	1	0	1	**5**	1	0	2	1	0	1
P61	no	6	1	0	2	1	0	2	**6**	1	0	2	1	0	2
P63	yes	6	1	1	1	2	0	1	**7**	1	1	1	2	1	1
P64	no	4	0	0	2	1	0	1	**4**	0	0	2	1	0	1
P65	no	5	0	0	2	1	0	2	**5**	0	0	2	1	0	2
P66	no	6	0	1	2	1	0	2	**6**	0	1	2	1	0	2
P69	no	6	1	0	2	1	0	2	**6**	1	0	2	1	0	2
P70	no	3	0	0	2	1	0	0	**3**	0	0	2	1	0	0
P72	no	6	1	0	2	1	0	2	**6**	1	0	2	1	0	2

P73	yes	6	1	1	2	1	0	2	**10**	1	3	2	1	1	2

3.2 Complete main and interaction effects for group, frequency band, and etiology as predictors of coherence within and between brain regions

Frontal coherence

Main effects:
Frequency: $x^2(5) = 86.357$. $p < .0001$
Group: $x^2(6) = 3.936$. $p = .047$
Etiology: $x^2(7) = 4.679$. $p = .030$

Interactions:
not significant ($p > .2$)

Parietal coherence

Main effects:
Frequency: $x^2(5) = 84.549$. $p < .0001$
Group: not significant ($p = .17$)
Etiology: $x^2(7) = 5.235$. $p = .02$

Interactions:
not significant ($p > .05$)

Fronto-Parietal coherence

Main effects:
Frequency: $x^2(5) = 91.640$. $p < .0001$
Group: not significant ($p = .522$)
Etiology: not significant (p = .052)

Interactions:
Frequency × Group:
$x^2(8) = 5.533$. $p = .018$
Frequency × Group × Etiology:
$x^2(10) = 6.614$. $p = .036$; $b = 0.088$. $t(228) = 3.086$. $p = .002$

Fronto-occipital coherence

Main effects:
Frequency: $x^2(5) = 82.289$. $p < .0001$
Group: $x^2(7) = 4.228$. $p = .039$
Etiology: not significant (p = .069)

Interactions:
Frequency × Group:
$x^2(10) = 6.092$. $p = .013$
Frequency × Group × Etiology:
$x^2(13) = 7.308$. $p = .025$; $b = -0.018$. $t(228) = -2.189$. $p = .029$

Fronto-temporal coherence

Main effects:
Frequency: $x^2(5) = 128.631$. $p < .0001$
Group: $x^2(7) = 8.451$. $p = .014$
Etiology: not significant (p = .088)

Interactions:
Frequency × Group:
$x^2(10) = 12.878$. $p = .001$; $b = -0.089$. $t(286) = -2.524$. $p = .012$
Frequency × Group × Etiology:
$x^2(13) = 15.749$. $p = .001$

3.3 Main and interaction effects for group, frequency band, and etiology as predictors of EEG power

Supplementary Table 3.2: Mean power values (percent of the individual overall power for each frequency band) and standard deviation for improved and unimproved patients

	Group „I“ = improved „U“ = unimproved	Mean	Standard Deviation
Frontal			
Delta	I	77.02	10.77
	U	70.40	14.03
Theta	I	17.69	8.17
	U	19.67	8.82
Alpha	I	3.84	3.71
	U	6.41	8.27
Beta	I	1.02	1.12
	U	2.22	4.06
Gamma	I	.40	.71
	U	1.27	2.65
Parietal			
Delta	I	77.11	9.78
	U	67.33	15.87
Theta	I	17.47	7.55
	U	21.90	10.09
Alpha	I	3.89	3.26
	U	8.15	10.12
Beta	I	1.12	1.15
	U	1.71	1.91
Gamma	I	.39	.59
	U	.88	1.59
Occipital			

Delta	I	75.31	11.27
	U	65.68	15.57
Theta	I	18.58	8.51
	U	22.49	9.55
Alpha	I	4.42	3.67
	U	8.58	11.40
Beta	I	1.25	1.24
	U	2.11	2.17
Gamma	I	.42	.73
	U	1.11	1.65
Temporal			
Delta	I	74.40	11.17
	U	65.43	14.93
Theta	I	19.44	9.60
	U	22.77	9.57
Alpha	I	4.19	3.33
	U	7.98	9.72
Beta	I	1.32	1.28
	U	2.41	2.82
Gamma	I	.63	1.25
	U	1.39	2.15

Frontal power:

Main effects:
Frequency: $x^2(5) = 301.480$. $p < .0001$

Interactions:
not significant ($p > .05$)

Parietal power:

Main effects:
Frequency: $x^2(5) = 312.105$. $p < .0001$
Group: not significant ($p = .058$)
Etiology: not significant ($p = .067$)

Interactions:
Frequency × Group:
$x^2(8) = 3.863$. $p = .049$
Frequency × Group × Etiology:
$x^2(10) = 6.241$. $p = .044$

Occipital power:

Main effects:
Frequency: $x^2(5) = 312.105$. $p < .0001$
Group: not significant ($p = .060$)
Etiology: not significant ($p = .070$)

Interactions:
Frequency × Group:
$x^2(8) = 3.978$. $p = .046$
Frequency × Group × Etiology:
$x^2(10) = 6.207$. $p = .044$

Temporal power:

Main effects:
Frequency: $x^2(5) = 319.133$. $p < .0001$
Group: not significant ($p = .061$)
Etiology: not significant ($p = .072$)

Interactions:
Frequency × Group:
$x^2(8) = 3.934$, $p = .047$
Frequency × Group × Etiology: not significant ($p > .05$)

III Consciousness Indexing and Outcome Prediction with Resting-State EEG in Severe Disorders of Consciousness

Reference: Stefan, S., Schorr, B., Lopez-Rolon, A., Kolassa, I.T., Shock, J.P., Rosenfelder, M., Heck, S., Bender, A. (2018). Consciousness Indexing and Outcome Prediction with Resting-State EEG in Severe Disorders of Consciousness. *Brain Topography*, (EPub) https://doi.org/10.1007/s10548-018-0643-x

Brain Topography
https://doi.org/10.1007/s10548-018-0643-x

ORIGINAL PAPER

Consciousness Indexing and Outcome Prediction with Resting-State EEG in Severe Disorders of Consciousness

Sabina Stefan[1] · Barbara Schorr[2,3] · Alex Lopez-Rolon[4] · Iris-Tatjana Kolassa[3] · Jonathan P. Shock[5] · Martin Rosenfelder[2,3] · Suzette Heck[4] · Andreas Bender[2,4]

Received: 30 May 2017 / Accepted: 7 April 2018

Abstract

We applied the following methods to resting-state EEG data from patients with disorders of consciousness (DOC) for consciousness indexing and outcome prediction: microstates, entropy (i.e. approximate, permutation), power in alpha and delta frequency bands, and connectivity (i.e. weighted symbolic mutual information, symbolic transfer entropy, complex network analysis). Patients with unresponsive wakefulness syndrome (UWS) and patients in a minimally conscious state (MCS) were classified into these two categories by fitting and testing a generalised linear model. We aimed subsequently to develop an automated system for outcome prediction in severe DOC by selecting an optimal subset of features using sequential floating forward selection (SFFS). The two outcome categories were defined as UWS or dead, and MCS or emerged from MCS. Percentage of time spent in microstate D in the alpha frequency band performed best at distinguishing MCS from UWS patients. The average clustering coefficient obtained from thresholding beta coherence performed best at predicting outcome. The optimal subset of features selected with SFFS consisted of the frequency of microstate A in the 2–20 Hz frequency band, path length obtained from thresholding alpha coherence, and average path length obtained from thresholding alpha coherence. Combining these features seemed to afford high prediction power. Python and MATLAB toolboxes for the above calculations are freely available under the GNU public license for non-commercial use (https://qeeg.wordpress.com)

Keywords Quantitative EEG · Unresponsive wakefulness syndrome · Minimally conscious state · Outcome prediction · Microstate analysis · Sequential floating forward selection

Introduction

Severe disorders of consciousness (DOC) are states of unconsciousness caused by injury or malfunction of neural systems which regulate arousal and awareness (Posner et al. 2007; Giacino et al. 2014). Despite significant advances in medical technology, patients with DOC may remain in a vegetative state, also known as unresponsiveness wakefulness syndrome (UWS), characterised by arousal without awareness (Laureys et al. 2010), or a minimally conscious state (MCS), defined by definite but minimal behavioural signs of awareness of oneself and one's environment, which may wax and wane (Giacino et al. 2002). For ethical, therapeutic and economic reasons, it is important to predict outcome as early, reliably and sensitively as possible (Graf et al. 2008; Grill et al. 2013; Lopez-Rolon et al. 2015).

The best criterion available to date for establishing the diagnosis of UWS or MCS is behavioural assessment by means of the clinical scales such as the revised version of

Handling Editor: Christoph M. Michel.

Electronic supplementary material The online version of this article (https://doi.org/10.1007/s10548-018-0643-x) contains supplementary material, which is available to authorized users.

✉ Jonathan P. Shock
jonathan.shock@uct.ac.za

[1] School of Engineering, Brown University, 182 Hope Street, Box D, Providence, RI 02912, USA

[2] Department of Neurology, Therapiezentrum Burgau, Kapuzinerstrasse 34, 89331 Burgau, Germany

[3] Clinical and Biological Psychology, Institute of Psychology and Education, Ulm University, 89081 Ulm, Germany

[4] Department of Neurology, University of Munich, Marchioninistrasse 15, 81377 Munich, Germany

[5] Department of Mathematics and Applied Mathematics, University of Cape Town, Rondebosch, Private Bag X1, Cape Town 7701, South Africa

Published online: 17 April 2018

the coma recovery scale (CRS-R). However, although every effort is made in clinical settings to avoid it, patients who do understand CSR-R commands, but are unable to follow them due to motor impairments could potentially receive a wrong UWS diagnosis.

Finding more accurate methods for discriminating DOC diagnostic groups is imperative, considering that diagnosis has a direct impact on decisions regarding life-sustaining therapy (Howell et al. 2013), and misdiagnosis prevalence has been reported to be possibly as high as 43% (Howell et al. 2013).

Electroencephalography (EEG) is a non-invasive, safe and relatively easy method for gauging the function of the brain, which allows the application of quantitative methods to better understand and interpret patterns of EEG data related to DOC (Kondziella et al. 2016). Applied to DOC, as expected these methods are focussed on the objective assessment of EEG signals and aim to detect subtleties that may escape visual inspection, thus minimising subjectivity and human error in prognostication (Schorr et al. 2015, 2016). Thus, these methods may expand the manner in which EEG is currently used in clinical practice by providing a more rigorous, objective and statistically coherent analysis of the data through the mathematical extraction of descriptive parameters (Gosseries et al. 2011). High-density EEG techniques in particular are a promising avenue of research, which is playing increasingly an important role in diagnosis and prognosis (Noirhomme and Laureys 2014).

However, researchers are still to find EEG features, which could index consciousness in such a manner as to be able to substitute reliably behavioural assessment in diagnosis and outcome prediction, where outcome categories are defined here as UWS or dead, and MCS or better.

In the present exploratory study we applied to resting-state, high-density EEG data from patients with DOC the following methods to examine the extent to which they could be used for consciousness indexing and outcome prediction: microstates, entropy (i.e. approximate, permutation), power in alpha and delta frequency bands, and connectivity (i.e. weighted symbolic mutual information, symbolic transfer entropy, complex network analysis). These are techniques that are commonly applied in EEG studies, but it remains unclear the relative performance of each metric in assessing consciousness. The aim then is to be able to assess these measures on a single dataset as well as apply and evaluate EEG measures that aren't ordinarily applied in DOC studies. This allows us then to apply machine-learning techniques to build a model to predict coma outcome, which may be a viable method to provide information on an individual basis, as opposed to group differences, as often done in DOC studies (Noirhomme et al. 2015).

To build the model, we extracted an optimal subset of features using sequential forward floating selection (SFFS), which is an algorithm selects a subset of EEG features by starting from an empty set and adding incrementally one feature at a time and deleting them conditionally while avoiding partially the local optima of the correct classification rate (Ververidis and Kotropoulos 2008).

The present exploratory study used standardized clinical evaluations at baseline and follow-up by means of the CRS-R to minimize misdiagnosis, which could also influence the analysis of EEG features. As noted in the review by Noirhomme et al. considerable limitations of machine-learning applied to EEG is the difficulty in establishing a reliable behavioural assessment and fluctuations in the patient's level of arousal (Noirhomme et al. 2015). In the absence of a gold standard to assess consciousness, consilience between multiple independent assessments might be a rational way forward as applied in the study by Chennu et al. (2017). In this study, the authors compared EEG measures to results obtained from positron emission tomography, which may be a useful method of validating EEG studies. Another important consideration is the sample size needed in such machine-learning studies to ensure robustness and generalizability of results—for example, in the review by Noirhomme et al., they only consider studies with over 50 patients, but it remains unclear whether that is sufficient. However, it may still be illuminating as a starting point to observe how various biomarkers compare on a small sample size.

We must also note that we do not aim to address known limitations of the techniques evaluated in this study, but to investigate several EEG biomarkers of consciousness on the same dataset to be able to compare the relative usefulness of these features. We also aimed to apply measures that are ordinarily applied to index consciousness to instead predict outcome, thus avoiding the complication of assessing prognosis through diagnosis.

Microstate Analysis

Microstate analysis is a spatio-temporal method that analyses the topographical maps of electrical potentials over the electrode array as well as the temporal evolution of these topographies, such that multichannel EEG data is essentially considered as a series of sequential topographies of electric fields (Pascual-Marqui et al. 1995). Interestingly, most studies find that four archetypal maps account for over 70% of total topographical variance, and furthermore that EEG topography remains quasi-stable for about 80–120 ms before abruptly changing into a topography represented by a different archetypal map (Murray et al. 2008). Microstates are thus defined as these archetypal maps of quasi-stability, during which global topography is invariant, although electric field strength may vary and polarity invert (Lehmann et al. 1987). The four topographies that are the most commonly exhibited are,

A right-frontal to left-posterior
B left-frontal to right-posterior
C frontal to occipital
D mostly frontal and medial to slightly less occipital activity than class C

It has been suggested that microstates reflect primitive information processing such that their generation is likely the result of the activity of distinct neural arrays associated with specific neural functions (Lehmann et al. 1998). Microstate analyses have proven to be useful in classifying transitive brain states. For example, it has been shown that microstate B in schizophrenics displays significantly different field configurations and shorter durations in patients than controls (Lehmann et al. 2005). Furthermore, microstate analyses have been applied to investigate differences in sleep stages between narcoleptic patients and controls and to probe the brain in different sleep stages (Kuhn et al. 2015; Brodbeck et al. 2012). This is a promising avenue of research considering that microstate analyses have been successful in probing the brain in different states, potentially allowing for the discrimination of patients in UWS/MCS states. Furthermore, such analyses might help us to understand key differences in the brain functions of patients with different severities of coma. As far as we know, microstate analyses have not previously been employed in this manner for the investigation of DOC and DOC outcome prediction, and may be an interesting topic of future research. In this paper, however, we do not intend to make biological claims between DOC patients in different outcome groups, but rather assess how predicative this common EEG technique in assessing consciousness as well as coma outcome.

Entropy

Measures of entropy applied to EEG signals aim to quantify the unpredictability of outputs of the complex system of neural networks underlying consciousness. Numerous measures of entropy have been applied to the analysis of EEG signals, particularly in the studies of anesthesia and epilepsy (Bruhn et al. 2000; Kannathal et al. 2005). However, measures of entropy, such as approximate entropy (ApEn) and permutation entropy specifically, are increasingly being investigated with relation to coma and consciousness, with some interesting preliminary results. For example, Sarà et al. have shown a correlation between *ApEn* measures and outcome of patients with UWS (Sarà et al. 2011), although Gosseries et al. found entropy to only be useful in diagnosis, and not prognosis (Gosseries et al. 2011). The present study extends the work of previous studies in analysing *ApEn* as a predictor of DOC outcome, and also investigates the prognostic value of permutation entropy as explored for the first time, as far as we know. These measures of entropy are potentially useful because they are scale-invariant, robust to noise, and discriminate series for which clear feature recognition is difficult (Pincus 1995; Pincus and Singer 2014).

Approximate Entropy

Conceptually, approximate entropy (*ApEn*) is defined as the logarithmic likelihood that the patterns of data that are close to each other will remain close on following, incremental comparisons. Mathematically, *ApEn* is determined as follows: Given a segment of EEG of N time samples, $[u(1), u(2), \ldots, u(N)]$, and an arbitrary value m, a sequence of vectors $[x(1), x(2), \ldots, x(N-m+1)]$ in m-dimensional space can be constructed such that $x(i) = [u(i), u(i+1), \ldots, u(i+m-1)]$. Using $x(i)$, and additional quantity, $C^m{}_i$, can be calculated:

$$C^m{}_i(r) = \frac{\text{number of } x(j) \text{ such that } |x(i) - x(j)| < r}{N-m+1} \tag{1}$$

where r is an arbitrary tolerance. This can be used to define

$$\phi^m(r) = \frac{1}{N-m+1} \sum_{i=1}^{N-m+1} \log(C^m{}_i(r)) \tag{2}$$

such that

$$ApEn = \phi^m(r) - \phi^{m+1}(r) \tag{3}$$

Permutation Entropy

In contrast to *ApEn*, permutation entropy (*PerEn*) makes use of the symbolic transform, such that the signal is represented by a sequence of discrete symbols, the probability density of which is analysed to obtain the entropy. Symbolization of EEG data is a useful practice because it reduces sensitivity to noise, simplifies computational evaluations, and consequently increases efficiency in quantifying information from a complex dynamical system (Daw et al. 2003). The transformation involves the extraction of sub-vectors of the signal, like in the case of ApEn, each composed of voltages at m time points separated by a fixed time delay, τ . For example, given a segment of EEG of N time samples, $[u(1), u(2), \ldots, u(N)]$, a set of subvectors can be constructed, $[x(1), x(2), \ldots, x(N-m+1)]$, where a subvector is defined as $x(i) = [u(i), u(i+\tau), \ldots, u(i+(m-1) \times \tau)]$. Each $x(i)$ is then represented by a symbol (or equivalently a number between 1 and m!) dependent on the order of amplitudes of the signal which comprise the subvector. Permutation entropy can then be calculated as,

$$PerEn = -\sum_{i=1}^{m!} p_i \log(p_i) \tag{4}$$

where p_i is the probability of occurrence of the ith symbol.

Power in Alpha and Delta Frequency Bands

Some studies have shown that differences in power spectra exist between patients with DOC and healthy controls, as well as between UWS and MCS patients (Lehmann et al. 1987; Blume et al. 2015; Stender et al. 2015). In particular, these studies have indicated that patients with DOC exhibit reduced power in the alpha band and increased power in the delta band, with a more severe difference presented in the UWS than the MCS. We verified these results by establishing how accurately power in these bands differentiate patients in the UWS and MCS, and furthermore we determine the effectiveness of using spectral power in these frequency bands to prognosticate in DOC.

Connectivity

Previous research has been done into comparing the brain connectivity of UWS and MCS through indices such as coherence, the imaginary part of coherence, weighted symbolic mutual information and symbolic transfer entropy, all of which are further explored in this study (Lehembre et al. 2012; King et al. 2013; Lee et al. 2015). These indices provide insight into the degree of integration and connection of networks in the brain by assessing connectivity between electrode signals. Previous research tend to agree that patients in UWS display significantly lower connectivity than MCS patients in the theta and alpha bands, indicating that the level of connectivity could be related to the severity of the disorder. Connectivity is likely to correlate to greater brain activity in terms of information sharing and processing, and therefore also to behavioural signs of consciousness, thus warranting further investigation in this area.

Coherence

Coherence quantifies the degree of coupling of frequency spectra between two electrodes, and can be calculated for a frequency f as,

$$C_{xy}(f) = \frac{|G_{xy}(f)|^2}{G_{xx}(f)G_{yy}(f)} \tag{5}$$

where $G_{xy}(f)$ is the cross-spectral density of x and y, where x and y are time-series of voltages recorded at different electrodes, and $G_{xx}(f)$ and $G_{yy}(f)$ are the auto-spectral densities of x and y respectively. Coherence has the significant disadvantage of being contaminated by volume conduction, which is the transmission of electrical signals from a primary source through brain tissue (Nunez et al. 1997). To overcome this issue, and thereby provide a more accurate reflection of brain interactions, one approach is to consider only the imaginary part of coherence since volume conduction only affects the real part of coherence. It is not necessarily the intention of this paper to correct the shortcomings or address the limitations of techniques applied in EEG research, but rather investigate techniques that are commonly applied in EEG research. This paper thus considers both magnitude-squared coherence as well as imaginary coherence the both are measures often justified by EEG researchers. We also note that the position of the reference electrode affect the possible network topologies generated, but we do not intend to make claims about the absolute values of coherence, but rather differences between patients groups (for which the reference electrode was located at the vertex for all patients).

Weighted Symbolic Mutual Information

Weighted symbolic mutual information (*wSMI*) is based on principles of permutation entropy applied to the quantification of global information sharing (King et al. 2013). Once having symbolically-transformed the signal as in the case for permutation entropy, the method assesses the joint occurrences of symbolic or qualitative fluctuations in the signal, thus robustly detecting non-directional nonlinear coupling. To account for spurious correlations produced by artifacts (such as those from volume conduction), wSMI disregards trivial conjunctions of symbols across two signals, corresponding to conjunctions of identical symbols, as well as conjunctions of opposite symbols. This is achieved by attributing a zero weight to symbol pairs as indicated on the joint probability matrix illustrated in Fig. 1.

wSMI can then be calculated as,

$$wSMI(\hat{X}, \hat{Y}) = \frac{1}{\log(k!)} \sum_{\hat{x}\in\hat{X}} \sum_{\hat{y}\in\hat{Y}} w(\hat{x},\hat{y}) p(\hat{x},\hat{y}) \log \frac{p(\hat{x},\hat{y})}{p(\hat{x})p(\hat{y})} \tag{6}$$

where $\hat{x}$ and $\hat{y}$ are symbols present in signals $\hat{X}$ and $\hat{Y}$ respectively, $p(\hat{x},\hat{y})$ is the joint probability of co-occurrence of $\hat{x}$ and $\hat{y}$, $p(\hat{x})$ and $p(\hat{y})$ are the probabilities of $\hat{x}$ and $\hat{y}$ in $\hat{X}$ and $\hat{Y}$, respectively. Lastly, $w(\hat{x},\hat{y})$ represents the weights (0 or 1) as described in Fig. 1. The reasoning behind the zero-weighting is that conjunctions of identical symbols may be elicited by a common source, and conjunctions of opposite symbols may reflect opposite sides of a common electric dipole.

Symbolic Transfer Entropy

Transfer entropy (*TE*) quantifies the directional transfer of information by assessing the uncertainty of the current value of voltage at one electrode position Y knowing past voltages at another position X compared to the uncertainty in the voltage at Y only knowing past voltages at Y. *TE* is based on

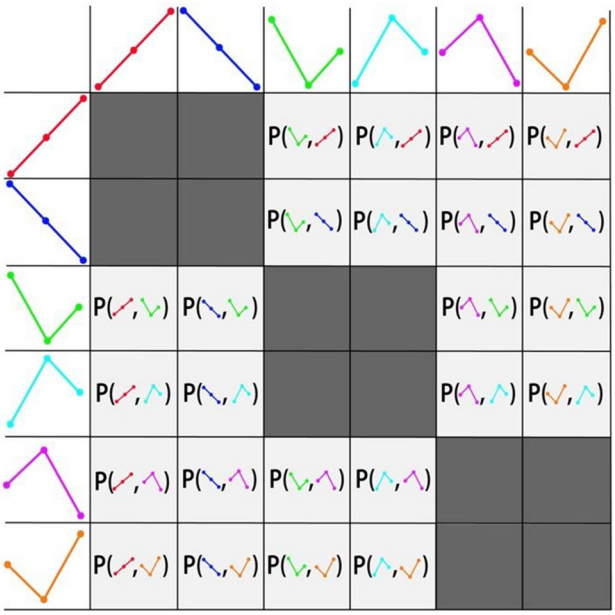

Fig. 1 The joint probability matrix for a symbol transformation with $m = 3$. Dark grey blocks are zero-weighted ($w = 0$) and do not contribute to the *wSMI*

Granger Causality, a linear regression model that quantifies the causal interaction between a source signal *X* and target signal *Y*:*X* is said to Granger-cause *Y* if the inclusion of the past of *X* improves the prediction of *Y* (Barnett et al. 2009) . *TE* thus differs from Granger Causality in that it is framed in terms of resolution of uncertainty, not in terms of prediction. However, it has been shown that *TE* is equivalent to Granger causality under Gaussian assumptions (Barnett et al. 2009). Granger Causality is known to produce spurious results due to its linearity, sensitivity to noise, and sensitivity to band-pass filtering. *TE* is a robust, nonlinear approach that was consequently introduced to address these limitations (Lee et al. 2015). However, we did not evaluate the possibility of spuriousness correlation with regards to *TE*, but instead employed this technique as is commonly performed in EEG research.

TE offers a model-free estimation of the direction and strength of connectivity between two signals, X and Y, and can be defined as the measure of mutual information between the past of *X*, (*XP*), and the future of *Y*, (*YF*), when the past of *Y*, (*YP*) is already known.

Mathematically,

$$TE_{X\rightarrow Y} = \sum P(Y_F, Y_P, X_P) \log \left[\frac{P(Y_f | Y_P, X_P)}{P(Y_F, Y_P)} \right] \quad (7)$$

TE can be quite complex to determine because of the difficulty in estimating probability density functions from finite, irregular data. Moreover, to do so, data is quantised into equally-spaced bins, and it has been shown that *TE* estimates are dependent on this arbitrary choice in bin-size. To overcome this, we investigated symbolic transfer entropy, which quantifies *TE* of symbolically transformed data without the need for binning or advanced estimators of the probability density function.

Complex Network Analysis

Measures of connectivity can be employed in complex network analysis which aims to represent complex systems as networks and extract meaningful information from the topologies of these networks. Complex network analysis may be a particularly insightful tool because it allows for the exploration of structural–functional connectivity relationships by defining functional connections with respect to the spatial map of the brain. In EEG analyses, networks can be constructed by considering the electrode positions as nodes and the links between nodes as functional connections, as quantified by measures described above. The topology of these networks can be assessed and compared through graph-theoretical measures, such as the clustering coefficient and characteristic path length. The clustering coefficient of a network can be computed by examining triplets, which are defined as three nodes with at least two links. Specifically, the clustering coefficient is defined as the number of closed triplets (groups of three nodes which are maximally interconnected) divided by the total number of triplets. The clustering coefficient is thus a micro-scale measure that provides an indication of clustered connectivity around individual nodes, which in turn is indicative of segregated neural processing. Conversely, characteristic path length provides insight into macro-scale functioning by quantifying functional integration: the ability to combine specialized information from distributed brain regions. Characteristic path length is defined as the average number of steps along the shortest paths for all possible pairs of nodes, where each path represents a potential route of information flow between two brain regions.

Complex network analyses applied to EEG analysis are beginning to gain interest with promising results. Chennu et al. calculated numerous graph theoretic statistics from EEG data including the clustering coefficient, path length, modularity, participation coefficient and network-level modular span and found that connectivity as assessed by these metrics correlated well with positron emission tomography (Chennu et al. 2017). Furthermore, they found that these networks correlate strongly with brain metabolism.

In EEG studies, a network topology can be created by thresholding measures of connectivity between electrodes, such that a link is said to exist between two electrodes if the connectivity between those two electrodes exceed a certain threshold. In the study by Chennu et al. graph-theoretic

statistics are calculated by thresholding debiased weighted phase lag index, but in the present study we threshold the coherence because of its prevalence in coma research. The position of the reference electrode affects the descriptions of connectivity between electrodes, and consequently also the network topologies generated, but we do not intend to make claims about the absolute values, but rather differences between patients groups (for which the reference electrode was located at the vertex for all patients).

Method

Selection of Participant Sample

After receiving approval from the local ethics committee, we recruited DOC patients consecutively during admission to same intensive inpatient neurorehabilitation center in the German state of Bavaria. Legal representatives of participants gave written informed consent. Patients were not under sedation during EEG recording. The resulting participant sample contains only data from patients, who were available for a follow-up on their consciousness level at or after discharge from neurorehabilitation. The state of consciousness both at baseline and follow-up was assessed with the CRS-R. Details on inclusion and exclusion criteria as well as other study protocol related information have been published elsewhere (Grill et al. 2013).

Procedure

Prior to recording 5 min of high-density resting state EEG for each patient, we assessed the level of consciousness of patients with the CRS-R. Patients were in the supine position with eyes closed. The standard CRS-R arousal facilitation protocol was used to maintain the patient in a state of arousal during EEG recording.

Data

Data consists of resting-state data recorded at a sampling rate of 1000 Hz with a 256 channel high-density geodesic sensor net with Net Amps 300 amplifier and Net Station 4.5. software (Electrical Geodesic Inc., Eugene, OR, USA). During recording, electrodes were referenced to the vertex and impedances were kept under 50 kΩ. Data were high-pass filtered at 0.1 Hz to eliminate slow drifts and subsequently segmented into trials of two seconds, such that all described analyses are performed on the same resting-state data of two seconds in duration. Trials with eye-movement artefacts exceeding 55 µV and eye-blinks artefacts exceeding 140 µV were automatically removed. To determine channel outliers, we examined the distributions of the maximum voltage difference across all channels in that trial. If a channel exhibited a maximum change that was greater than five standard deviations, that channel was removed from analysis in that trial. This resulted in at most one to two channels being excluded in a single trial. Each analysis described in this paper was performed using ten trials.

Statistical Analysis

We analysed data using both MATLAB Release 2014b (Mathworks, Sherborn, Massachusetts, USA) and Python. To determine the predictive power of the measures explored in this study, patients were classified into one of two groups (UWS or MCS for diagnosis and UWS or dead, and MCS or better for prognosis) by fitting a generalised linear model (GLM) on training data, and testing the model on test data. Additionally, to avoid over-fitting and circular analysis, a ten-fold stratified cross-validation scheme was implemented. The performance of the classifiers was then investigated using receiver operating characteristic (ROC) curves. The ROC curve illustrates the performance of a binary classifier by plotting the true positive rate (sensitivity) against the false positive rate (1—specificity) as the threshold is varied. The outputs of the GLM are thresholded at values ranging between 0 and 1, thus binarizing the output of the GLM. These binary outputs are then compared to the actual labels (UWS vs. MCS, or improved vs. unimproved) represented by 0 and 1 s, allowing for the calculation of specificity and sensitivity. Each threshold yields a pair of values (one value for specificity and one for sensitivity), corresponding to one point on the ROC curve.

We calculated the area under the curve (AUC) of ROC curves to determine which features exhibited significant differences across groups of patients. The area under the curve (AUC) of a ROC provides a measure of classification accuracy, such that an of 100% indicates perfect classification (there is some value of the threshold parameter for which there is both perfect sensitivity and specificity) and 50% indicates random classification. Significance of the AUC was established by randomly permuting the elements of feature vectors and comparing the results using the non-parametric Kruskal–Wallis test (Mason and Graham 2002).

Finally, to account for multiple comparisons, the false discovery rate was controlled by employing the Benjamini–Hochberg procedure at level = 0.05. The procedure is as follows: the p values, $p_1, \ldots, p_m$, corresponding to the null hypotheses (features tested), $H_1, \ldots, H_m$, are sorted in increasing order. Each p value is compared to the Benjamini–Hochberg critical value, $\frac{i}{m}\alpha$, where i is the rank and m is the number of hypotheses. The largest p value that is less than the critical value is considered to be significant, as well as all p values smaller than it. Adjusted p values are

calculated as raw p values multiplied by $\frac{m}{i}$, and are reported in this study as q values.

Microstate Analysis

We performed a microstate segmentation following a protocol employed in previous studies (Koenig and Melie-Garca 2010). Specifically, we transformed EEG data to the average-reference, calculated the global field power (GFP) for each trial, and extracted topographic maps at time points of GFP local maxima, which correspond to times of greatest signal-to-noise ratio. The GFP is the standard deviation of the voltages recorded at all channels at each time point, and can be calculated as,

$$GFP = \sqrt{\frac{\sum_{i=1}^{N}(u_i - \bar{u}_i)^2}{N}} \tag{8}$$

where u_i is the voltage at electrode i, $\bar{u}_i$ is the average voltage of all electrodes, and N is the number of electrodes.

These maps at GFP maxima are assimilated for all trials, and clustered into a predetermined number of clusters using both a modified k-means and a "topographical atomise and agglomerate hierarchical clustering" algorithm (Murray et al. 2008). Here, the data was analysed using both clustering methods to account for potential differences in the microstates obtained using the different clustering methods.

Microstates in the delta (0–4 Hz), theta (4–8 Hz), alpha (8–13 Hz), and 2–20 Hz frequency bands were obtained after having filtered data in the respective frequency bands using a second-order Butterworth filter. For each frequency band, the following outputs were obtained for each patient,

- EEG scalp topographies when data is segmented into four microstates.
- The average number of times a microstate appears in a trial of EEG data.
- The average duration of each microstate in a trial.
- The average percentage of time spent in each microstate.

To achieve this, firstly four global microstates were obtained by pooling all patient data and clustering topographies to obtain the four microstates: *A*, *B*, *C* and *D*. Figure 2 shows global microstates obtained for patients in the two different outcome groups. We note that in our microstate analysis we use the same archetypal microstates (calculated by pooling data for both improved and unimproved conditions) which have the same general characteristics as those shown in Fig. 2 for classes A, B, C and D.

For each patient, the topographies at GFP maxima were then compared with each global microstate by computing squared correlation coefficients so as to disregard polarity.

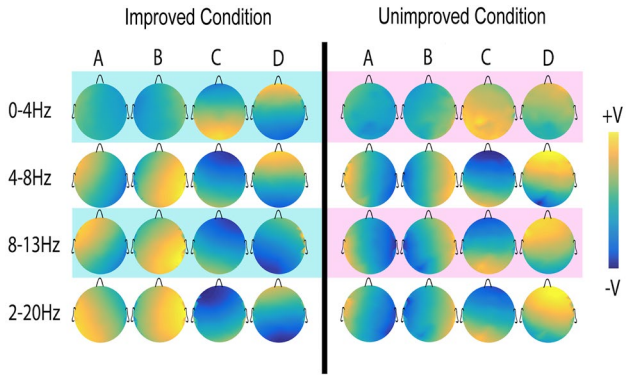

Fig. 2 Global microstate classes, *A*, *B*, *C* and *D*, obtained in the 0–4, 4–8, 8–13 and 0–20 Hz frequency bands, obtained globally for patients in the different outcome groups

Each topography was then assigned to a microstate class *A*, *B*, *C* or *D* dependent on the global microstate with which it best correlated, so that this process is much like a modified k-means clustering algorithm with the global maps as seed maps. The first spatial principal component was calculated for each microstate class to obtain four representative maps for each patient, which were then used in subsequent analyses.

For each patient, topographies at GFP maxima were compared to each microstate class by calculating squared correlation coefficients, and assigned to the class with which they best correlated. The average frequency, duration and percentage of time spent in each microstate were then determined, considering that EEG topographies remain stable between GFP minima as determined by previous research (Michel 2009). This procedure is illustrated in Fig. 3.

Entropy

Approximate Entropy

In order to be able to compare the *ApEn* of both patient groups we calculated *ApEn* with a short embedded dimension (m) template of 2, and a wide tolerance (r) and time delay (tau) equal to 0.2 × (standard deviation of data), as suggested by previous seminal research aiming to avoid the penalties associated with parameters lacking sufficient rigor (Pincus and Goldberger 1994; Pincus 1995; Bruhn et al. 2000; Pincus 2001). This approach has been adopted widely in EEG studies within and outside DOC research because such a normalization of r allows *ApEn* to remain "unchanged under uniform process magnification, reduction, or constant shift to higher or lower values" (Abásolo et al. 2005), which yields an *ApEn* unaffected by scale and translation (Ocak 2009; Sarà et al. 2011; Liang et al. 2015). *ApEn* was calculated separately for ten trials for each patient in

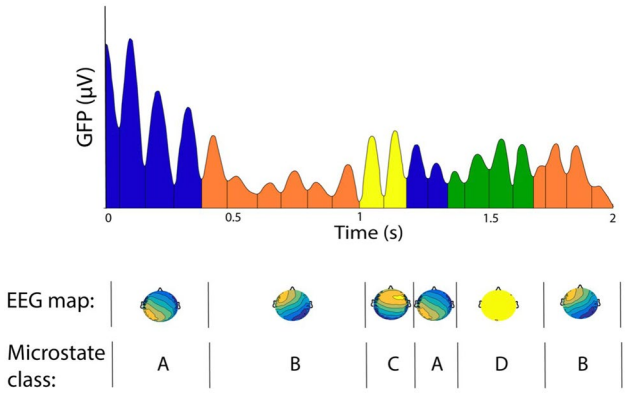

Fig. 3 The microstate analysis for one trial of data for one patient. Firstly, microstate classes, *A*, *B*, *C* and *D*, are obtained for each patient using a clustering algorithm, and then topographic maps at each time point are assigned to a microstate class. The different colours of the GFP curve represent the four microstate classes. The corresponding microstate topography at each time point, as well as the microstate class, are illustrated beneath the GFP curve

the delta, theta, alpha and beta (13–35 Hz) frequency bands for each channel. Furthermore, it is not within the scope of this paper to attempt to optimize various parameter values, but rather to explore existing quantitative methods in the way that they are currently implemented. Additionally, it is the comparison of the ApEn in the two different patient groups that is important (not the absolute value of ApEn) that is important in this study. These values were then averaged over the trials and over the channels to obtain a single descriptor as a feature in the classification scheme.

Permutation Entropy

We calculated permutation entropy over ten trials for each channel in the delta, theta, alpha and beta bands separately, using a time delay of one sample and an embedding dimension m of 3: Fig. 1 provides an illustration of the $3! = 6$ possible symbol representations of sub-vectors. Feature vectors for the classification scheme were obtained in a similar manner to those in the *ApEn* analysis.

Power in Alpha and Delta Frequency Bands

We obtained relative power values in the alpha and delta bands by computing the power in these bands as a fraction of the power across 1–50 Hz, which were then used as features in the classification scheme. We employed a multitaper method to overcome some of the limitations of conventional Fourier analysis. In principle, to describe a system in the frequency domain, an output sample of infinite length is needed. Moreover, infinitely many realisations of this output are needed to capture stochastic properties, which in most scenarios is not possible. Typically, the output is only observed as a single realisation with finite length, which often results in spectral estimates that are biased and exhibit high error variance (Babadi and Brown 2014).

To remedy this, we obtained several periodograms by multiplying the EEG signal with Slepian sequences, a family of mutually orthogonal tapers (windows), which additionally have optimal time–frequency concentration properties (Van De Ville et al. 2002) These periodograms (each one obtained using a different Slepian sequence as a window) were then averaged to produce the multitaper power spectral density estimate. Slepian sequences, $\hat{h}_n$, are defined as the eigenvectors of,

$$\sum_{n=0}^{N-1} \frac{\sin(2\pi W(m-n))}{\pi(m-n)} \hat{g}_n = \lambda \hat{g}_n \tag{9}$$

where N is the number of time samples of EEG data for one channel, and W is a half-bandwidth that defines a small frequency band centred around [1] f. Here, we chose [2] W of 0.002, and made use of the first 7 Slepian sequences based on the value of the corresponding eigenvalues.

Connectivity

Coherence

Magnitude-squared coherence and the imaginary part of coherence were calculated for each patient for each pair of electrodes in the delta, theta, alpha and beta frequency bands and averaged over 10 trials. [3] The median value of coherence for each electrode was then determined, and the mean of these median values used as a feature in the classification scheme.

Weighted Symbolic Mutual Information

To calculate wSMI, we transformed EEG data symbolically in the same way as has been described for the calculation of permutation entropy: data points are divided into subvectors of dimension m, with each element in the sub-vector separated by a fixed time delay, τ, similarly to the embedding performed for the calculation of permutation entropy. wSMI was calculated as described previously in the delta, theta, alpha and beta frequency bands with m of 3 and of 4, 8 and 32 time samples. These parameters were chosen based on the work of King et al. who first described the method (King et al. 2013). The authors note that different τ values are specific to different frequency bands, and note the importance of applying an appropriate low-pass filter before analysis to prevent aliasing. By band-pass filtering the signal, one can address the potential problem of aliasing as well as further

isolate the frequencies responsible of the wSMI differences across consciousness states.

Figure 1 shows the probability matrix used to calculate *wSMI* for an m of 3, and illustrates the $3! = 6$ possible symbol representations of sub-vectors. For each patient, wSMI was calculated over all electrode pairs and the median value determined for each trial. The median values for each of the ten trials were then averaged to obtain one value.

Symbolic Transfer Entropy

We transformed EEG data symbolically as described previously with an embedding dimension of $m = 3$ and time delay $\tau = 1$, and *TE* calculated for each patient in the delta, theta, alpha and beta frequency bands. Feature vectors were obtained by averaging *TE* over all electrodes and over 10 trials of data.

Complex Network Analysis

The present study makes use of non-directional binary links, which incorporates EEG results as shown in Fig. 4, such that a link is either present or absent depending on a threshold value of the connectivity measure.

We examined both average clustering coefficient and characteristic path length, with links between nodes determined by thresholding values for coherence between electrodes. Coherence in the delta, theta, alpha and beta ranges were thresholded at values of coherence of 0.8–0.95, incrementing by 0.01. We can thus define a binary link between two nodes if the magnitude-squared coherence between the two corresponding electrodes is above the threshold. If the threshold is too high, very few links between electrodes remain making it difficult to infer connectivity patterns, and if the threshold is too low very few differences in the connectivity graphs are present, making comparisons difficult. As noted in literature (Bordier et al. 2017), methods of determining? optimal? thresholds are widely discussed and researched, although it appears that no real consensus has been reached on how best to choose such thresholds. Thus, we observed empirically (on a different set of data) that 0.8–0.95 represented a broad enough range such that thresholds within this range represented a compromise between overly connected and overly sparse connectivity graphs.

Results

Obtained Participant Sample

As shown in Tables 1 and 2 we performed consciousness indexing with EEG data from 62 patients and predicted outcome with a subset of 39 patients, who had follow-up

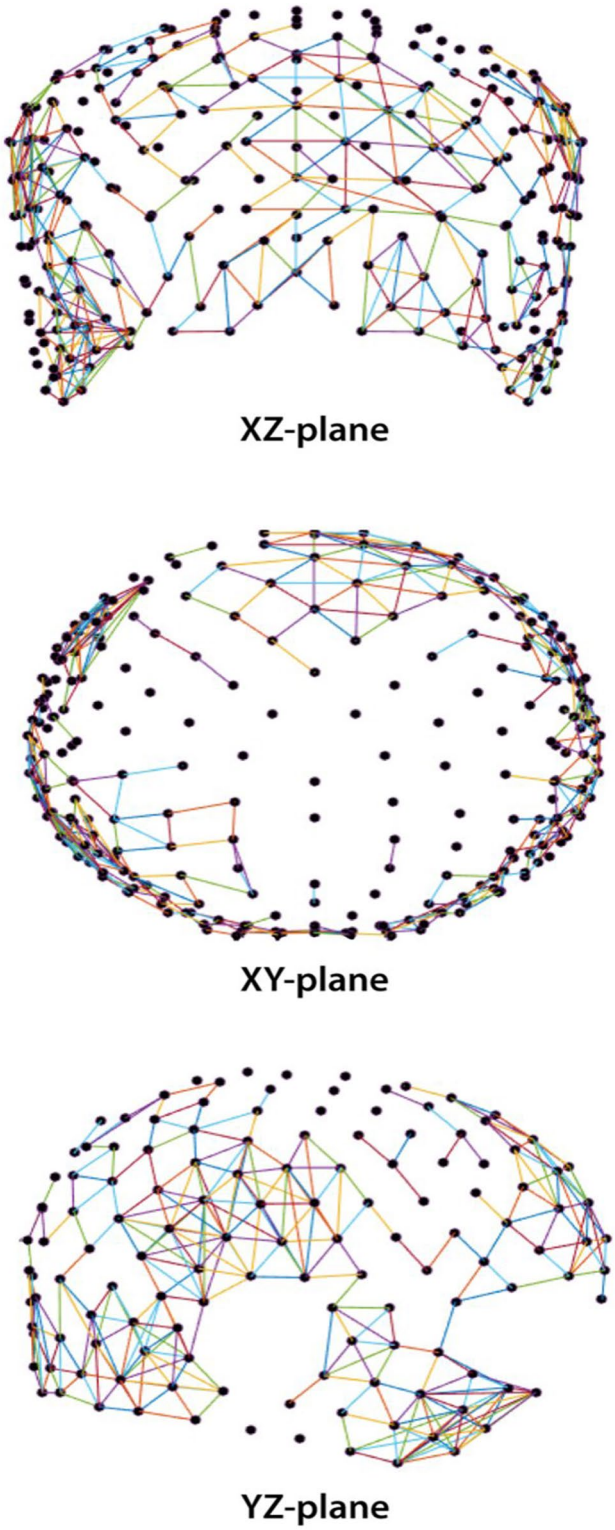

Fig. 4 A visualisation in the XZ-, XY- and YZ-planes of complex network analysis applied to EEG: this is an example of the network obtained for one patient when thresholding coherence in the beta range at 0.94. The nodes are represented by electrodes and binary non-directional links between two electrodes indicate a coherence of greater than 0.94 between those electrodes

Table 1 Characteristics of patients in the consciousness indexing group ($N = 62$)

Etiology	Age at admission in years	Gender		DOC category at baseline	
		M	F	UWS	MCS
Hypoxia	56.17 ± 14.08	17	12	28	1
TBI	39.71 ± 17.7	9	5	12	2
Ischemic stroke	47.00 ± 25.24	1	2	3	0
Brain tumor	74	0	1	0	1
ICH	62.33 ± 5.61	6	0	3	3
SAH	46.50 ± 9.59	3	5	4	4
Cerebral venous sinus thrombosis	25	0	1	1	0
Total	51.15 ± 16.42	36	26	51	11

EEG data. Mean time elapsed from baseline to follow-up was 589.26 ± 1125.32 days. Additional data on the obtained sample is available in the online resource.

Consciousness Indexing

Microstate

Percentage of time spent in microstate *D* in the alpha range ($AUC = 74 \pm 5\%, q < 0.0001$) was the best performing feature extracted at discriminating between MCS and UWS patients.

Entropy

ApEn in all frequency ranges was higher for MCS patients than UWS patients (delta: $AUC = 57 \pm 5\%$, $q < 0.01$, theta: $AUC = 55 \pm 2\%$, $q < 0.01$, alpha: $AUC = 57 \pm 5\%$, $q < 0.001$, beta: $AUC = 68 \pm 2\%$, $q < 0.001$). Permutation entropy in the alpha range was also significantly higher for MCS patients ($AUC = 61 \pm 2\%, q < 0.0001$).

Power in Alpha and Delta Frequency

Power in both the alpha frequencies was greater for MCS patients than UWS patients, and conversely for power in the delta frequencies. The measures performed similarly at distinguishing between UWS and MCS patients ($AUC = 54 \pm 3\%$, $q < 0.01$ for alpha range and $AUC = 58 \pm 7\%, q < 0.01$ for delta range).

Connectivity

Only imaginary coherence in the theta band yielded significant results. We found that coherence in the alpha and beta frequencies were higher for patients in UWS ($AUC = 64 \pm 4\%$, $q < 0.001$ in the alpha band and $AUC = 61 \pm 2\%, q < 0.001$ in the beta band). We also found that wSMI performed significantly in the theta range with t = 4 ($AUC = 60 \pm 3\%, q < 0.01$), the alpha range with t = 4 ($AUC = 56 \pm 4\%, q < 0.01$) and the delta range with t = 8 ($AUC = 69 \pm 1\%, q < 0.001$). Transfer entropy performed similarly in all frequency bands, with transfer entropy in the alpha band yielding the best results ($AUC = 67 \pm 3\%$, $q < 0.0001$).

Complex Network Analysis

We represented EEG signals as complex network graphs by thresholding coherence in the delta, theta, alpha and beta ranges, and found that both the characteristic path length and the clustering coefficient of these graphs successfully classified patients into UWS/MCS. The clustering coefficient of complex networks obtained by thresholding alpha coherence yielded reasonable classification accuracy on average ($AUC = 64 \pm 1\%, q < 0.001$), without the threshold having any significant effect. Similar results are obtained for

Table 2 Characteristics of patients in the outcome prediction subgroup ($N = 39$)

Etiology	Age at admission in years	Gender		DOC category at baseline		DOC category at follow-up			Time from admission to follow-up in days
		M	F	UWS	MCS	UWS	MCS	MCS+	
Hypoxia	56.95 ± 16.19	13	7	20	0	18	2	0	457.70 ± 824.21
TBI	42.88 ± 17.08	8	1	9	0	8	0	1	434.67 ± 796.26
Ischemic stroke	61.5 ± 3.54	1	1	2	0	1	0	1	32.00 ± 32.53
ICH	65.00 ± 4.24	3	0	3	0	1	1	1	386.00 ± 614.89
SAH	46.00 ± 1.41	0	4	4	0	1	1	2	165.75 ± 231.56
Cerebral venous sinus thrombosis	25	0	1	1	0	0	0	1	153
Total	51.85 ± 17.57	25	14	39	0	29	4	6	386.36 ± 717.06

average path length in the obtained by thresholding alpha coherence ($AUC = 65 \pm 4\%, q < 0.001$) and beta coherence ($AUC = 65 \pm 5\%, q < 0.001$). See Supplementary Figs. 1 and 2 for the distributions of clustering coefficients and path lengths with respect to state of consciousness.

Outcome prediction

Microstates

It appears that microstate *A* was particularly informative in predicting coma outcome. We found that the duration of microstate *A* in the delta band ($AUC = 75 \pm 5\%$, $q < 0.001$), the frequency of microstate *A* in the theta band ($AUC = 75 \pm 10\%, q < 0.01$), the percentage of time spent in microstate *A* in the theta band ($AUC = 85 \pm 2\%, q < 0.0001$) and the frequency of microstate *A* in the 2–20Hz band ($AUC = 73 \pm 3\%, q < 0.0001$) all perform significantly.

Entropy

ApEn in the alpha band efficiently predicted outcome ($AUC = 67 \pm 5\%, q < 0.001$), however permutation entropy performed better than *ApEn*: permutation entropy in the delta ($AUC = 71 \pm 5\%, q < 0.0001$), theta ($AUC = 83 \pm 3\%$, $q < 0.0001$) bands yielded promising results.

Power in the Alpha and Delta Frequency

Power in the alpha ($AUC = 64 \pm 4\%, q < 0.001$) and delta ($AUC = 68 \pm 9\%, q < 0.01$) performed better at discriminating outcome than indexing consciousness.

Connectivity

Coherence in the theta band yielded high classification accuracy ($AUC = 78 \pm 2\%$, $q < 0.0001$). Alpha ($AUC = 62 \pm 4\%$, $q < 0.001$) and beta coherence ($AUC = 67 \pm 1\%, q < 0.0001$) were also successful. Coherence in all frequency ranges was greater for patients who improved condition. Interestingly, only the imaginary part of coherence in the beta band achieved significant results ($AUC = 75 \pm 2\%, q < 0.0001$) and did not offer an advantage to magnitude-squared coherence as a classifier.

TE and *wSMI* also predicted patient outcome effectively. We found that TE was successful at predicting outcome both in the delta ($AUC = 70 \pm 3\%, q < 0.001$) and alpha band ($AUC = 78 \pm 3\%, q < 0.001$). We also found that *wSMI* in the alpha band with a time delay of 32 s ($AUC = 73 \pm 4\%, q < 0.0001$) exhibited the most notable prognostic power, but *wSMI* in the alpha band with $t = 8$ s ($AUC = 71 \pm 5\%, q < 0.001$) and in the delta band with $t = 8$ s ($AUC = 69 \pm 8\%, q < 0.001$) also yielded significant results.

Complex Network Analysis

We found that clustering coefficients, calculated from beta coherence ($AUC = 82 \pm 1\%, q < 0.0001$) and alpha coherence ($AUC = 82 \pm 2\%, q < 0.0001$) performed best at classifying patients into the two outcome categories, without the thresholds having much effect. Clustering coefficients in the theta (mean $AUC = 72 \pm 1\%, q < 0.0001$) range also exhibited significant results. However, path length did not show a strong association with outcome. Here, the two outcomes correspond to emergence from UWS to MCS, or death or a persistent DOC. See Supplementary Figs. 2 and 4 for the distributions of clustering coefficients and path lengths with respect to outcome.

Automated Outcome Prediction

We selected an optimal subset of features with SFFS for an automated outcome prediction scheme. To avoid selection bias, we apply feature selection to each fold within cross-validation and select the three features that are most represented to select features for a final model. A larger sample size, however, is needed to validate the robustness of these features as well as the risk of overfitting. It is our hope that this may at least demonstrate promise for approaches to EEG data analysis and coma studies that are grounded in quantification.

It consisted of the following three features: frequency of microstate A in the 2–20 Hz frequency band, path length obtained from thresholding alpha coherence, and clustering coefficient obtained from thresholding alpha coherence. Combining these features seemed to afford high prediction power ($AUC = 92 \pm 4\%$), as shown in Fig. 5.

Python and MATLAB toolboxes for the above calculations are freely available under the GNU public license for non-commercial use (https://qeeg.wordpress.com). Results are presented in greater detail in the online supplementary material.

Discussion

Most measures performed significantly better at predicting outcome of coma than at discriminating between UWS and MCS patients, indicating perhaps that the link between diagnosis and prognosis is not as compelling as originally thought, or perhaps that some patients had been erroneously classified, considering that in clinical practice misdiagnoses occur in up to 43% of cases, especially when an inappropriate behavioural scale is used (Schnakers et al.

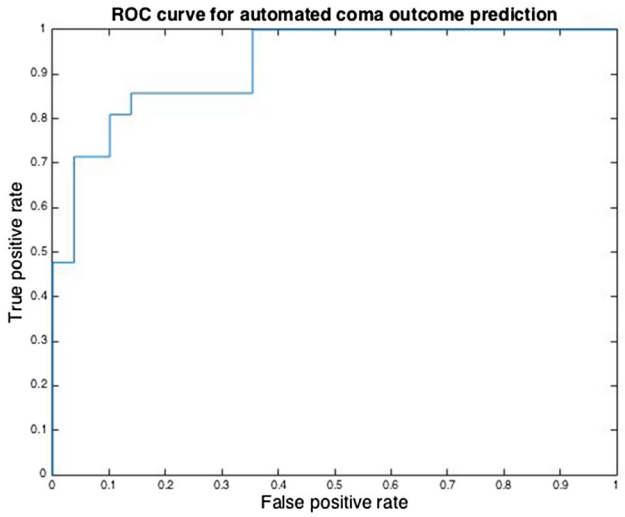

Fig. 5 ROC curve showing the performance of the combination of the three features selected using *SFFS*, namely the frequency of microstate A in the 2–20 Hz frequency band, path length obtained from thresholding alpha coherence and clustering coefficient obtained from thresholding alpha coherence

2009). Additionally, these strictly-defined categories do not take into account that UWS patients may actually be minimally or even fully conscious (van Erp et al. 2015). As mentioned, we found that all connectivity measures were not significantly different for UWS and MCS patients, although many of these metrics were greater in UWS patients than MCS patients. This is in direct contrast to previous research on *wSMI* and *TE* which indicates that measures of connectivity systematically increase with degree of consciousness, although in previous work auditory paradigm data was analysed whereas resting-state data was used in the present study (King et al. 2013; Thul et al. 2016). We did however find greater *wSMI*, *TE* and coherence (in all frequency ranges) in patients with improved outcome than those with unimproved outcome, indicating possible power of connectivity measures in prognosis instead of diagnosis.

Similarly, Lehembre et al. (2012) found that patients in UWS had significantly lower coherence than MCS patients in the theta and alpha bands. We did also observe this relationship, but the result was not significant. However, in a more recent study, Schorr et al. (2016) found that coherence could not be used to differentiate UWS and MCS patients, but could instead predict the recovery of UWS to MCS. The present study however did not find significant differences in the coherence between patients with improved and unimproved condition. This may be a consequence of averaging the coherence across all parts of the brain instead of investigating the connectivity between different parts of the brain separately, as was done by Schorr et al. (2016).

There were however significant differences between entropy of MCS and UWS patients, with permutation entropy and *ApEn* significantly higher in MCS patients, in accordance with the previous findings (Thul et al. 2016; Gosseries et al. 2011). Similarly, we found that patients with improved outcome exhibited greater EEG entropy than those with unimproved outcomes. It is hypothesised that the increased entropy is reflective of the increased complexity of neural networks that are necessary to support consciousness.

Power in the alpha band was greater for MCS patients than for UWS patients, and delta power was greater for UWS patients compared to MCS patients as also found by Lehembre et al. (2012), although the differences were not significant. The power in the delta band, however, was significantly smaller for patients who improved condition.

Our analysis of the topologies of the different patient groups largely agrees with the findings presented in the study by Chennu et al., and we highlight their work in comparing EEG-based connectivity hubs to PET data and glucose metabolism itself (Chennu et al. 2017). They show that these measures of connectivity correlate with the potential physiological underpinnings of consciousness, which may help to explain the relatively high performance of these measures at predicting outcome. Like in their work, we find that patients who improved condition exhibited greater connectivity, indicated by higher average clustering coefficients, and shorter characteristic path lengths (see Supplementary Figures).

We also draw attention to work by Sitt et al. which similarly to this study aimed to perform a large-scale analysis of the EEG measures in discriminating UWS and MCS patients (Sitt et al. 2014). This study complements much of this work, and further demonstrates differences in EEG features in predicting outcome as opposed to indexing consciousness.

Collectively, the comparison between these results seems to indicate that the results are dependent on the type of paradigm used, and possibly various other specific parameters used in calculations, like the length of each trial. It is also interesting to note that the number of electrodes used in this study is significantly higher than those used in many previous studies, providing information at more locations across the scalp, potentially allowing for more robust results. This is by virtue of the fact that high channel-density recordings may provide information from more regions of the brain (and thus more reflective of overall brain dynamics) than low channel-density recordings, as well as by providing more data over the same period of time.

With regards to the microstate analysis, we found a very pronounced difference in the percentage of time spent in microstate *D* in the alpha frequency in the two patient groups with respect to outcome, with patients with unimproved outcome spending more time in microstate *D*. It is possible that each microstate reflects an underlying neurological function,

as activity of different neural populations is responsible for the different landscapes of electrical potentials characterized by each microstate (Lehmann et al. 2006) This possibly indicates that improved outcome patients spend more time on other neurological tasks (represented by the other microstates) than unimproved outcome patients.

While effective and accurate, it is questionable whether the methods and measures studied here may perform sufficiently well to replace current practice for prognosticating coma on an individual basis. However, the automatic classification scheme is simple and cost-effective to implement and may indeed provide supplemental information to better inform medical practitioners when assessing prognosis. Moreover, the results of this study may not only be useful in clinical practice, but also in better understanding the nature of consciousness and the roots of disorders of consciousness. However, an important goal of the present study was to investigate several EEG biomarkers of consciousness on the same dataset to be able to compare the relative usefulness of these features. Most features presented here are commonly applied in EEG analyses of consciousness, but it has remained unclear how they perform comparatively. We also aimed to apply measures that are ordinarily applied to index consciousness to instead predict outcome, thus avoiding the problem of misdiagnoses.

Recent theories attribute disorders of consciousness to the disconnection of different cortical networks, rather than the dysfunction of a single area of the brain (Ovadia-Caro et al. 2012; Vanhaudenhuyse et al. 2010). For this reason, it may be important to investigate the network structures and motifs underlying consciousness and their interconnectedness through measures of functional connectivity, like those explored in this study. It is possible that disorders of consciousness stem from a functional isolation within the cerebral cortex, due to a derangement of neural networks and a consequent decrease in connectivity. The measures of connectivity, entropy and graph-theoretical statistics investigated here directly assess the degree of functional isolation through the investigation of the interconnectedness of subdivisions within the neural networks, as well as the complexity of these neural networks through the quantification of the unpredictability of its outputs. While the measures studied here do support this proposed theory of consciousness to some extent, it is entirely possible that other measures may better reflect true brain interactions, and consequently be more successful at interrogating differences between positive and negative outcome patients. It is thus necessary to continue to propose EEG methods to accurately reveal interactions between different cortical networks, and compare the results to those from other brain imaging methods, such as fMRI. These new methods of analysis may then firstly contribute additional evidence to the leading theory or otherwise, and secondly prove to be more useful in prognosticating coma than the methods studied here.

Conclusion

Our results suggest that several mathematically precise biomarkers perform significantly better than expected by chance at predicting outcome of coma, with the most promising results obtained through the analysis of EEG signals represented as microstates. These series of sequential topographies of electrical fields possibly provide insight into the differences between UWS and MCS patients, as well as key differences between patients with improved and unimproved outcomes. As far as we know, microstate analysis had not previously been applied to outcome prediction in this manner, such that this study is the first indication of the potential promise of this method.

An important goal of the study was to investigate several EEG biomarkers of consciousness on the same dataset to be able to compare the relative usefulness of these features. Most features presented here are commonly applied in EEG analyses of consciousness, but it has remained unclear how they perform comparatively. We also aimed to apply measures that are ordinarily applied to index consciousness to instead predict outcome, thus avoiding the problem of misdiagnoses.

Lastly, we aimed to design an automated classification scheme using SFFS: we found that combining metrics such frequency of microstate A in the 2–20 Hz frequency band, path length obtained from thresholding alpha coherence, and clustering coefficient obtained from thresholding alpha coherence affords high prediction power with an *AUC* of $92 \pm 4\%$. While this may still not be ideal for prognostication of individuals, it may indeed serve to better inform medical practitioners when assessing prognosis.

Acknowledgements The authors wish to thank patients and their caregivers as well as the Information and Communication Technology High Performance Computing Team of the University of Cape Town. Part of this study was supported by Grant 2011013 of the Hannelore-Kohl-Stiftung, and the Deutsche Stiftung Neurologie.

Compliance with Ethical Standards

Conflict of interest The authors declare that they have no conflict of interest.

Ethical Approval All procedures performed in the present study involving human participants were approved by the institutional review board of the University of Munich and were in accordance with the ethical standards of the 1964 Helsinki declaration and its later amendments.

References

Babadi B, Brown EN (2014) A review of multitaper spectral analysis. IEEE Trans Biomed Eng 61:1555–1564. https://doi.org/10.1109/TBME.2014.2311996

Barnett L, Barrett AB, Seth AK (2009) Granger causality and transfer entropy are equivalent for Gaussian variables. Phys Rev Lett 103:238701. https://doi.org/10.1103/PhysRevLett.103.238701

Blume C, Del Giudice R, Wislowska M et al (2015) Across the consciousness continuum-from unresponsive wakefulness to sleep. Front Hum Neurosci 9:105. https://doi.org/10.3389/fnhum.2015.00105

Bordier C, Nicolini C, Bifone A (2017) Graph analysis and modularity of brain functional connectivity networks: searching for the optimal threshold. arXiv preprint arXiv:1705.0648

Brodbeck V, Kuhn A, von Wegner F et al (2012) EEG microstates of wakefulness and NREM sleep. NeuroImage 62:2129–2139. https://doi.org/10.1016/j.neuroimage.2012.05.060

Bruhn J, Rpcke H, Hoeft A (2000) Approximate entropy as an electroencephalographic measure of anesthetic drug effect during desflurane anesthesia. Anesthesiology 92:715–726

Chennu S et al (2017) Brain networks predict metabolism, diagnosis and prognosis at the bedside in disorders of consciousness. Brain 140(8):2120–2132

Daw CS, Finney CEA, Tracy ER (2003) A review of symbolic analysis of experimental data. Rev Sci Instrum 74:915–930. https://doi.org/10.1063/1.1531823

Giacino JT, Ashwal S, Childs N et al (2002) The minimally conscious state: definition and diagnostic criteria. Neurology 58:349–353

Giacino JT, Fins JJ, Laureys S, Schiff ND (2014) Disorders of consciousness after acquired brain injury: the state of the science. Nat Rev Neurol 10:99–114. https://doi.org/10.1038/nrneurol.2013.279

Gosseries O, Schnakers C, Ledoux D et al (2011) Automated EEG entropy measurements in coma, vegetative state/unresponsive wakefulness syndrome and minimally conscious state. Funct Neurol 26:25–30

Graf J, Mhlhoff C, Doig GS et al (2008) Health care costs, long-term survival, and quality of life following intensive care unit admission after cardiac arrest. Crit Care 12:R92. https://doi.org/10.1186/cc6963

Grill E, Klein A-M, Howell K et al (2013) Rationale and design of the prospective German registry of outcome in patients with severe disorders of consciousness after acute brain injury. Arch Phys Med Rehab 94:1870–1876. https://doi.org/10.1016/j.apmr.2012.10.040

Howell K, Grill E, Klein A-M et al (2013) Rehabilitation outcome of anoxic-ischaemic encephalopathy survivors with prolonged disorders of consciousness. Resuscitation 84:1409–1415. https://doi.org/10.1016/j.resuscitation.2013.05.015

Kannathal N, Choo ML, Acharya UR, Sadasivan PK (2005) Entropies for detection of epilepsy in EEG. Comput Methods Progr Biomed 80:187–194. https://doi.org/10.1016/j.cmpb.2005.06.012

King J-R, Sitt JD, Faugeras F et al (2013) Information sharing in the brain indexes consciousness in noncommunicative patients. Curr Biol 23:1914–1919. https://doi.org/10.1016/j.cub.2013.07.075

Koenig T, Melie-Garca L (2010) A method to determine the presence of averaged event-related fields using randomization tests. Brain Topogr 23:233–242. https://doi.org/10.1007/s10548-010-0142-1

Kondziella D, Friberg CK, Frokjaer VG et al (2016) Preserved consciousness in vegetative and minimal conscious states: systematic review and meta-analysis. J Neurol Neurosurg Psychiatry 87:485–492. https://doi.org/10.1136/jnnp-2015-310958

Kuhn A, Brodbeck V, Tagliazucchi E et al (2015) Narcoleptic patients show fragmented EEG-microstructure during early NREM sleep. Brain Topogr 28:619–635. https://doi.org/10.1007/s10548-014-0387-1

Laureys S, Celesia GG, Cohadon F et al (2010) Unresponsive wakefulness syndrome: a new name for the vegetative state or apallic syndrome. BMC Med 8:68. https://doi.org/10.1186/1741-7015-8-68

Lee U, Blain-Moraes S, Mashour GA (2015) Assessing levels of consciousness with symbolic analysis. Philos Trans A 373(2034):20140117. https://doi.org/10.1098/rsta.2014.0117

Lehembre R, Marie-Aurlie B, Vanhaudenhuyse A et al (2012) Resting-state EEG study of comatose patients: a connectivity and frequency analysis to find differences between vegetative and minimally conscious states. Funct Neurol 27:41–47

Lehmann D, Faber PL, Gianotti LR et al (2006) Coherence and phase locking in the scalp EEG and between LORETA model sources, and microstates as putative mechanisms of brain temporo-spatial functional organization. J Physiol 99(1):29–36

Lehmann D, Faber PL, Galderisi S et al (2005) EEG microstate duration and syntax in acute, medication-naive, first-episode schizophrenia: a multi-center study. Psychiatry Res 138:141–156. https://doi.org/10.1016/j.pscychresns.2004.05.007

Lehmann D, Ozaki H, Pal I (1987) EEG alpha map series: brain microstates by space-oriented adaptive segmentation. Electroencephalogr Clin Neurophysiol 67:271–288

Lehmann D, Strik WK, Henggeler B et al (1998) Brain electric microstates and momentary conscious mind states as building blocks of spontaneous thinking I: visual imagery and abstract thoughts. Int J Psychophysiol 29:1–11

Liang Z, Wang Y, Sun X et al (2015) EEG entropy measures in anesthesia. Front Comput Neurosci 9:16. https://doi.org/10.3389/fncom.2015.00016

Lopez-Rolon A, Bender A (2015) Hypoxia and Outcome Prediction in Early-Stage Coma (Project HOPE): an observational prospective cohort study. BMC Neurol 15:82. https://doi.org/10.1186/s12883-015-0337-x

Mason SJ, Graham NE (2002) Areas beneath the relative operating characteristics (ROC) and relative operating levels (ROL) curves: statistical significance and interpretation. Q J R Meteorol Soc 128:2145–2166. https://doi.org/10.1256/003590002320603584

Michel CM (2009) Electrical neuroimaging. Cambridge University Press, Cambridge

Murray MM, Brunet D, Michel CM (2008) Topographic ERP analyses: a step-by-step tutorial review. Brain Topogr 20:249–264. https://doi.org/10.1007/s10548-008-0054-5

Noirhomme Q, Laureys S (2014) Consciousness and unconsciousness: an EEG perspective. Clin EEG Neurosci 45:4–5. https://doi.org/10.1177/1550059413519518

Noirhomme Q et al (2015) Look at my classifier's result?: disentangling unresponsive from (minimally) conscious patients. Neuroimage 145:288–303

Nunez PL, Srinivasan R, Westdorp AF et al (1997) EEG coherency I: statistics, reference electrode, volume conduction, Laplacians, cortical imaging, and interpretation at multiple scales. Clin Neurophysiol 103:499–515

Ocak H (2009) Automatic detection of epileptic seizures in EEG using discrete wavelet transform and approximate entropy. Expert Syst Appl 36(2):2027–2036. https://doi.org/10.1016/j.eswa.2007.12.065

Ovadia-Caro S, Nir Y, Soddu A et al (2012) Reduction in inter-hemispheric connectivity in disorders of consciousness. PLoS ONE 7:e37238. https://doi.org/10.1371/journal.pone.0037238

Pascual-Marqui RD, Michel CM, Lehmann D (1995) Segmentation of brain electrical activity into microstates: model estimation and validation. IEEE Trans Biomed Eng 42:658–665. https://doi.org/10.1109/10.391164

Pincus SM (1995) Approximate entropy (ApEn) as a complexity measure. Chaos 5:110–117. https://doi.org/10.1063/1.166092

Pincus SM (2001) Assessing serial irregularity and its implications for health. Ann N Y Acad Sci 954:245–267

Pincus SM, Goldberger AL (1994) Physiological time-series analysis: what does regularity quantify? Am J Physiol 266:H1643–1656

Pincus S, Singer BH (2014) Higher-order dangers and precisely constructed taxa in models of randomness. Proc Nat Acad Sci 111(15):5485–5490. https://doi.org/10.1073/pnas.1402621111

Posner JB, Saper CB, Schiff N, Plum F (2007) Plum and posner's diagnosis of stupor and coma, 4th edn. Oxford University Press, Oxford

Sarà M, Pistoia F, Pasqualetti P et al (2011) Functional isolation within the cerebral cortex in the vegetative state: a nonlinear method to predict clinical outcomes. Neurorehabilit Neural Repair 25:35–42. https://doi.org/10.1177/1545968310378508

Schnakers C, Vanhaudenhuyse A, Giacino J et al (2009) Diagnostic accuracy of the vegetative and minimally conscious state: clinical consensus versus standardized neurobehavioral assessment. BMC Neurol 9:35. https://doi.org/10.1186/1471-2377-9-35

Schorr B, Schlee W, Arndt M et al (2015) Stability of auditory event-related potentials in coma research. J Neurol 262:307–315. https://doi.org/10.1007/s00415-014-7561-y

Schorr B, Schlee W, Arndt M, Bender A (2016) Coherence in resting-state EEG as a predictor for the recovery from unresponsive wakefulness syndrome. J Neurol 263:937–953. https://doi.org/10.1007/s00415-016-8084-5

Sitt JD et al (2014) Large scale screening of neural signatures of consciousness in patients in a vegetative or minimally conscious state. Brain 137.8:2258–2270

Stender J, Gjedde A, Laureys S (2015) Detection of consciousness in the severely injured brain. In: Vincent J-L (ed) Annual update in intensive care and emergency medicine 2015. Springer, Cham, pp 495–506

Thul A, Lechinger J, Donis J et al (2016) EEG entropy measures indicate decrease of cortical information processing in disorders of consciousness. Clin Neurophysiol 127(2):1419–1427

Van De Ville D, Philips W, Lemahieu I (2002) On the n-dimensional extension of the discrete prolate spheroidal window. IEEE Signal Process Lett 9:89–91

van Erp WS, Lavrijsen JCM, Vos PE et al (2015) The vegetative state: prevalence, misdiagnosis, and treatment limitations. J Am Med Dir Assoc 16:85.e9–85.e14. https://doi.org/10.1016/j.jamda.2014.10.014

Vanhaudenhuyse A, Noirhomme Q, Tshibanda LJ-F et al (2010) Default network connectivity reflects the level of consciousness in non-communicative brain-damaged patients. Brain J Neurol 133:161–171. https://doi.org/10.1093/brain/awp313

Ververidis D, Kotropoulos C (2008) Fast and accurate sequential floating forward feature selection with the Bayes classifier applied to speech emotion recognition. Signal Process 88(12):2956–2970. https://doi.org/10.1016/j.sigpro.2008.07.001

Appendix: Supplementary Tables

Table A1 Characteristics of patients with hypoxia in the obtained patient sample ($N = 29$)

Gender	Age at Admission in years	Time from Admission to Follow-up in days	DOC Category at Baseline	DOC Category at Follow-up	CRS-R at Baseline	CRS-R at Follow-up
F	26	1043	UWS	UWS	7	7
F	46	29	UWS	N/A	4	N/A
F	47	66	MCS	N/A	10	N/A
F	47	50	UWS	UWS	5	6
F	50	73	UWS	N/A	6	N/A
F	53	5316	UWS	UWS	7	7
F	58	63	UWS	UWS	2	5
F	66	415	UWS	UWS	7	7
F	68	442	UWS	UWS	3	3
F	68	1109	UWS	UWS	6	6
F	69	35	UWS	N/A	1	N/A
F	75	79	UWS	UWS	3	3
M	20	25	UWS	MCS	6	7
M	32	56	UWS	UWS	6	6
M	42	3256	UWS	UWS	4	4
M	47	49	UWS	MCS	5	11
M	52	38	UWS	N/A	3	N/A
M	52	25	UWS	UWS	3	3
M	54	25	UWS	UWS	3	3
M	57	509	UWS	N/A	7	N/A
M	58	21	UWS	N/A	1	N/A
M	63	48	UWS	UWS	2	5
M	64	35	UWS	N/A	1	N/A
M	65	37	UWS	UWS	2	6
M	66	49	UWS	UWS	4	6
M	67	33	UWS	UWS	3	3
M	69	414	UWS	UWS	6	6
M	73	1900	UWS	UWS	3	4
M	75	36	UWS	UWS	4	4

Table A2 Characteristics of patients with traumatic brain injury in the obtained patient sample ($N = 14$)

Gender	Age at Admission (years)	Time from Admission to Follow-up in days	DOC category at Baseline	DOC Category at Follow-up	CRS-R at Baseline	CRS-R at Follow-up
M	49	30	UWS	UWS	1	7
M	24	1062	UWS	UWS	7	7
M	24	34	UWS	MCS+	6	23
F	18	1022	UWS	N/A	9	N/A
M	48	89	UWS	UWS	5	5
M	18	56	UWS	N/A	3	N/A
M	42	53	UWS	UWS	8	8
M	64	185	UWS	UWS	1	1
F	59	19	UWS	N/A	4	N/A
M	66	38	UWS	MCS+	4	21
F	52	120	MCS	N/A	14	N/A
M	19	1205	UWS	N/A	6	N/A
F	47	29	MCS	N/A	6	N/A
F	26	2365	UWS	UWS	6	6

Table A3 Characteristics of patients with ischemic brain injury in the obtained patient sample ($N = 3$)

Gender	Age at Admission in years	Time from Admission to Follow-up in days	DOC category at Baseline	DOC Category at Follow-up	CRS-R at Baseline	CRS-R at Follow-up
F	18	88	UWS	N/A	5	N/A
M	59	9	UWS	UWS	5	5
F	64	55	UWS	MCS+	2	20

Table A4 Characteristics of patient with a brain tumor in the obtained patient sample ($N = 1$)

Gender	Age at Admission in years	Time from Admission to Follow-up in days	DOC category at Baseline	DOC Category at Follow-up	CRS-R at Baseline	CRS-R at Follow-up
F	74	34	MCS	N/A	16	N/A

Table A5 Characteristics of patients with intracraneal hemorrhage in the obtained patient sample ($N = 6$)

Gender	Age at Admission in years	Time from Admission to Follow-up in days	DOC category at Baseline	DOC Category at Follow-up	CRS-R at Baseline	CRS-R at Follow-up
M	54	50	MCS	N/A	4	N/A
M	68	34	UWS	MCS	3	9
M	59	69	MCS	N/A	8	N/A
M	62	1096	UWS	UWS	3	3
M	62	76	MCS	N/A	8	N/A
M	69	28	UWS	MCS+	5	11

Table A6 Characteristics of patients with subarachnoid hemorrhage in the obtained patient sample ($N = 8$)

Gender	Age at Admission in years	Time from Admission to Follow-up in days	DOC category at Baseline	DOC Category at Follow-up	CRS-R at Baseline	CRS-R at Follow-up
F	45	120	MCS	N/A	13	N/A
F	45	513	UWS	MCS	7	9
M	50	142	MCS	N/A	1	N/A
M	47	63	MCS	N/A	12	N/A
F	47	51	UWS	UWS	5	5
M	49	744	MCS	N/A	9	N/A
F	27	56	UWS	MCS+	6	20
F	62	43	UWS	MCS+	4	15

Table A7 Characteristics of patients with Cerebral venous thrombosis ($N = 1$)

Gender	Age at Admission in years	Time from Admission to Follow-up in days	DOC category at Baseline	DOC Category at Follow-up	CRS-R at Baseline	CRS-R at Follow-up
F	25	117	UWS	MCS+	7	21

Table A8 Area Under Curve (AUC) Scores for consciousness indexing and outcome prediction of delta microstates

	AUC Score	
Delta Microstates	Consciousness Indexing	Outcome Prediction
Microstate class A: frequency, delta	68% ± 3%	60% ± 6%
Microstate class B: frequency, delta	57% ± 3%	56% ± 3%
Microstate class C: frequency, delta	67% ± 4%	66% ± 6%
Microstate class D: frequency, delta	58% ± 2%	57% ± 2%
Microstate class A: duration, delta	51% ± 1%	75% ± 5%
Microstate class B: duration, delta	61% ± 3%	53% ± 10%
Microstate class C: duration, delta	63% ± 1%	59% ± 2%
Microstate class D: duration, delta	60% ± 1%	70% ± 1%
Microstate class A: percentage, delta	68% ± 3%	58% ± 4%
Microstate class B: percentage, delta	56% ± 2%	55% ± 7%
Microstate class C: percentage, delta	74% ± 5%	50% ± 1%
Microstate class D: percentage, delta	59% ± 6%	69% ± 4%

Table A9 Area Under Curve (AUC) Scores for consciousness indexing and outcome prediction of theta microstates

	AUC Score	
Theta Microstates	Consciousness Indexing	Outcome Prediction
Microstate class A: frequency, theta	50% ± 2%	75% ± 10%
Microstate class B: frequency, theta	64% ± 3%	57% ± 7%
Microstate class C: frequency, theta	65% ± 2%	67% ± 1%
Microstate class D: frequency, theta	61% ± 1%	63% ± 4%
Microstate class A: duration, theta	70% ± 2%	51% ± 4%
Microstate class B: duration, theta	50% ± 2%	54% ± 2%
Microstate class C: duration, theta	64% ± 3%	57% ± 2%
Microstate class D: duration, theta	56% ± 1%	52% ± 4%
Microstate class A: percentage, theta	65% ± 3%	85% ± 2%
Microstate class B: percentage, theta	60% ± 2%	59% ± 8%
Microstate class C: percentage, theta	53% ± 2%	55% ± 4%
Microstate class D: percentage, theta	60% ± 2%	62% ± 3%

Table A10 Area Under Curve (AUC) Scores for consciousness indexing and outcome prediction of alpha microstates

	AUC Score	
Alpha Microstates	Consciousness Indexing	Outcome Prediction
Microstate class A: frequency, alpha	57% ± 5%	51% ± 10%
Microstate class B: frequency, alpha	60% ± 5%	59% ± 2%
Microstate class C: frequency, alpha	56% ± 2%	55% ± 5%
Microstate class D: frequency, alpha	62% ± 2%	62% ± 5%
Microstate class A: duration, alpha	62% ± 10%	76% ± 10%
Microstate class B: duration, alpha	53% ± 7%	67% ± 3%
Microstate class C: duration, alpha	70% ± 7%	51% ± 4%
Microstate class D: duration, alpha	67% ± 5%	61% ± 7%
Microstate class A: percentage, alpha	54% ± 4%	51% ± 3%
Microstate class B: percentage, alpha	59% ± 5%	55% ± 5%
Microstate class C: percentage, alpha	50% ± 4%	66% ± 4%
Microstate class D: percentage, alpha	74% ± 3%	63% ± 3%

Table A11 Area Under Curve (AUC) Scores for consciousness indexing and outcome prediction of $2-20Hz$ microstates

	AUC Score	
2-20Hz Microstates	Consciousness Indexing	Outcome Prediction
Microstate class A: frequency, $2-20Hz$	59% ± 1%	73% ± 3%
Microstate class B: frequency, $2-20Hz$	58% ± 1%	67% ± 1%
Microstate class C: frequency, $2-20Hz$	56% ± 1%	56% ± 4%
Microstate class D: frequency, $2-20Hz$	62% ± 4%	70% ± 10%
Microstate class A: duration, $2-20Hz$	62% ± 10%	62% ± 5%
Microstate class B: duration, $2-20Hz$	73% ± 4%	74% ± 5%
Microstate class C: duration, $2-20Hz$	53% ± 4%	58% ± 4%
Microstate class D: duration, $2-20Hz$	55% ± 1%	57% ± 1%
Microstate class A: percentage, $2-20Hz$	64% ± 7%	62% ± 4%
Microstate class B: percentage, $2-20Hz$	60% ± 1%	55% ± 4%
Microstate class C: percentage, $2-20Hz$	58% ± 1%	54% ± 5%
Microstate class D: percentage, $2-20Hz$	60% ± 1%	71% ± 3%

Table A12 Area Under Curve (AUC) Scores for consciousness indexing and outcome prediction of *ApEn*

	AUC Score	
ApEn	Consciousness Indexing	Outcome Prediction
alpha	57% ± 5%	67% ± 5%
beta	68% ± 2%	59% ± 4%
delta	58% ± 5%	51% ± 2%
theta	55% ± 2%	51% ± 6%

Table A13 Area Under Curve (AUC) Scores for consciousness indexing and outcome prediction of *PEn*

	AUC Score	
PEn	Consciousness Indexing	Outcome Prediction
alpha	61% ± 2%	53% ± 2%
beta	67% ± 1%	58% ± 2%
delta	62% ± 2%	71% ± 5%
theta	66% ± 7%	83% ± 3%

Table A14 Area Under Curve (AUC) Scores for consciousness indexing and outcome prediction of alpha and delta power

	AUC Score	
Power	Consciousness Indexing	Outcome Prediction
alpha	54% ± 3%	64% ± 4%
delta	58% ± 7%	68% ± 9%

Table A15 Area Under Curve (AUC) Scores for consciousness indexing and outcome prediction of alpha, beta delta and theta coherence

	AUC Score	
Coherence	Consciousness Indexing	Outcome Prediction
alpha	64% ± 4%	62% ± 4%
beta	61% ± 2%	67% ± 1%
delta	59% ± 3%	56% ± 7%
theta	51% ± 4%	78% ± 2%

Table A16 Area Under Curve (AUC) Scores for consciousness indexing and outcome prediction of alpha, beta delta and Imag coherence

	AUC Score	
Imag Coherence	Consciousness Indexing	Outcome Prediction
alpha	53% ± 9%	63% ± 6%
beta	50% ± 3%	55% ± 4%
delta	52% ± 5%	54% ± 7%
theta	60% ± 4%	75% ± 5%

Table A17 Area Under Curve (AUC) Scores for consciousness indexing and outcome prediction of $wSMI$

	AUC Score	
$wSMI$	Consciousness Indexing	Outcome Prediction
Alpha		
t = 4	56% ± 4%	50% ± 4%
t = 8	58% ± 2%	71% ± 5%
t = 32	62% ± 3%	73% ± 4%
Beta		
t = 4	67% ± 2%	58% ± 3%
t = 8	68% ± 2%	72% ± 3%
t = 32	68% ± 3%	58% ± 3%
Delta		
t = 4	63% ± 3%	63% ± 5%
t = 8	69% ± 1%	69% ± 8%
t = 32	65% ± 2%	62% ± 8%
Theta		
t = 4	60% ± 3%	63% ± 5%
t = 8	54% ± 10%	51% ± 1%
t = 32	65% ± 3%	61% ± 6%

Table A18 Area Under Curve (AUC) Scores for consciousness indexing and outcome prediction of TE

	AUC Score	
TE	Consciousness Indexing	Outcome Prediction
alpha	67% ± 3%	78% ± 3%
beta	62% ± 2%	62% ± 5%
delta	66% ± 2%	70% ± 3%
theta	66% ± 3%	60% ± 4%

Table A19 Area Under Curve (AUC) Scores for consciousness indexing and outcome prediction of the average path length

	AUC Score	
Average Path Length	Consciousness Indexing	Outcome Prediction
alpha	65% ± 4%	61% ± 4%
beta	65% ± 5%	60% ± 5%
delta	60% ± 1%	59% ± 4%
theta	59% ± 1%	60% ± 5%

Table A20 Area Under Curve (AUC) Scores for consciousness indexing and outcome prediction of the average clustering coefficient

	AUC Score	
Average Clustering Coefficient	Consciousness Indexing	Outcome Prediction
alpha	63% ± 5%	80% ± 3%
beta	62% ± 4%	82% ± 3%
delta	58% ± 4%	57% ± 7%
theta	60% ± 5%	73% ± 4%

Appendix: Supplementary Figures

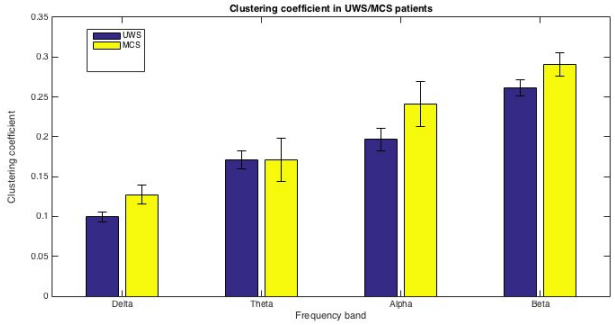

Supplementary Figure 1 Distribution of average clustering coefficients for UWS/ MCS patients, averaged over all thresholds.

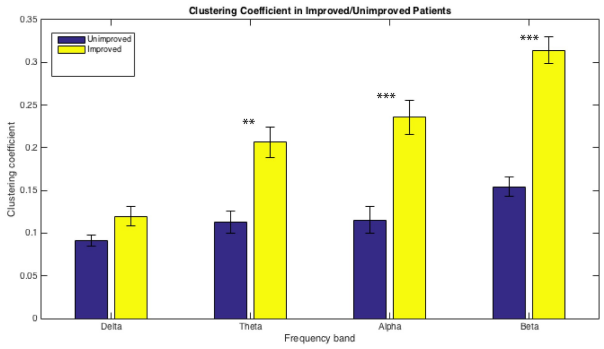

Supplementary Figure 2 Distribution of average clustering coefficients for improved/ unimproved patients, averaged over all thresholds.

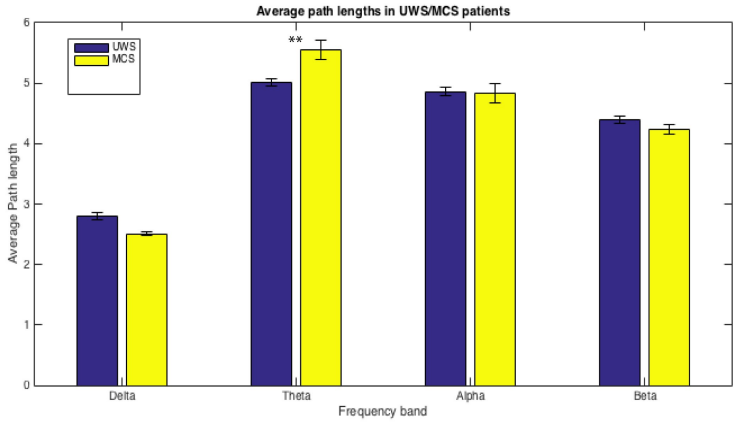

Supplementary Figure 3 Distribution of average path lengths for UWS/MCS patients, averaged over all thresholds.

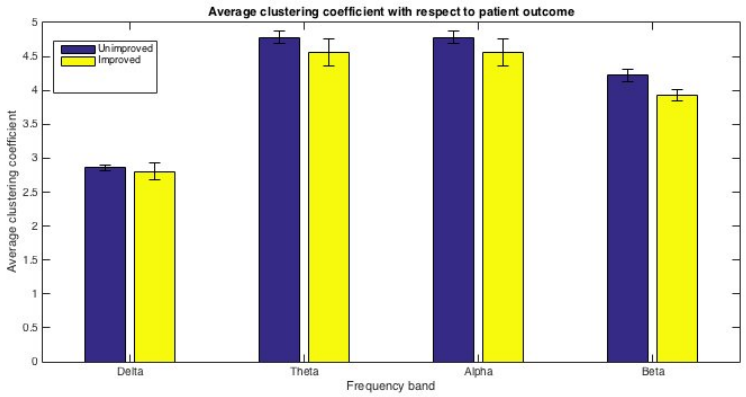

Supplementary Figure 4 Distribution of average path lengths for improved/unimproved patients, averaged over all thresholds.

Erklärung

Ich versichere hiermit, dass ich die Arbeit selbständig angefertigt habe und keine anderen als die angegebenen Quellen und Hilfsmittel benutzt sowie die wörtlich oder inhaltlich übernommenen Stellen als solche kenntlich gemacht und die zur Zeit gültige Satzung der Universität Ulm zur Sicherung guter wissenschaftlicher Praxis beachtet habe (§ 6 Abs. 2 Satz 2 Promotionsordnung).

....

(Datum) (Unterschrift)

Lebenslauf aus Gründen des Datenschutzes entfernt.